



**ORGANOMETALLIC COMPOUNDS AND METAL NANOPARTICLES AS
CATALYSTS IN LOW ENVIRONMENTAL IMPACT SOLVENTS**
Martha Verónica Escárcega Bobadilla

ISBN: 978-84-694-1249-7

Dipòsit Legal: T-324-2011

ADVERTIMENT. La consulta d'aquesta tesi queda condicionada a l'acceptació de les següents condicions d'ús: La difusió d'aquesta tesi per mitjà del servei TDX (www.tesisenxarxa.net) ha estat autoritzada pels titulars dels drets de propietat intel·lectual únicament per a usos privats emmarcats en activitats d'investigació i docència. No s'autoritza la seva reproducció amb finalitats de lucre ni la seva difusió i posada a disposició des d'un lloc aliè al servei TDX. No s'autoritza la presentació del seu contingut en una finestra o marc aliè a TDX (framing). Aquesta reserva de drets afecta tant al resum de presentació de la tesi com als seus continguts. En la utilització o cita de parts de la tesi és obligat indicar el nom de la persona autora.

ADVERTENCIA. La consulta de esta tesis queda condicionada a la aceptación de las siguientes condiciones de uso: La difusión de esta tesis por medio del servicio TDR (www.tesisenred.net) ha sido autorizada por los titulares de los derechos de propiedad intelectual únicamente para usos privados enmarcados en actividades de investigación y docencia. No se autoriza su reproducción con finalidades de lucro ni su difusión y puesta a disposición desde un sitio ajeno al servicio TDR. No se autoriza la presentación de su contenido en una ventana o marco ajeno a TDR (framing). Esta reserva de derechos afecta tanto al resumen de presentación de la tesis como a sus contenidos. En la utilización o cita de partes de la tesis es obligado indicar el nombre de la persona autora.

WARNING. On having consulted this thesis you're accepting the following use conditions: Spreading this thesis by the TDX (www.tesisenxarxa.net) service has been authorized by the titular of the intellectual property rights only for private uses placed in investigation and teaching activities. Reproduction with lucrative aims is not authorized neither its spreading and availability from a site foreign to the TDX service. Introducing its content in a window or frame foreign to the TDX service is not authorized (framing). This rights affect to the presentation summary of the thesis as well as to its contents. In the using or citation of parts of the thesis it's obliged to indicate the name of the author.

UNIVERSITAT ROVIRA I VIRGILI
ORGANOMETALLIC COMPOUNDS AND METAL NANOPARTICLES AS CATALYSTS IN LOW ENVIRONMENTAL IMPACT SOLVENTS
Martha Verónica Escárcega Bobadilla
ISBN:978-84-694-1249-7/DL:T-324-2011

UNIVERSITAT ROVIRA I VIRGILI
ORGANOMETALLIC COMPOUNDS AND METAL NANOPARTICLES AS CATALYSTS IN LOW ENVIRONMENTAL IMPACT SOLVENTS
Martha Verónica Escárcega Bobadilla
ISBN:978-84-694-1249-7/DL:T-324-2011

Martha Verónica Escárcega Bobadilla

ORGANOMETALLIC COMPOUNDS AND METAL NANOPARTICLES AS CATALYSTS IN LOW ENVIRONMENTAL IMPACT SOLVENTS

PhD Thesis

Supervised by Dr. Anna Maria Masdeu i Bultó
and Prof. Montserrat Gómez Simón

Departament de Química Física i Inorgànica



UNIVERSITAT ROVIRA I VIRGILI
TARRAGONA, SPAIN

Laboratoire Hétérochimie Fondamentale et Appliquée



UNIVERSITÉ TOULOUSE III - PAUL SABATIER
TOULOUSE, FRANCE

TARRAGONA
2010

UNIVERSITAT ROVIRA I VIRGILI
ORGANOMETALLIC COMPOUNDS AND METAL NANOPARTICLES AS CATALYSTS IN LOW ENVIRONMENTAL IMPACT SOLVENTS
Martha Verónica Escárcega Bobadilla
ISBN:978-84-694-1249-7/DL:T-324-2011



UNIVERSITAT ROVIRA I VIRGILI
Departament de Química Física i
Inorgànica

La Dra. ANNA MARIA MASDEU I BULTÓ i la Prof. MONTSERRAT GÓMEZ SIMÓN,
Professora Titular d'Universitat del Departament de Química Física i Inorgànica de la
Facultat de Química de la Universitat Rovira i Virgili i Professeur des Universités de la
Université Toulouse III - Paul Sabatier (França)

CERTIFIQUEN:

Que la present memòria que porta per títol “ORGANOMETALLIC COMPOUNDS AND METAL NANOPARTICLES AS CATALYSTS IN LOW ENVIRONMENTAL IMPACT SOLVENTS” per a l’obtenció del títol de Doctor, ha estat realitzada per MARTHA VERÓNICA ESCÁRCEGA BOBADILLA sota la nostra direcció a l’àrea de Química Inorgànica del Departament de Química Física i Inorgànica d’aquesta Universitat i al Laboratoire Hétérochimie Fondamentale et Appliquée de la Université Toulouse III - Paul Sabatier, i que compleix els requeriments per poder optar a Menció Europea.

Tarragona, Octubre de 2010

Dra. Anna Maria Masdeu i Bultó

Prof. Montserrat Gómez Simón

UNIVERSITAT ROVIRA I VIRGILI
ORGANOMETALLIC COMPOUNDS AND METAL NANOPARTICLES AS CATALYSTS IN LOW ENVIRONMENTAL IMPACT SOLVENTS
Martha Verónica Escárcega Bobadilla
ISBN:978-84-694-1249-7/DL:T-324-2011

Ha llegado el momento de agradecer a toda la gente que ha hecho posible, de una manera u otra, el desarrollo de la presente Tesis.

En primer lugar me gustaría agradecer a las Doctoras Anna Masdeu y Montserrat Gómez por la confianza depositada en mí para el desarrollo de este trabajo, así como el apoyo, la paciencia y los consejos que en todo momento me han brindado, sinceramente gracias por todo.

Me gustaría también agradecer a los miembros del tribunal, Dr. Miquel Pericàs, por los consejos brindados, al Dr. David Madec, merci pour le soutien le temps qu'on a passé ensemble à Toulouse, a la Dra. Montserrat Diéguez, por los consejos brindados desde hace ya algunos años en el máster, en el inicio de este trabajo, al Prof. Michel Etienne y a la Dra. Victoria Jiménez por aceptar ser miembros del jurado y por el tiempo dedicado a la presente Tesis.

Je voudrais aussi remercier au Dr. Antoine Baceiredo pour me recevoir au sein du Laboratoire Hétérochimie Fondamentale et Appliquée, merci pour tout. Aussi même je voudrais remercier à tous les permanents du « LHFA », spécialement à : Christian Pradel pour les photos TEM, Maryse pour tout le support administrative, Marie-Jo pour l'aide offert, Olivier et Pierre pour le soutien logistique au labo, à Marc, Pierre et Claude pour toute l'aide donnée pour les RMN. Danielle pour l'aide à la bibliothèque, Corinne pour les spectres infrarouge et Raman et finalement au service de spectrométrie de masse, Tsuyoshi pour les conseils à la pause café et Eddy pour ton soutien au labo.

En ce qui concerne aux membres « non permanents » du labo, je voudrais remercier à : Susana pour tous les discussions chimiques et non chimiques aussi de m'introduire à la vie française et aux « sevillanas », merci beaucoup et bonne chance au Mexique doctoresa ! Ricardo je t'écris en français parce que je sais que probablement ton niveau doit être maintenant très bon, merci pour ton soutien et les conversations chimiques et quotidiennes et aussi pour toute l'aide que m'as donné, merci beaucoup « mañico »! Aux membres et ex-membres du LPBP (eh ! je l'ai écrit correctement !) Olivier merci pour tes conseils et pour ton soutien au labo et au

Acknowledgements / Remerciements / Agradecimientos / Agraciements

bureau, on se verra pour aller découvrir la France, je suis sûre ! Aurèlie pour les coups et les conseils dans le labo et dans la cuisine, nouvelle doctoresa, j'attends pour ce que tu m'as promis he he, Marie bonne chance et merci pour ton soutien, Pauline merci pour tout, princesse et bonne chance, Fany merci pour tout ! Ça a été un vrai plaisir partager tous ces moments à Toulouse, bonne continuation et courage ma petite asturienne ! Noël comme j'ai dit pour Ricardo, j'espère que ton français a été avancé pendant ce temps à Toulouse, merci pour tes conseils et puxa Asturies !, Bea une autre asturienne qui est venue pour découvrir Toulouse avec moi, merci pour partager ces deux mois avec moi, courage pour la partie finale de la Thèse, Eric merci pour tout mon canadien préféré, je t'attends à Tarragona Canadian guy, Jérôme pour ton bonheur, merci pour me montrer Rodrigo y Gabriela, bonne continuation, Fethi pour ton bonheur, bonne chance, Colin, Pascal et Damien. Un grand merci aussi aux membres de autres équipes du labo, Florie ne te stresse pas et bonne chance pour la fin de la thèse, Sophie merci pour tout, Hélène avec ton bonheur ma copine du bureau, bonne chance, Nico Toselli bonne chance et ton espagnol est magnifique, Nico Dellus courage l'aveyronnais, Thibault bonne chance, Juan, Damien, Etienne, Aurèlie et Aymeric.

Un grand merci pour les membres de l'équipe « SYMAC » avec qui j'ai partagé des bons moments pendant le cours de cette Thèse : Emma pour tes blagues et ton soutien quotidiennes, David pour tes conseils au labo et au salle de lecture, Fernando avec qui tout a commencé une fois à Barcelone... bonne chance ! Isabelle pour m'introduire au monde des nanoparticules et pour tes délicieuses truffes, Laura pour partager en toute moment tes connaissances du monde des nanotubes de carbone aussi que des conseils de la vie toulousaine et pour la soutenance, merci beaucoup ! Delphine pour ta sourisse quotidienne, Stephan pour tes blagues au labo, Ulrike pour me montrer la vie toulousaine, Mohamad pour les chansons arabes dans le labo, Raluca pour faire plus amusante le bureau, Susanna pour les conseils de la vie et du labo, Brito finalement on s'est revu à Toulouse et après... on verra ! Pauline bonne chance avec le M2 et les concours ! et à Bea et à les personnes de l'Universitat de Barcelona pour les moments vécus ensemble à Barcelone, à Montpellier et à Palermo.

Acknowledgements / Remerciements / Agradecimientos / Agraiaments

Un remerciement spécial à Soraya pour tout le soutien reçu pendant ce temps à l'École Doctorale Sciences de la Matière, et aussi à Marie Claude et Raphaël pour tout le temps qu'on a passé ensemble à Toulouse et pour me montrer les merveilles de la France, de la cuisine et la culture françaises, j'espère qu'on se verra prochainement pour continuer la découverte, à Rita, Pablo et Noura, merci pour le soutien quotidienne, et les moments musicales qu'on a passé ensemble, bonne chance !

También me gustaría agradecer a la Dra. Carmen Claver por acogerme en su grupo y por las cenas en su casa así como a los profesores del área de Inorgánica de la Universitat Rovira i Virgili : Elena, Pilar, Montse, Aurora, Yolanda y Núria por los consejos y el haberme recibido dentro del grupo. Así como un agradecimiento especial al Prof. Piet van Leeuwen por los consejos y apoyo brindados.

No podía faltar un agradecimiento especial a María José y Jordi por todo el apoyo brindado durante este tiempo, a Ramón por ayudarme a ahondar más en la RMN, a Rosa por los espectros de masas, a Mercè, Mariana, Núria y Lucas por las largas horas en la TEM así como también a las secretarias del departamento: Yolanda, Silvia y Cristina por todo el apoyo brindado en logística.

Agradezco a la gente del grupo y de la Facultad, a los doctores: Aitor por tu buen sentido del humor, Alí por tu paciencia, apoyo “docente” y ayuda y Cyril, así como a los compañeros: Pep, David F., Isidro, Andrea, Lucas, Isabel por tu simpatía y buen humor ¡áñimos!, a Vane por estar siempre allí y por brindarme tu amistad desde mi llegada a Tarragona, Idoia suerte y ánimos que esto se pasa muy rápido, Mariam bonne continuation, Surya thank you for your friendship and good luck! and Ailis for the scientific discussions and your energy. Good luck!

Agradezco especialmente a la gente del grupo de scCO₂: Clara quien fue mi compañera de labo al inicio de la Tesis, Arantxa por toda la ayuda con los reactores, Siham merci pour le coucou et bonne continuation!, Gil thank you for the good time in Liverpool, Lara por las risas en el labo, Eva C. por el apoyo y consejos brindados tanto en Tarragona como en Toulouse, suerte en Madrid, Raquel suerte en lo que viene y Ariadna.

Acknowledgements / Remerciements / Agradecimientos / Agraiaments

Un agradecimiento especial a Carlos, Eréndira y a los Marios, por los buenos momentos vividos por Tarragona y alrededores, así como por el apoyo brindado este tiempo que llevamos de conocernos.

Por último me gustaría agradecer a mi familia, a mis padres, hermanos, abue y tía Rosy por todo el gran apoyo brindado a lo largo de todo este tiempo, a los que ya no están con nosotros pero que siempre me apoyaron, así como a Gustavo Z. por estar siempre allí apoyándome en todo, a Caridad F. por su amistad, apoyo y el gusto por la química y a Bernardo F. por iniciarme en el mundo de la investigación, por los consejos y la amistad brindada.

UNIVERSITAT ROVIRA I VIRGILI
ORGANOMETALLIC COMPOUNDS AND METAL NANOPARTICLES AS CATALYSTS IN LOW ENVIRONMENTAL IMPACT SOLVENTS
Martha Verónica Escárcega Bobadilla
ISBN:978-84-694-1249-7/DL:T-324-2011

UNIVERSITAT ROVIRA I VIRGILI
ORGANOMETALLIC COMPOUNDS AND METAL NANOPARTICLES AS CATALYSTS IN LOW ENVIRONMENTAL IMPACT SOLVENTS
Martha Verónica Escárcega Bobadilla
ISBN:978-84-694-1249-7/DL:T-324-2011

Table of Contents

Abbreviations / 1

Chapter 1. Introduction / 3

- 1.1. Sustainable chemistry and catalysis / **5**
- 1.2. Non-conventional solvents in catalysis / **8**
 - 1.2.1. Water / **9**
 - 1.2.2. Fluorous solvents / **10**
 - 1.2.3. Supercritical fluids (SCFs) / **11**
 - 1.2.3.1. Supercritical carbon dioxide (scCO₂) / **12**
 - 1.2.4. Ionic liquids (ILs) / **14**
- 1.3. Metallic nanoparticles in catalysis / **18**
 - 1.3.1. Synthesis of MNP / **18**
 - 1.3.1.1. Organometallic approach in the synthesis of MNP / **19**
 - 1.3.2. Stabilisation of MNP / **20**
 - 1.3.2.1. Electrostatic stabilisation / **20**
 - 1.3.2.2. Steric stabilisation / **21**
 - 1.3.2.3. Electrosteric stabilisation / **22**
 - 1.3.3. Catalytic applications / **22**
 - 1.3.3.1. Non-conventional solvents / **23**
- 1.4. References / **25**

Chapter 2. Objectives / 31

Chapter 3. Rh and Ru Nanoparticles in Catalytic Arene Hydrogenation in Supercritical Carbon Dioxide / 35

- 3.1. Introduction / **37**
- 3.2. Results and Discussion / **39**
 - 3.2.1. Synthesis of rhodium and ruthenium nanoparticles / **39**
 - 3.2.2. Catalytic reactivity of rhodium and ruthenium nanoparticles / **45**
- 3.3. Conclusions / **49**
- 3.4. Experimental / **50**

Table of Contents

3.4.1. Synthesis of metallic nanoparticles / 51
3.4.1.1. General synthesis of Ru nanoparticles stabilized by phosphine ligands / 51
3.4.1.2. General synthesis of Rh nanoparticles stabilized by phosphine ligands / 52
3.4.2. Catalytic reactions / 52
3.4.2.1. Hydrogenation of arenes using metallic nanoparticles in THF / 52
3.4.2.2. Hydrogenation of arenes using metallic nanoparticles in scCO ₂ / 53
3.4.3. Ligand exchange reaction monitored by NMR / 53
3.5. References / 54

Chapter 4. New Bicyclic P-donor Ligands: Synthesis, Structure and Applications in Pd-Catalysed C-C Bond Formation in Ionic Liquids / 57

4.1. Introduction / 59
4.2. Results and Discussion / 63
4.2.1. Synthesis and characterization of azadioxaphosphabicyclo [3.3.0]octane compounds / 63
4.2.2. Preparation of palladium complexes / 69
4.2.3. Catalytic results / 70
4.2.3.1. Suzuki C-C cross-couplings / 70
4.2.3.2. Recycling experiments / 74
4.2.3.3. Asymmetric Suzuki C-C cross-coupling / 75
4.2.3.4. Asymmetric allylic alkylation / 76
4.3. Conclusions / 78
4.4. Experimental / 79
4.4.1. Synthesis of P-donor ligands / 79
4.4.1.1. (3 <i>S</i> ,4 <i>S</i>)-1-benzylpyrrolidine-3,4-diol, 4 / 79
4.4.1.2. (3 <i>S</i> ,4 <i>S</i>)-1-benzyl-3,4-bis(diphenylphosphinoxy)pyrrolidine, 3 / 80
4.4.1.3. (3a <i>S</i> ,6a <i>S</i>)-5-benzyl-2-phenyltetrahydro-3aH-[1,3,2]dioxaphospholo[4,5-c]pyrrole, 1 / 80
4.4.1.4. (3a <i>S</i> ,6a <i>S</i>)-5-benzyl-2-phenoxytetrahydro-3aH-[1,3,2]dioxaphospholo[4,5-c]pyrrole, 2 / 81

4.4.2. Synthesis of Pd(II) complexes / 82
4.4.2.1. Dichloro- κ^1 -P-bis-{(3aS,6aS)-5-benzyl-2-phenyltetra-hydro-3aH-[1,3,2]dioxaphospholo[4,5-c]pyrrole]}palladium(II), Pd1 / 82
4.4.2.2. Dichloro- κ^2 -P,P-(3S,4S)-1-benzyl-3,4-bis(diphenylphosphinoxy)-pyrrolidine]palladium(II), Pd3 / 83
4.4.3. Catalytic experiments / 83
4.4.3.1. General procedure for catalytic Suzuki C-C coupling in ionic liquid / 83
4.4.3.2. General procedure for catalytic Suzuki C-C coupling in toluene / 84
4.4.3.3. General procedure for catalytic asymmetric allylic alkylation in [BMI][PF ₆] / 84
4.4.3.4. General procedure for catalytic asymmetric allylic alkylation in dichloromethane / 84
4.5. References / 85

Chapter 5. Rh-catalysed Asymmetric Hydrogenation in Non-Conventional Solvents / 89

5.1. Introduction / 91
5.2. Results and Discussion / 94
5.2.1. Synthesis of BINOL derived chiral fluorinated ligands 1 and 2 / 94
5.2.2. Synthesis of Rh(I) complexes, Rh1 and Rh3 / 95
5.2.3. Supported catalytic ionic liquid phase / 96
5.2.4. Rh-catalysed asymmetric hydrogenation / 98
5.2.4.1. Rh-catalysed asymmetric hydrogenation in CH ₂ Cl ₂ / 98
5.2.4.2. Rh-catalysed asymmetric hydrogenation in scCO ₂ / 99
5.2.4.3. Rh-catalysed asymmetric hydrogenation in [BMI][PF ₆] / 100
5.2.4.4. Rh-catalysed asymmetric hydrogenation in [BMI][PF ₆]/scCO ₂ / 101
5.2.4.5. Recycling experiments / 102
5.2.4.6. Rh-catalysed asymmetric hydrogenation in supported ionic liquid phase / 103
5.2.5. Confined catalytic ionic liquid phase / 104
5.3. Conclusions / 107

Table of Contents

5.4. Experimental / **107**

5.4.1. Synthesis of P-donor ligands / **108**

5.4.1.1. (11b*R*)-4-(3,5-bis(trifluoromethyl)phenoxy)dinaphtho[2,1-d:1',2'f]

[1,3,2] dioxaphosphepine **1** / **108**

5.4.1.2. Synthesis of (11b*R*)-4-(2,2,2-trifluoroethoxy)dinaphtho[2,1-d:1',2'-f][1,3,2]dioxaphosphepine, **2** / **109**

5.4.1.3. (3a*S*,6a*S*)-5-benzyl-2-phenyltetrahydro-3aH-[1,3,2]dioxaphospholo[4,5-c]pyrrole, **3** / **110**

5.4.1.4. (3a*R*,6a*R*)-5-benzyl-2-phenoxytetrahydro-3aH-[1,3,2]dioxaphospholo[4,5-c]pyrrole, **4** / **110**

5.4.2. Synthesis of Rh(I) complexes / **110**

5.4.2.1. Cyclooctadiene-bis-(11b*R*)-4-(2,2,2-trifluoroethoxy)di naphtho[2,1-d:1',2'-f][1,3,2]dioxaphosphepine)rhodium(I) hexafluorophosphate **Rh1** / **110**

5.4.2.2. Cyclooctadiene-bis-((3a*S*,6a*S*)-5-benzyl-2-phenyltetrahy-dro-3aH-[1,3,2]dioxaphospholo[4,5-c]pyrrole)rhodium(I) hexafluorophosphate **Rh3** / **111**

5.4.3. Immobilization of [Rh(COD)(**1**)₂]PF₆ over a supported ionic liquid phase (SILP), **Rh1-IL-MWCNT**, **Rh1-IL-SiO₂** / **111**

5.4.4. Immobilization of [Rh(COD)(**1**)₂]PF₆ over a supported ionic liquid phase (SILP) inside of CNTs, **Rh1-ILinMWCNT** / **112**

5.4.5. Catalytic experiments / **112**

5.4.5.1. General procedure for catalytic asymmetric hydrogenation in organic solvent / **112**

5.4.5.2. General procedure for catalytic asymmetric hydrogenation in [BMI][PF₆] / **112**

5.4.5.3. General procedure for catalytic asymmetric hydrogenation in supercritical carbon dioxide (scCO₂) / **113**

5.4.5.4. General procedure for catalytic asymmetric hydrogenation in supercritical carbon dioxide/[BMI][PF₆] (scCO₂/[BMI][PF₆]) / **113**

5.4.5.5. General procedure for catalytic asymmetric hydrogenation in suported ionic liquid phase (SILP) / **113**

5.5. References / **114**

Chapter 6. Conclusions / 117

6.1. Concluding remarks / **119**

6.2. Conclusions / **123**

6.3. Conclusiones / **127**

6.4. Conclusions / **131**

Summary / 135

Summary / **137**

Résumé / **139**

Resumen / **142**

Resum / **145**

Scientific contributions / 149

UNIVERSITAT ROVIRA I VIRGILI
ORGANOMETALLIC COMPOUNDS AND METAL NANOPARTICLES AS CATALYSTS IN LOW ENVIRONMENTAL IMPACT SOLVENTS
Martha Verónica Escárcega Bobadilla
ISBN:978-84-694-1249-7/DL:T-324-2011

Abbreviations

acac	acetylacetone
AgNP	Silver nanoparticles
BARF	tetrakis-(3,5-bis-trifluoromethylphenyl)borate
BASIL™	Biphasic Acid using Ionic Liquids
BINAP	2,2'-bis(diphenylphosphino)-1,1'-binaphthyl
BINOL	1,1'-Bi-2,2'-naphtol
BMI	1-butyl-3-methylimidazolium
BSA	Bis(trimethylsilyl)acetamide
C-CVD	Catalytic chemical vapour deposition
COD	Cyclooctadiene
COT	cyclooctatriene
DFT	Density functional theory
DIOP	((4 <i>R</i> ,5 <i>R</i>)-2,2-dimethyl-1,3-dioxolane-4,5-diyl)bis(methylene))bis(diphenylphosphine)
<i>ee</i>	Enantiomeric excess
EMI	1-ethyl-3-methylimidazolium
ESI	Electrospray ionization
GC	Gas chromatography
HAPs	Hazardous air pollutants
hcp	Hexagonal cubic packing
HRMS	High resolution mass spectrometry
HR-TEM	High resolution transmission electron microscopy
HSQC	Heteronuclear Single-Quantum Correlation
ICP	Inductively coupled plasma
ILs	Ionic liquids
IR	Infrared spectroscopy
L	Ligand
M	Metal
MNP	Metal nanoparticles
MS	Mass spectrometry
MWCNT	Multi-walled carbon nanotubes

Abbreviations

NBD	norbornadiene
NMR	Nuclear magnetic resonance
NOESY	Nuclear Overhauser Effect Spectroscopy
P	Pressure
P _c	Critical pressure
PdNP	Palladium nanoparticles
PM3	Parameterized Model number 3
PPh ₃	Triphenylphosphine
RhNP	Rhodium nanoparticles
RuNP	Ruthenium nanoparticles
scCO ₂	Supercritical carbon dioxide
SCFs	Supercritical fluids
T	Temperature
T _c	Critical temperature
TEM	Transmision electron microscopy
THF	Tetrahydrofurane
TOF	Turn over frequency
TON	Turn over number
TPPTS	Triphenylphosphine trisulphonate
VOCs	Volatile organic compounds
XRD	R-ray diffraction

Chapter 1

Introduction

UNIVERSITAT ROVIRA I VIRGILI
ORGANOMETALLIC COMPOUNDS AND METAL NANOPARTICLES AS CATALYSTS IN LOW ENVIRONMENTAL IMPACT SOLVENTS
Martha Verónica Escárcega Bobadilla
ISBN:978-84-694-1249-7/DL:T-324-2011

1.1. Sustainable chemistry and catalysis

In 1990s, the concept of sustainable chemistry was simultaneously initiated in US and Europe, and after that has been widely adopted by the chemical industry.¹ The sustainable chemistry message is simple: “seek prevention not cure”. Anastas and Warner postulated in 1998 the 12 principles of “green chemistry”.²

Roger Sheldon has proposed a reasonable working definition of sustainable chemistry: *Green chemistry efficiently uses (preferably renewable) raw materials, eliminates waste and avoids the use of toxic and/or hazardous reagents and solvents in the manufacture and application of chemical products.*³

Waste is defined as “everything produced in the process, except the desired product.”⁴ The environmental impact of a chemical process can be evaluated by the E factor, or environmental factor, defined as the mass ratio of waste to desired product. E factor significantly increases its value going from bulk to fine chemicals (Table 1.1).⁵

Table 1.1. The E factor depending on the industrial sector.⁵

Industry segment	Product Tonnage / year	E [kg waste / kg product]
Oil refining	$10^6\text{-}10^8$	<1
Bulk chemicals	$10^4\text{-}10^6$	<1-5
Fine chemicals	$10^2\text{-}10^4$	>50
Pharmaceuticals	$10\text{-}10^3$	>100

One of the key objectives of sustainable chemistry is to diminish the waste production, as stated above. Moreover, a sustainable process is one that optimises the use of starting materials, while still leaving sufficient for future generations. Actually, catalysis can play an important role. Indeed, as far as chemistry is concerned, catalysis is the key to sustainability.⁴ In fact, the definition to describe a catalyst reads as follows: *A catalyst is a substance that increases the rate at which a chemical reaction approaches equilibrium without becoming itself permanently involved.*⁶ Thus, improving the efficiency of the process.

Introduction

The "catalyst" can be added to the reactants under different forms, the named catalyst precursor, which has to be brought into the active form. During the catalytic cycle, the catalyst evolves to lead to several intermediate species. An active catalyst can be involved several times through this cycle; in this sense, the catalyst remains unaltered but dynamic. The number of moles of substrate that a mole of catalyst can convert into product molecules through this cycle before becoming inactivated is called the turnover number (TON) and is a measure of the catalyst stability. The turnover frequency (TOF) is the number of moles of product per mole of catalyst per unit time or the TON in a certain period and is a measure of the catalyst efficiency.⁷

Catalysis is traditionally divided into heterogeneous and homogeneous catalysis. In heterogeneous catalysis, the catalyst and the reactants are in different phase. Usually the catalyst is in a solid phase providing a surface on which the reactants are temporarily adsorbed. Bonds in the substrate became sufficiently weakened by chemisorption to favour the formation of new bonds. Syngas conversion, hydrogenation and oxidation processes are by far the most important industrial applications. Catalyst synthesis technology is applied to the manufacture of high surface area metal species, including metallic nanoparticles (which will be further discussed in the section 1.3 of this Chapter) and metal oxides, usually supported on inorganic materials such as alumina, silica and zeolites.⁸

Homogeneous catalysis refers to a catalytic system in which the reactants and the catalyst are in one phase. In contrast to the heterogeneous catalysis, advanced levels in terms of understanding the elementary steps characterizing the catalytic cycle, bringing molecular insight into the design of new catalysts and even allowing the discovery of new reactions have been reached. The advantages of homogeneous catalysts are often the activity and mainly the selectivity induced, however their separation from organic products and their recycling remain often troublesome.^{6,9}

In 1980s, Schwartz pointed an expanded and better consideration for defining a catalysts as "homogeneous", relating it to its possessing only a single type of active site and if having many active sites as "heterogeneous" catalysts.¹⁰

In particular, homogeneous asymmetric catalysis provides a powerful tool for the synthesis of optically active molecules such as fine chemicals (pharmaceuticals and biocides). Although numerous highly selective chiral catalysts have been developed over the past three decades, their practical applications in industrial processes are hindered by their high costs as well as difficulties in removing traces of toxic metals from the organic product produced. In this case, costly and time-consuming unit operations, such as crystallization, chromatography or distillation, are necessary to both purify and recover (and eventually reuse) the catalyst.¹¹

In an effort to solve the problem of catalyst recovery, the concept of catalyst immobilization has been developed. It is defined as the transformation of a homogeneous catalyst into a heterogeneous one, which is able to be separated from the reaction mixture and preferably be reused multiple times. Specially in asymmetric catalysis, the main goal for the development of an immobilized chiral catalyst is to combine the positive aspects of a homogeneous catalyst (*e.g.* high activity, high enantioselectivity, good reproducibility) with those of a heterogeneous catalyst (*e.g.* ease of separation, stability, reusability). Depending on whether the modifications are made on the catalyst structure or on the reaction medium, the immobilization techniques are categorized into two general types, namely heterogenised enantioselective catalysts and multiphase catalysis in non-conventional media (Figure 1.1).¹²

Taking into account the solubility criteria, the immobilized chiral catalysts can be further subdivided into several types:

- Insoluble chiral catalysts bearing stationary supports such as inorganic materials or organic crosslinked polymers, or homochiral organic – inorganic coordination polymeric catalysts without using any external support and supported metal nanoparticles bearing chiral ligands.¹³
- Soluble chiral catalysts bearing linear polymer supports or dendritic ligands, unsupported metal nanoparticles bearing chiral ligands.

Introduction

- Chiral catalysts soluble in a non-conventional reaction medium as ‘mobile carrier’, such as aqueous phase, fluorous phase, ionic liquid and supercritical carbon dioxide (scCO_2).¹⁴

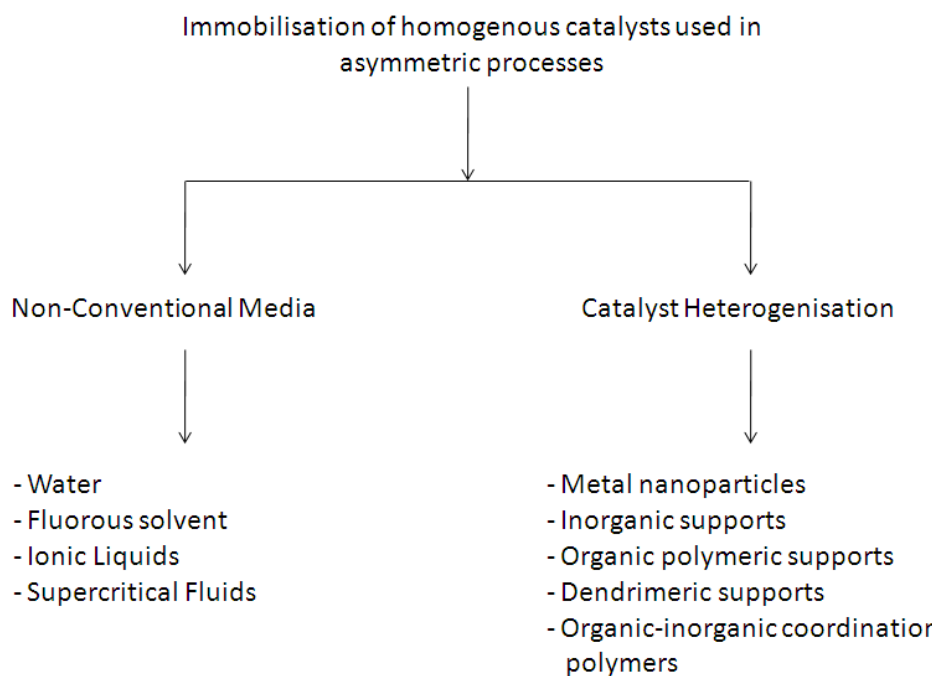


Figure 1.1. Immobilisation of homogenous catalysts used in asymmetric processes.

Some of these aspects will be developed in the subsequent sections of this Chapter, such as non-conventional solvents and metal nanoparticles.

1.2. Non-conventional solvents in catalysis

The use of a solvent in chemical transformations is an important issue for different good reasons:¹⁵

- Reactions proceed faster and more smoothly when the reactants are dissolved due to diffusion reasons.
- The solvent may trigger a positive effect on the rate and selectivity of the reaction.

-The solvent acts as a heat transfer medium, removing heat liberated in an exothermic process. It reduces thermal gradients in a reaction vessel, allowing a soft and safe transformation.

However, organic solvents cause a particular concern to the chemical industry because of the sheer volume used in synthesis, processing and separations. The main part of them behaves as volatile organic compounds (VOCs) or hazardous air pollutants (HAPs) and exhibits flammable, toxic and/or carcinogenic characteristics. Thus, the involvement of solvents requires a major rethink in terms of sustainability issues; this need is driving the research for alternative reaction media.

In this context, alternative reaction media (*neoteric* solvents) present the great issue of recovery and reuse of the catalyst. This is highly important from both an environmental and an economic point of view because the catalysts used in fine chemicals manufacture often contain highly expensive noble metals and/or optically pure ligands.

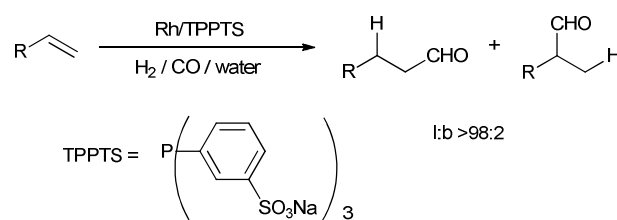
Typical non-conventional solvents are supercritical carbon dioxide,¹⁶ water,¹⁷ room temperature ionic liquids¹⁸ and fluorous solvents.¹⁹ For the purposes of this Thesis, only a general outlook is given for water and fluorous systems. Ionic liquids and supercritical fluids (especially supercritical CO₂) as *neoteric* reaction media will be specifically discussed in sections 1.2.3 and 1.2.4, respectively.

1.2.1. Water

Water is the most abundant, inexpensive and safe solvent available. However, it has not been intensively used as reaction solvent because of the lack of solubility of most organic compounds and catalysts, chemical reactivity and purification cost. Transition metal catalysts are often coordinated to tertiary phosphorus donor ligands. In the case of water as solvent, the most studied ligands, since mid-1980s, are water soluble tertiary phosphines containing ionic groups, such as sulphonate, sulphate, phosphate, carboxylate, quaternary ammonium, phosphonium, as well as neutral polyether or polyamide substituents.^{8,20}

Introduction

In the field of the homogenous catalysis, applications of water soluble phosphines are limited. In 1984, the first hydroformylation unit employing an aqueous biphasic system, the “Ruhrchemie/Rhône-Poulenc oxo process”, emerged with an initial capacity of 100,000 tons per year, using triphenylphosphine trisulphonate (TPPTS) as water soluble ligand (Scheme 1.1).²¹ This process produces over 10% of the world’s C4-C5 aldehyde requirement.²²



Scheme 1.1. Ruhrchemie/Rhône Poulenc oxo process in water.

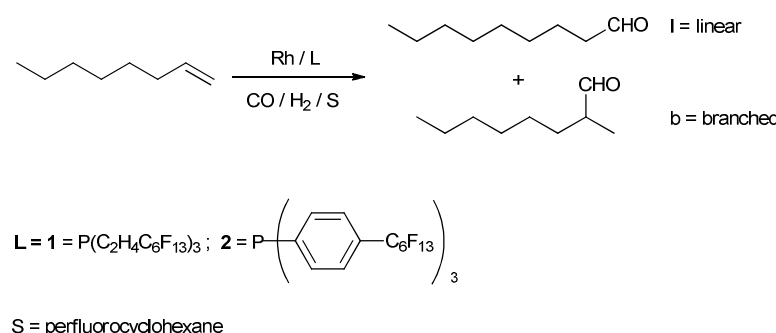
Further development towards the asymmetric version of this reaction, has been achieved by the synthesis of chiral water-soluble phosphines.^{20,23}

1.2.2. Fluorous solvents

Horváth and Rabai coined the term “fluorous” by analogy with “aqueous” to describe highly fluorinated alkanes, ethers and tertiary amines in their pioneering works in fluorous biphasic catalysis.²⁴ This kind of compounds markedly differs from the corresponding hydrocarbon compounds, and presents immiscibility with many common organic solvents at room temperature, but they can become miscible at higher temperatures. This behaviour provides the basis for using monophasic catalysis at high temperatures with biphasic product/catalyst separation, by temperature decrease.

Fluorous and organic solvent mixtures were first used by Horváth for hydroformylation reactions, at room temperature (Scheme 1.2). Precatalyst [Rh(acac)(CO)₂] (acac = acetylacetone) in the presence of **1** in a mixture of perfluorocyclohexane and toluene gave good rates for hydroformylation of 1-octene and leaching of rhodium into the organic phase was very limited (4.2% after nine runs). The linear:branched isomer ratio was high (8:1), but *ca.* 10% of the starting alkene was

lost through isomerisation.²⁵ Even higher rates were obtained when toluene was omitted and the ligand was replaced by **2**. In this case, rhodium leaching was reduced to 0.05% per run.²⁶ The lack of toluene removes the energetic requirement for fractional distillation to separate the catalyst from the solvent.²⁷



Scheme 1.2. Hydroformylation of 1-octene in fluorous solvent.

1.2.3. Supercritical fluids (SCFs)

The use of supercritical fluids has been successfully applied in the basic research as well as in industry. Supercritical fluids offer a number of benefits, such as the potential of combining both reaction and separation processes as well as the ability to tune the solvent through variations concerning temperature and pressure.^{2a}

In a general phase diagram schematised in Figure 1.2, the curves represent the coexistence between two phases. The liquid becomes less dense because of the thermal expansion and the gas becomes denser as the pressure rises. Eventually, the densities of the two phases become identical, the distinction between gas and liquid disappears, the curve ends at the critical point and the substance becomes a fluid.²⁸ Supercritical fluids exhibit properties between gas and liquid, such as giving compressibility and homogeneity.

Critical temperature and pressure are characteristic for each substance; in Table 1.2, some data is collected.²⁹

Introduction

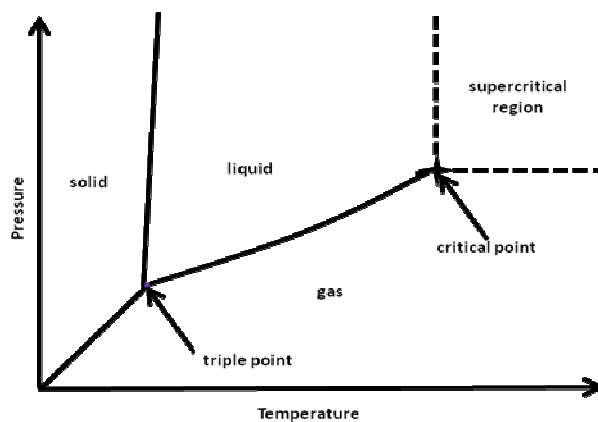


Figure 1.2. Schematised phase diagram of a single substance.

Table 1.2. Critical parameters for some substances.^{29b}

Substance	T_c [K]	P_c [bar]
carbon dioxide	304	74
water	647	221
ethane	305	49
ethene	282	50
propane	370	43
xenon	290	58
fluoroform	299	49

1.2.3.1. Supercritical carbon dioxide ($scCO_2$)

Several features of $scCO_2$ make it an interesting solvent in the context of sustainable chemistry and catalysis.³⁰ It has so far been the most widely used supercritical fluid, because of its convenient critical parameters ($P_c = 74$ and $T_c = 31$ °C),³⁰ cheapness, chemical stability, non-flammability and non-toxicity. It is an environmentally friendly substitute for other organic solvents, mainly due to the fact that the CO_2 is obtained in large quantities as a by-product of fermentation combustion, and ammonia synthesis and after recovery, can be used as supercritical fluid.^{29a}

Due to its non-polar nature, the solubility of a solute in $scCO_2$ is extremely dependent on its chemical properties. Different strategies are used to increase the solubility of the solutes, such as the introduction of some specific low polar groups like

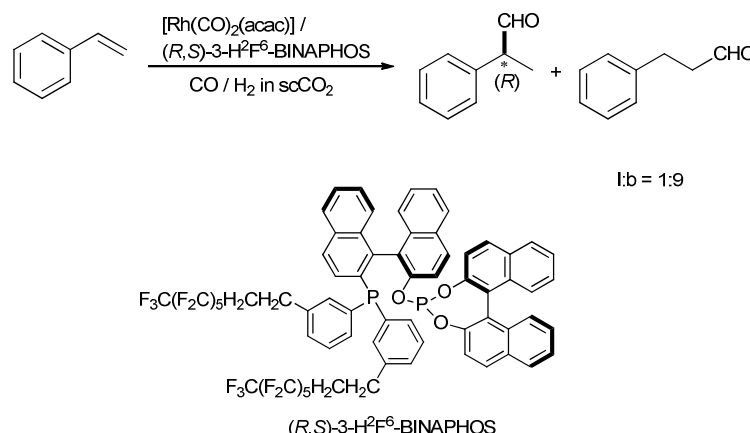
perfluoroalkyl and polysiloxane or polyether/polycarbonate, in order to lead to compounds exhibiting high affinity to compressed CO₂.^{16b}

Many organometallic complexes show relative low solubility in scCO₂, too low even for catalytic applications under single-phase conditions. That is the case of catalysts containing aryl phosphine ligands, which are often used in enantioselective catalysis. The problem can be overcome introducing perfluoroalkyl groups in the ligand, as is the case, of the catalytic asymmetric hydrogenation reaction using chiral aryl phosphine ligands bearing fluoroalkyl groups.³¹ Another strategy adopted to increase the catalyst solubility of cationic catalysts in scCO₂ is the modification of the anion, an example of such anion is tetrakis-(3,5-bis-trifluoromethylphenyl)borate, BARF; excellent enantioselectivities (up to 99.5%) comparable with those obtained in organic solvent, were reported in Rh-catalysed asymmetric hydrogenations using BARF or trifluoromethane sulphonate as counteranions.³²

Another typical example of the application of scCO₂ in homogenous catalysis is the hydroformylation reaction. Rhodium catalysts containing scCO₂-philic phosphine and scCO₂-philic phosphite ligands, were applied in the hydroformylation reactions have led similar results than those obtained in other reaction media, improving the selectivity towards the linear regioisomer and giving efficient separation and recycling, with less than 1 ppm of rhodium in the organic product.³³

Rh-catalysed asymmetric hydroformylation of styrene using scCO₂-philic ligand (*R,S*)-3-H²F⁶-BINAPHOS were carried out giving a TON higher than 12,000 after eight successive runs (Scheme 1.3). Both the catalytic reaction and extraction process using scCO₂, allowed the free-solvent quantitative product recovery with a rhodium content in the products ranging from 0.36 to 1.94 ppm. The branched aldehyde was obtained with an enantiomeric excess up to 93.6% and with a regioselectivity more than 1:9 *l:b* ratio.³⁴

Introduction



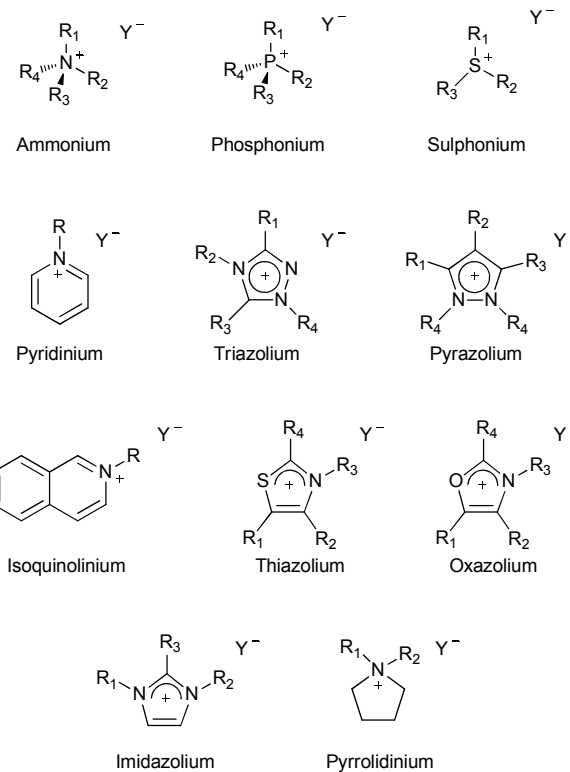
Scheme 1.3. Asymmetric hydroformylation of styrene in scCO₂.

1.2.4. Ionic liquids (ILs)

Ionic liquids are molten salts containing only ions, which exhibit melting points at temperatures below 100 °C. The reason for the relatively low melting point of these salts is the low energy of their crystalline network. They are usually composed of a bulky and non-symmetric organic cation with low charge density and low tendency to establish intermolecular interactions, and an inorganic anion. Currently, there is a large number of commercially available ILs, which are liquid at room temperature.³⁵ Despite that, only in the past few years significant literature has become available in this area. ILs are not recent discovered compounds, some of them have been known for many years, such as [EtNH₃][NO₃], which was described in 1914 possessing melting point of 12 °C.³⁶ In the last decade, the interest of researchers in this field has exponentially grown, representing one of the most attractive alternatives to conventional organic solvents. The most common encountered cations and anions are illustrated in Figure 1.3.

The chemical, physical and solvent properties of the ILs depend on both the cation and anion. Thus, it is possible to design new ionic liquids with the desired properties by the appropriate choice of the cation and its countering ion.

CATIONS :



ANIONS :

$\text{Y} = \text{Cl}, \text{Br}, \text{BF}_4^-, \text{ClO}_4^-, \text{PF}_6^-, \text{SbF}_6^-, \text{NO}_3^-, \text{MeCO}_2^-, \text{CH}_2(\text{OH})\text{CO}_2^-$
 $\text{CF}_3\text{SO}_3^-, \text{MeSO}_3^-, \text{OTs}, \text{N}(\text{CF}_3\text{SO}_2)_2, \text{EtSO}_4^-, \text{C}_8\text{H}_{17}\text{SO}_4^-$
 $(\text{CF}_3\text{CF}_2)_3\text{PF}_3, (\text{MeO})_2\text{PO}_2^-, \text{PH(O)OMe}, \text{CB}_{11}\text{H}_{12}$,
 $\text{Al}(\text{OC}(\text{CF}_3)_2\text{Ph})_4, \text{Al}_2\text{Cl}_7, \text{BARF}$

Figure 1.3. Some examples of frequent ions involved in usual ILs.

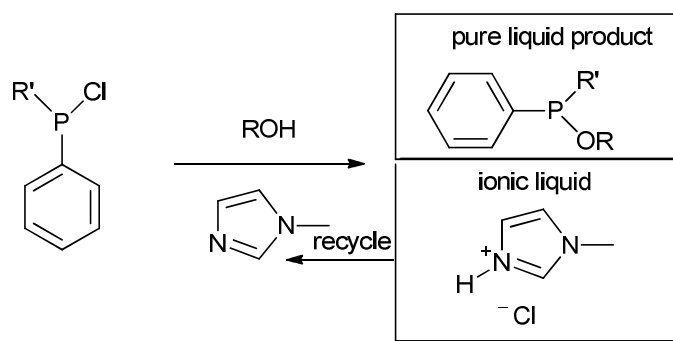
Some simple physical properties of ILs that make them suitable solvents for catalysis are the following:³⁵

1. ILs are good solvents for a wide range of both inorganic and organic materials.
 2. ILs are often composed by poorly coordinating ions, giving high polar but non-coordinating solvents.
 3. ILs are immiscible with a number of organic solvents and provide a non-aqueous, polar alternative for biphasic systems. Hydrophobic ionic liquids can be also used as immiscible polar phases with water.

Introduction

4. ILs have negligible vapour pressure, which minimises the risk of atmospheric contamination and reduces associated health concerns.³⁷
5. Their polarity and hydrophilicity/hydrophobicity can be tuned by a suitable combination of ions.

Although academic research has produced a great number of works in which ILs are used as solvents, co-solvents and/or catalysts, they have not found yet many industrial applications.^{36a} The probably currently most successful example of these applications is the BASILTM (Biphasic Acid Scavenging utilising Ionic Liquids) process, which is used to produce the generic photoinitiator precursor alkoxyphenylphosphines (Scheme 1.4). This process presents the following advantages: the use of a smaller reactor than the conventional process, the space-time yield increase (from 8 kg m⁻³ h⁻¹ to 690,000 kg m⁻³ h⁻¹) and the yield increase (from 50% to 98%).³⁸

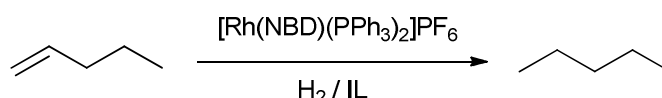


Scheme 1.4. The BASILTM process.

Hazardous properties of ILs have become an important area of research but unfortunately only few data about this feature is yet available and the requirement to consider toxicity, biodegradation and bioaccumulation data has become a priority in this field.³⁹ Consequently, ILs are not necessarily non-toxic and “green” solvents, as often stated, in the absence of the corresponding biological and physico-chemical studies. However, the great advantage of ILs is that they are non-volatile and as a result, ILs do not exhibit serious health risk.⁴⁰

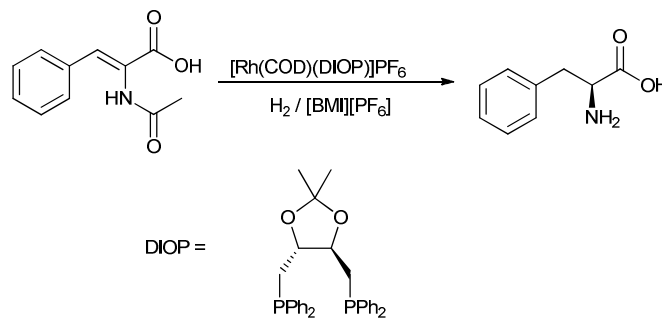
ILs were first introduced in catalysis by Yves Chauvin in 1990s,⁴¹ for the biphasic hydrogenation of 1-pentene (Scheme 1.5), dissolving [Rh(NBD)(PPh₃)₂]PF₆ (NBD =

norbornadiene) in $[\text{BMI}][\text{SbF}_6]$, $[\text{BMI}][\text{PF}_6]$ and $[\text{BMI}][\text{BF}_4]$ (BMI = 1-butyl-3-methylimidazolium). Although the reactants exhibited only limited solubility in the catalyst phase, the rates of hydrogenation in $[\text{BMI}][\text{SbF}_6]$ were almost five times faster than for the comparable reaction in acetone. However, the reaction was found to be much slower using $[\text{BMI}][\text{PF}_6]$. This effect was attributed to the better solubility of pentene in $[\text{BMI}][\text{SbF}_6]$. However, the very poor yield in $[\text{BMI}][\text{BF}_4]$ was due to a high amount of residual Cl^- ions in the ionic liquid, which led to a deactivation by catalyst poisoning. Ionic catalytic phases could be repeatedly reused.



Scheme 1.5. Rh-catalysed hydrogenation of 1-pentene in ILs.

The same group also described the first example of asymmetric hydrogenation of α -acetamido cinnamic acid in $[\text{BMI}][\text{SbF}_6]$ using $[\text{Rh}(\text{COD})(\text{DIOP})]\text{PF}_6$ (COD = cyclooctadiene, DIOP = (((4*R*,5*R*)-2,2-dimethyl-1,3-dioxolane-4,5-diyl)bis(methylene))bis(diphenylphosphine)) as catalyst to obtain (*S*)-phenylalanine with 64% of enantiomeric excess (Scheme 1.6).



Scheme 1.6. Rh-catalysed asymmetric hydrogenation in $[\text{BMI}][\text{PF}_6]$.

After these studies, the use of ILs in catalysis has received a considerable attention.^{42,18} In terms of catalytic applications, as mentioned above, the possibility of the catalyst recovery for further recycling is one of the most important potentials that ILs offer as solvents.

Introduction

Investigations concerning chiral trivalent phosphorus compounds and ionic liquids are mainly focused on the immobilization of metal catalyst bearing phosphorus ligand(s) in mono- or biphasic systems, being some of the most common asymmetric catalytic processes C-C coupling and hydrogenation reactions (which will be discussed in Chapter 4 and Chapter 5, respectively).⁴³

In the last part of this Chapter, a general introduction to nanocatalysis as well as some applications in non-conventional media are given.

1.3. Metallic nanoparticles in catalysis

Metal nanoparticles (MNP) or nanoclusters are entities exhibiting a diameter less than 100 nm. They have generated great interest during the last years, mainly because their unique properties, between bulk metal and single-particle species.⁴⁴

In catalysis, MNP can be supported over a solid support (supported MNP) or dispersed in solution. MNP have significant potential as catalysts showing high activity and selectivity for some processes.⁴⁵ This effect has been attributed to the fact that the large percentage of a MNP's metal atoms lie on the surface,⁴⁶ but it is also important to note that the surface atoms placed at different sites (faces, edges, corners) generate different reactivity depending on their coordination number.

1.3.1. Synthesis of MNP

Two main methodological approaches are generally used to synthesise MNP (Figure 1.4):

1. The physical method – *top-down* – that consists in mechanic subdivision of metallic aggregates, leading to broad particle size distribution, not appropriate for catalytic purposes.⁴⁷
2. The chemical approach – *bottom-up* – that consists in nucleation and growth of metallic atoms.

The chemical methodology offers many advantageous characteristics in MNP that make them suitable as catalysts, such as good control of shape and size (narrow size

distributions), and well-defined surface composition. This procedure leads to reproducible synthesis, and in general the MNP obtained are isolable and redissolvable (“bottleable”).⁴⁸⁵² Perhaps the most important fact of this procedure is that offers the possibility of controlling both the MNP size and the coordination chemistry at the surface in a quantitative and modifiable way.

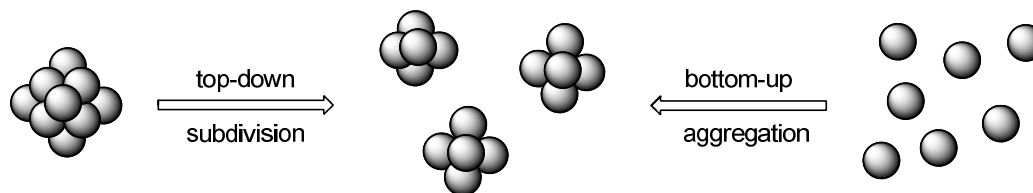


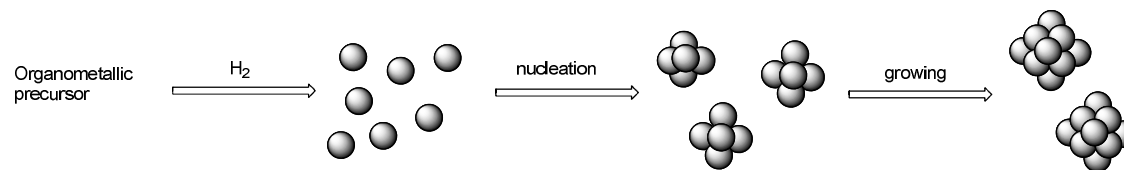
Figure 1.4. The two main approaches for producing MNP.

1.3.1.1. Organometallic approach in the synthesis of MNP

Different strategies have been used in the chemical approach for MNP synthesis, such as: a) chemical reduction of transition metal salts, b) thermal, photochemical or sonochemical decomposition, c) metal vapour synthesis, d) electrochemical reduction and e) ligand reduction and displacement from organometallics.⁴⁸

In this work, the also named organometallic approach, developed by the group of B. Chaudret,⁴⁹ has been employed. This methodology starts from organometallic precursors under mild reaction conditions (generally under reducing atmosphere) to obtain reproducible, uniform and small size MNP (1 – 3 nm).⁴⁹

An organometallic complex containing preferentially olefinic-type ligands represents an ideal precursor for this methodology, since, after hydrogenation, they are reduced to alkanes, which are innocent towards MNP surfaces (Scheme 1.7). One of these precursors largely used in the synthesis of ruthenium nanoparticles is [Ru(COD)(COT)] (COT = cyclooctatriene), which decomposes satisfactorily under low dihydrogen pressure at room temperature.⁵⁰



Scheme 1.7. General MNP synthetic method followed.

Introduction

1.3.2. Stabilisation of MNP

MNP present, as a main characteristic, small sizes, but unfortunately, are unstable with respect to agglomeration towards the bulk metal, and in most cases, this agglomeration leads to the loss of the properties associated with them. Thus, the stabilisation of MNP and the means to preserve them finely dispersed is a crucial aspect to consider during their synthesis. In addition, they can leach metallic atoms from the surface, mainly working under wet conditions. These metallic atoms can be further adsorbed on the metallic surface by sintering processes, such as coalescence and Ostwald ripening.⁵¹

Stabilisation of MNP can essentially be achieved by electrostatic, steric or electrosteric (combination of both) effect. The ligand coordination at the metallic surface, sometimes considered as a steric stabilization, can also avoid the agglomeration.⁵²

1.3.2.1. Electrostatic stabilisation

This kind of stabilisation is produced by ionic compounds such as halides, carboxylates or polyoxoanions salts in aqueous medium. The adsorption of these ionic compounds on the metallic surface generates an electrical double layer around the particles, which results in a Coulombic repulsion between them (Figure 1.5). If the electric potential associated with this double layer is high enough, then the particle aggregation is prevented by electrostatic repulsion. This kind of MNP is, in solution, highly sensitive to any phenomenon able to disrupt the double layer (like ionic strength). The control of these parameters is essential to guarantee an effective electrostatic stabilization.^{44,45,48}

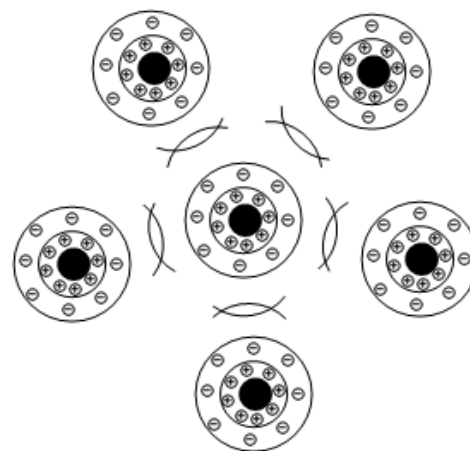


Figure 1.5. MNP electrostatic stabilisation (black circles denote MNP)

1.3.2.2. Steric stabilisation

The adsorption of macromolecules, such as dendrimers,^{52a,53} polymers or oligomers⁵⁴, or ligands,^{52b} such as phosphines, thiols, amines or carbon monoxide as well as solvent molecules, can prevent aggregation of MNP (Figure 1.6). As mentioned in 1.3.2.1 section, electrostatic stabilisation is often produced in aqueous medium, however steric stabilization can be triggered in both organic and aqueous phase.

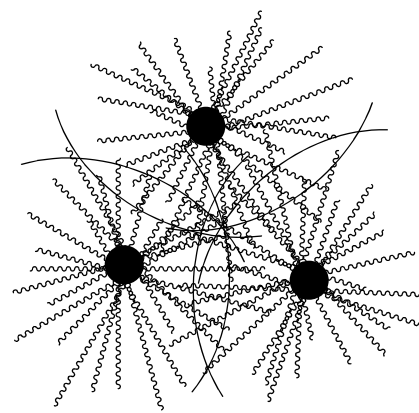


Figure 1.6. MNP steric stabilisation (black circles denote MNP).

In relation to small organic molecules, such as ligands employed in molecular coordination chemistry, their coordination nature as well as the length and nature of ligand substituents, influence the thickness of the protective layer and in consequence the stability of the MNP.

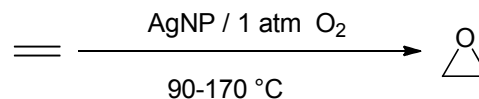
1.3.2.3. Electrosteric stabilisation

Steric and electrostatic stabilisation can be combined to prevent MNP agglomeration in solution. This is generally provided by the use of ionic surfactants, which bear a polar group able to generate an electric double layer and a hydrophilic side chain able to provide steric repulsion.⁵⁵

1.3.3. Catalytic applications

MNP have proven to be efficient catalysts in a large number of reactions such as C-C coupling, hydrogenation, hydrosilylation, hydroxycarbonylation of olefins and amination, which are also catalysed by molecular complexes, as well as for reactions where molecular species are not or are poorly active like hydrogenation of arenes.^{42b,45,52,56}

AgNP stabilized by sodium polyacrylate have been used in catalytic epoxidation of ethane under oxygen atmosphere (Scheme 1.8). AgNP exhibited higher activities than commercial Ag catalyst and an important thermal stability.⁵⁷



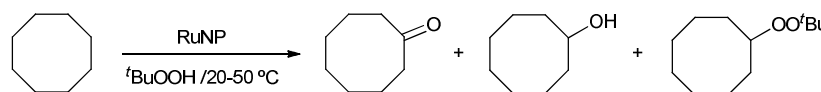
Scheme 1.8. AgNP catalysed oxidation of ethane.

MNP have also proven to be efficient catalysts in enantioselective catalysis,⁵⁸ *e. g.* Hydrogenation,⁵⁹ hydrosilylation,⁶⁰ Suzuki-Miyaura coupling⁶¹ and allylic alkylation.⁶²

The most studied reaction using MNP is the arene hydrogenation, which has an important industrial impact, being rhodium and ruthenium MNP the most employed catalysts. The compounds $[\text{Rh}(\mu\text{-Cl})(\text{COD})]_2$, $\text{RhCl}_3\cdot\text{H}_2\text{O}$, $\text{RuCl}_3\cdot\text{H}_2\text{O}$ and $[\text{Ru}(\text{COD})(\text{COT})]$ are commonly used as MNP precursors. In general, the arene hydrogenation reaction is a biphasic – aqueous/organic solvent – system and takes place under mild conditions.^{56c} This reaction will be further discussed in Chapter 3.

1.3.3.1. Non-conventional solvents

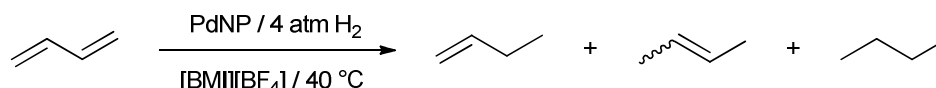
Crooks and Gladysz groups have applied “Fluorous” strategies for MNP synthesis (stabilisation) and catalysis. Fluorous surfactants can also stabilise MNP in water-in-scCO₂ microemulsions that have been used as catalysts for hydrogenation of olefins and citral.⁶³ Functional olefins such as 4-methoxycinnamic acid as well as nitrobenzene (to aniline), were selectively hydrogenated using PdNP in a water-in-scCO₂ microemulsion.⁶⁴ Cyclooctane oxidation by *tert*-butylhydroperoxide was catalysed by RuNP in a biphasic water/organic solvent with recycling of the catalyst without loss of activity (Scheme 1.9).⁵²



Scheme 1.9. Cyclooctane oxidation catalysed by RuNP in biphasic water/organic system.

As mentioned in section 1.2.4, Yves Chauvin introduced the imidazolium salts that are the most frequently used ILs in catalysis. This is a valuable medium for catalysis using MNP because the imidazolium cation is bulky, thus favouring the stabilization of MNP.⁵² ILs-stabilised MNP have been used in several catalytic reactions over the last years,⁶⁵ such as arene hydrogenation,⁶⁶ methoxycarbonylation,⁶⁷ hydrosilylation⁶⁸ and C-C- cross coupling reactions.⁶⁹

Dupont *et al.* tested preformed PdNP in the hydrogenation of butadiene towards 1-butene in [BMI][BF₄] (Scheme 1.10), taking advantage of the fact that the latter is four times more insoluble than butadiene, and by this way, the selectivity was better controlled in this reaction medium. Total conversion and selectivities up to 72% were achieved.⁷⁰



Scheme 1.10. PdNP catalysed hydrogenation of butadiene in IL.

Introduction

However, ligand-free PdNP dispersed in simple ILs are not stable and tend to agglomerate after hydrogenation of alkenes or dialkenes, while phenantroline-PdNP in [BMI][PF₆] have showed high activities and selectivities for the hydrogenation of olefins and can be reused several times without reducing the activity.⁷¹

1.4. References

- ¹ J. H. Clark. *Green Chem.* **2007**, 8, 17.
- ² a) P. T. Anastas and J. Warner. *Green chemistry : Theory and practice*, Oxford University Press, New York, **2000**. b) P. T. Anastas and M. M. Kirchhoff. *Acc. Chem. Res.* **2002**, 35, 686
- ³ R. A. Sheldon. *C. R. Acad. Sci. Paris, IIc, Chimie/Chemistry.* **2000**, 3, 541.
- ⁴ R. Sheldon. *Pure Appl. Chem.* **2000**, 72, 1233.
- ⁵ A. Moore in “*Green Catalysis*”. Ed. P. T. Anastas. Wiley-VCH, Weinheim, **2009**.
- ⁶ a) L. A. Oro and E. Sola (Eds). *Fundamentos y aplicaciones de la Catálisis Homogénea*, CYTED. 2^a Ed. Zaragoza, **2000**. b) P. W. N. M. van Leeuwen. *Homogeneous Catalysis. Understanding the Art*. Kluwer Academic Publishers. Amsterdam, **2004**.
- ⁷ R. H. Crabtree. *The Organometallic Chemistry of the Transition Metals*. 5th ed. New Jersey, **2009**.
- ⁸ G. Rothenberg. *Catalysis: Concepts and Green Applications*. Wiley-VCH, Weinheim, **2008**.
- ⁹ B. Cornils and W. A. Herrmann. *Applied Homogeneous Catalysis with Organometallic Compounds*. WILEY-VCH, Weinheim, **1996**.
- ¹⁰ a) J. Schwartz. *Acc. Chem. Res.* **1985**, 18, 302. b) M. Gómez and I. Favier in *Metal Nanoclusters in Catalysis and Materials Science: The Issue of Size Control*. Eds. B. Corain, G. Schmidt and N. Toshima. Elsevier Amsterdam, **2008**.
- ¹¹ R. Noyori. *Asymmetric Catalysis in Organic Synthesis*. John Wiley & Sons, New York, **1993**.
- ¹² Z. Wang, K. Ding and Y. Uozumi in *Handbook of Asymmetric Heterogeneous Catalysis*. Eds. K. Ding and Y. Uozumi. WILEY-VCH, Weinheim, **2008**.
- ¹³ a) C. Copperet, M. Chabanas, R. P. Saint-Arroman and J-M. Basset. *Angew. Chem. Int. Ed.* **2003**, 42, 156. b) J-M. Basset, C. Coperet, D. Saulivong, M. Taoufik and J. Thivolle-Cazat. *Angew. Chem. Int. Ed.* **2006**, 45, 6082.
- ¹⁴ a) *Multiphase Homogeneous Catalysis*, Eds. B. Cornils, W. A. Herrman, I. T. Horvath, W. Leitner, S. Mecking, H. Olivier-Bourbigou and D. Vogt. Wiley-VCH, Weinheim, **2005**. b) *Recovery and Recycling in Homogeneous Catalysis*, Eds. D. J. Cole-Hamilton and R.

- P. Tooze. Dordrecht, **2005**. c) M. Benaglia, A. Puglisi and F. Cozzi, *Chem. Rev.* **2003**, 103, 3401. d) F. Cozzi, *Adv. Synth. Catal.* **2006**, 348, 1367.
- ¹⁵ a) M. Lombardo and C. Trombini. *Eco-Friendly Synthesis of Fine Chemicals*. RSC Green Chemistry Book Series, London, **2009**. b) M. Poliakoff and P. License. *Nature*. **2007**, 450, 810.
- ¹⁶ a) C. M. Gordon and W. Leitner in *Catalyst separation, recovery and recycling* . Eds D. Cole-Hamilton and R. Tooze, Springer, Netherlands, **2006**, 215. b) W. Leitner. *Acc. Chem. Res.* **2002**, 35, 746.
- ¹⁷ a) C- J. Li. *Chem. Rev.* **2005**, 105, 3095. b) R. Poli. *Chem. Eur. J.* **2004**, 10, 332.
- ¹⁸ H. Olivier-Bourbigou, L. Magna and D. Morvan. *Appl. Cat. A: General*. **2010**, 373, 1.
- ¹⁹ L. P. Barthel-Rosa and J. A. Gladysz. *Coord. Chem. Rev.* **1999**, 190, 587.
- ²⁰ C. Präsang and E. Bauer in *Phosphorous ligands in Asymmetric Catalysis*. Vol 3. Ed. A. Börner. Wiley-VCH, Weinheim, **2008**.
- ²¹ a) E. Kuntz. *CHEMTECH*. **1987**, 570-575. b) C. W. Kohlpaintner, R. W. Fischer and B. Cornils. *Appl. Cat. A: General*. **2001**, 221, 219.
- ²² B. Cornils. *Org. Process Res- Devel.* **1998**, 2, 121.
- ²³ a) Y. Amrani, L. Lecompte, D. Sinou, J. Bakos, I. Toth and B. Heil. *Organometallics*. **1989**, 8, 542. b) M. D. Serrano, A. M. Masdeu-Bultó, C. Claver and D. Sinou. *J. Mol. Cat. A*. **1999**, 143, 49.
- ²⁴ a) I. T. Horvath and J. Rabai. *Science*. **1994**, 266, 72. b) I. T. Horvath. *Acc. Chem. Res.* **1998**, 31, 641.
- ²⁵ I. T. Horvath, G. Kiss, R.A. Cook, J. E. Bond, P. A. Stevens, J. Rabai and E. J. Mozeleski. *J. Am. Chem. Soc.* **1998**, 120, 3133.
- ²⁶ D. F. Foster, D. Gudmunsen, D. J. Adams, A. M. Stuart, E. G. Hope, D. J. Cole-Hamilton, G. P. Schwartz and P. Pogorzelec. *Tetrahedron*. **2002**, 58, 3901.
- ²⁷ D. J. Cole-Hamilton. *Science*. **2003**, 299, 1702.
- ²⁸ P. G. Jessop and W. Leitner (Eds.). *Chemical Synthesis Using Supercritical Fluids*. Wiley-VCH, Weinheim, 1999.

- ²⁹ a) T. Clifford. *Fundamentals of supercritical fluids*, Oxford University Press, Oxford, **1999**. b) S. K. Kumar, S. P. Chhabria, R.C. Reid and U. W. Suter. *Macromolecules*. **1987**, *20*, 2550.
- ³⁰ R. Sheldon, I. W. C. E. Arends and U. Hanefeld. *Green chemistry and catalysis*. Wiley-VCH. Weinheim, **2007**.
- ³¹ a) S Lange, A. Brinkmann, P. Trautner, K. Woelk, J. Bargon and W. Leitner. *Chirality*. **2000**, *12*, 450. b) G. Franciò and W. Leitner. *Chem. Commun.* **1999**, 1663. c) D. J. Adams, W. P. Chen, E. G. Hope, S. Lange, A. M. Stuart, A. West and J. L. Xiao. *Green Chem.* **2003**, *5*, 118.
- ³² M. J. Burk, S. Feng, M. F. Gross and W. Tumas. *J. Am. Chem. Soc.* **1995**, *117*, 8277.
- ³³ a) D. Koch and W. Leitner. *J. Am. Chem. Soc.* **1998**, *120*, 13398. b) C. Tortosa, A. Orejón and A. M. Masdeu-Bultó. *Green Chem.* **2008**, *10*, 545. c) C. Tortosa, M. Giménez, A. M. Masdeu-Bultó, A. D. Sayede and E. Monflier. *Eur. J. Inorg. Chem.* **2008**, *46*, 2659.
- ³⁴ a) G. Franciò and W. Leitner. *Chem. Commun.* **1999**, 1663. b) G. Franciò, K. Wittmann and W. Leitner. *J. Organomet. Chem.* **2001**, *621*, 130.
- ³⁵ P. Wasserscheid and T. Welton. *Ionic Liquids in Synthesis*. 2nd Ed. Wiley-VCH, Weinheim, **2008**.
- ³⁶ a) N. V. Plechkova and K. R. Seddon. *Chem. Soc. Rev.* **2008**, *37*, 123. b) P. Walden. *Bull. Acad. Imper. Sci. (St. Petersburg)*. **1914**, 1800.
- ³⁷ M. J. Earle, J. M. S. S. Esperança, M. A. Gilea, J. N. Canongia Lopes, L. P. N. Rebelo, J. W. Magee, K. R. Seddon and J. A. Widgren. *Nature*. **2006**, *439*, 831.
- ³⁸ J. Baker. *Eur. Chem. News*. **2004**, 18.
- ³⁹ D. Zhao, Y. Liao and Z. Zhang. *Clean: Soil. Air, Water*. **2007**, *35*, 42-48. D. Coleman and N. Gathergood. *Chem. Soc. Rev.* **2010**, *39*, 600.
- ⁴⁰ P. Dyson and T. J. Geldbach. *Metal catalyzed reactions in ionic liquids*. Springer, Dordrecht, **2005**.
- ⁴¹ Y. Chauvin, L. O. Mussmann and H. Olivier. *Angew. Chem. Int. Ed. Engl.* **1995**, *34*, 2698.

Introduction

⁴² For some selected reviews, see: a) J. Dupont, R. F. de Souza and P. A. Z. Suarez.

Chem. Rev. **2002**, 102, 3667. b) J. Dupont, G. S. Fonseca, A. P. Umpierre, P. F. P. Fitchner and S. R. Teioxera. *J. Am. Chem. Soc.* **2002**, 124, 4228. c) V. I. Pârvulescu and C. Hardcare. *Chem. Rev.* **2007**, 107, 2615-2665. d) S. V. Malhotra, V. Kumat and V. S. Parmar. *Curr. Org. Chem.* **2007**, 4, 370. e) T. Welton. *Coord. Chem. Rev.* **2004**, 248, 1015.

⁴³ a) P. S. Schulz in *Phosphorous ligands in Asymmetric Catalysis*. Vol 3. Ed. A. Börner. Wiley-VCH, Weinheim, **2008**. b) J. Durand, E. Teuma and M. Gómez. *C. R. Chimie*. **2007**, 10, 152.

⁴⁴ a) G. Schmidt (Ed.). *Nanoparticles From Theory to Application*. Wiley-VCH, Weinheim, **2010**. b) G. Schmidt (Ed.). *Clusters and Colloids: From Theory to Applications*. VCH Publishers, New York, **1994**. c) L. J. de Jongh (Ed.), *Physics and Chemistry of Metal Nanocluster Compounds*. Kluwer Publishers, Dordrecht, **1994**.

⁴⁵ J. D. Aiken III and Richard G. Finke. *J. Mol. Catal. A: Chem.* **1999**, 145, 1 and references therein.

⁴⁶ R. Pool. *Science*. **1990**, 248, 1186.

⁴⁷ I. Willner and D. Mandler. *J. Am. Chem. Soc.* **1989**, 111, 1330.

⁴⁸ M. E. Labib. *Colloids Surf.* **1988**, 29, 293.

⁴⁹ a) B. Chaudret. *Top. Organomet. Chem.* **2005**, 16, 233. b) K. Philippot and B. Chaudret. *C. R. Chimie*. **2003**, 6, 1019.

⁵⁰ C. Pan, K. Pelzer, K. Philippot, B. Chaudret, F. Dassenoy, P. Lecante and M. -J. Casanove. *J. Am. Chem. Soc.* **2001**, 123, 7584.

⁵¹ a) L. Ratke and P. W. Voorhees. *Growth and Coarsening. Ripening in Material Processing*. Springer-Verlag. Berlin, **2002**. b) M. Bowker. *Nature Materials*. **2002**, 1, 205. c) C. T. Campbell, S. C. Parker and D. E. Starr. *Science*. **2002**, 298, 811.

⁵² a) D. Astruc (Ed.). *Nanoparticles and Catalysis*, Wiley-VCH Verlag GmbH & Co. KGaA, Weinheim, **2008**. b) A. Roucoux, J. Schulz and H. Patin. *Chem. Rev.* **2002**, 102, 3757.

⁵³ D. A. Tomalia, A. M. Naylor and A. Goddard III. *Angew. Chem. Int. Ed. Engl.* **1990**, 29, 138.

⁵⁴ D. H. Napper in *Polymeric Stabilization of Colloidal Dispersions*, Academic Press. London, **1983**.

- ⁵⁵ a) J. D. Aiken III, Y. Lin and R. G. Finke. *J. Mol. Catal. A: Chem.* **1996**, 114, 29-51. b) Y. Lin and R. G. Finke. *J. Am. Chem. Soc.* **1994**, 116, 8335.
- ⁵⁶ a) M. A. El-Sayed. *Acc. Chem. Res.* **2001**, 34, 257. b) H. Bönnemann and R. M. Richards. *Eur. J. Inorg. Chem.* **2001**, 2455. c) J. A. Widegren and R. G. Finke. *J. Mol. Catal. A: Chem.* **2003**, 191, 187. d) J. D. Aiken and R. G. Finke. *J. Am. Chem. Soc.* **1999**, 121, 8803. e) M. Boutonnet, J. Kizling, P. Stenius and G. Maire. *Colloids Surf.* **1982**, 5, 209. f) M. Boutonnet, J. Kizling, R. Tourode, G. Maire and J. Stenius. *Appl. Catal.* **1986**, 20, 163. g) G. Schmidt, H. West, H. Mehles and A. Lehnert. *Inorg. Chem.* **1997**, 36, 891. h) A. M. Caporusso, L. A. Aronica, E. Schiavi, G. Martra, G. Vitulli and P. Salvadori. *J. Organomet. Chem.* **2005**, 690, 1063. i) F. Bertoux, E. Monflier, Y. Castanet, and A. Mortreux. *J. Mol. Catal. A: Chem.* **1999**, 143, 23. j) R. Grigg, L. -X, Zhang, S. Collard and A. Keep. *Tetrahedron Lett.* **2003**, 44, 6979. k) J. Penzien, C. Haessner, A. Jentys, K. Köhler, T. E. Muller and J. A. Lercher. *J. Catal.* **2004**, 221, 302.
- ⁵⁷ a) Y. Shiraisi and N. Toshima. *J. Mol. Catal. A: Chem.* **1999**, 141, 187.
- ⁵⁸ For recent reviews see: a) S. Roy and M. A. Pericàs. *Org. Biomol. Chem.* **2009**, 7, 2669. b) I. Favier, D. Madec, E. Teuma and M. Gómez. *Curr. Org. Chem.* **2010**, accepted.
- ⁵⁹ a) K. Nasar, F. Fache, M. Lemaire, M. Draye, J. C. Béziat, M. Besson and P. Galez. *J. Mol. Catal. A: Chem.* **1994**, 87, 107. b) J. U. Kohler and J. S. Bradley. *Langmuir*. **1998**, 14, 2730. c) H. Bönnemann and G. A. Braun. *Angew. Chem. Int Ed.* **1996**, 35, 1992. d) M. Studer, H. U. Blaser and C. Exner. *Adv. Synth. Catal.* **2003**, 345, 45.
- ⁶⁰ M. Tamura and H. Fujihara. *J. Am. Chem. Soc.* **2003**, 125, 15742.
- ⁶¹ K. Sawai, R. Tatumi. Nakahodo and H. Fujihara. *Angew. Chem. Int. Ed.* **2008**, 47, 6917.
- ⁶² S. Jansat, M. Gómez, K. Philippot, G. Muller, E. Guiu, C. Claver, S. Castillón, B. Chaudret. *J. Am. Chem. Soc.* **2004**, 126, 1592.
- ⁶³ a) H. Ohde, C. M. Wai, H. Kim and M. Ohde, *J. Am. Chem. Soc.* **2002**, 124, 4540. b) P. Meric, K. M. K. Yu and S. C. Tsang. *Catal. Lett.* **2004**, 95, 39. c) P. Meric, K. M. J. Yu and S. C. Tsang. *Langmuir*. **2004**, 20, 8537. d) K. M. K. Yu, C. M. Y. Yeung, D. Thompsett and S. C. Tsang. *J. Phys. Chem. B.* **2003**, 107, 4515.

Introduction

- ⁶⁴ a) X. R. Ye, Y-H. Lin and C. M. Wai. *Chem. Commun.* **2003**, 642. b) A. M. Doyle, S. K. Shaikhutdinov, S. D. David Jackson and H. –J. Freund. *Angew. Chem. Int. Ed.* **2003**, 42, 5240.
- ⁶⁵ P. Migowski and J. Dupont. *Chem. Eur. J.* **2007**, 13, 32.
- ⁶⁶ a) C. W. Scheeren, G. Machado, J. Dupont, P. F. P. Fichtner and S. R. Teixeira. *Inorg. Chem.* **2003**, 42, 4738. b) E. T. Silveira, A. P. Umpierre, L. M. Rossi, G. Machado, J. Morais, G. V. Soares, I. L. R. Baumvol, S. R. Teixeira, P. F. P. Fichtner and J. Dupont. *Chem. Eur. J.* **2004**, 10, 3734. c) G. S. Fonseca, A. P. Umpierre, P. F. P. Fichtner, S. R. Teixeira and J. Dupont. *Chem. Eur. J.* **2003**, 9, 3263. d) L. M. Rossi, J. Dupont, G. Machado, P. F. P. Fichtner, C. Radtke, I. J. R. Baumvol and S. R. Teixeira. *J. Braz. Chem. Soc.* **2004**, 15, 904. e) X. D. Mu, J. O. Meng, Z. C. Li and Y. Kou. *J. Am. Chem. Soc.* **2005**, 127, 9694.
- ⁶⁷ W. Wojtkow, A. M. Trzeciak, R. Choukroun and J. L. Pellegatta. *J. Mol. Catal. A: Chem.* **2004**, 224, 81.
- ⁶⁸ T. J. Geldbach, D. B. Zhao, N. C. Castillo, G. Laurenczy, B. Meyer, B. Weyershausen and P. J. Dyson. *J. Am. Chem. Soc.* **2006**, 128, 9773.
- ⁶⁹ M. H. G. Prechtl, J. D. Scholten and J. Dupont. *Molecules*. **2010**, 15, 3441.
- ⁷⁰ A. P. Umpierre, G. Machado, G. H. Fecher, J. Morris and J. Dupont. *Adv. Synth. Catal.* **2005**, 347, 1404.
- ⁷¹ J. Huang, T. Jiang, B. X. Han, H. X. Gao, Y. H. Chang, G. Y. Zhao and W. Z. Wu. *Chem. Commun.* **2003**, 1654.

Chapter 2

Objectives

UNIVERSITAT ROVIRA I VIRGILI
ORGANOMETALLIC COMPOUNDS AND METAL NANOPARTICLES AS CATALYSTS IN LOW ENVIRONMENTAL IMPACT SOLVENTS
Martha Verónica Escárcega Bobadilla
ISBN:978-84-694-1249-7/DL:T-324-2011

The objective of this Thesis is to study the catalytic behaviour of different organometallic molecular catalysts and metallic nanocatalytic systems in low environmental impact solvents, such as supercritical carbon dioxide (scCO_2) and ionic liquids (ILs). For this purpose, three different catalytic systems have been selected: Rh and Ru nanoparticles, Pd molecular systems and Rh complexes. These systems were chosen to be applied in arene hydrogenation (scCO_2), C-C bond formation reactions (ILs) and asymmetric hydrogenation (scCO_2 , ILs and scCO_2 /IL mixture) processes, respectively.

Therefore, one of the chapters (**Chapter 3**) deals with the synthesis and characterisation of new Rh and Ru nanoparticles stabilised by mono-phosphines and their use as catalysts for the arene hydrogenation reaction in organic solvent as well as in scCO_2 .

The aim of **Chapter 4** concerns the synthesis and characterisation of new azaphosphabicyclo[3,3,0]octane ligands, which were conformationally studied and applied in Pd-catalysed Suzuki C-C cross-coupling reactions in ILs between different aryl halides and boronic acids as well as in the asymmetric allylic alkylation reaction.

Chapter 5 focuses on the synthesis and characterisation of novel BINOL-derived P-donor ligands and their application in the Rh-catalysed asymmetric hydrogenation reaction of functionalised olefins in non-conventional solvents such as scCO_2 and ILs. Immobilization of the catalyst-IL phase over/inside functionalised multi-walled carbon nanotubes (MWCNTs) was also studied to improve the catalyst recycling.

UNIVERSITAT ROVIRA I VIRGILI
ORGANOMETALLIC COMPOUNDS AND METAL NANOPARTICLES AS CATALYSTS IN LOW ENVIRONMENTAL IMPACT SOLVENTS
Martha Verónica Escárcega Bobadilla
ISBN:978-84-694-1249-7/DL:T-324-2011

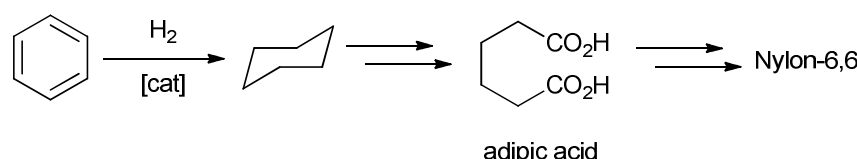
Chapter 3

Rh and Ru
Nanoparticles in
Catalytic Arene
Hydrogenation in
Supercritical
Carbon Dioxide

UNIVERSITAT ROVIRA I VIRGILI
ORGANOMETALLIC COMPOUNDS AND METAL NANOPARTICLES AS CATALYSTS IN LOW ENVIRONMENTAL IMPACT SOLVENTS
Martha Verónica Escárcega Bobadilla
ISBN:978-84-694-1249-7/DL:T-324-2011

3.1. Introduction

The recent developments in the field of metallic nanoparticles (MNP) have demonstrated that they are excellent catalytic materials for the hydrogenation of alkenes and arenes under mild conditions.¹ Selective hydrogenation is an efficient and widely applied synthetic procedure for industrial processes and syntheses of fine chemicals.² Hydrogenation of arenes to produce cyclohexanes is an important reaction, especially the hydrogenation of benzene, which is used for the industrial production of adipic acid, a precursor for the nylon manufacture Scheme 3.1.³ This process is performed using heterogeneous catalysts, usually under harsh conditions.



Scheme 3.1. Catalytic hydrogenation of benzene for Nylon-6,6 production.

Concerning nanocatalysts, hydrogenation reactions are mostly performed in organic solvents.⁴ As discussed in Chapter 1, from an environmental point of view, advices to reduce the use of volatile organic compounds in all kind of processes are strongly encouraged.⁵ One alternative for catalysed reactions is the use of supercritical carbon dioxide (scCO₂), considered as a green solvent.⁶ Its low polarity and variable density with pressure and temperature make it an appropriate medium for reactions involving a wide variety of organic reagents. In addition, scCO₂ shows a high miscibility with gases, rendering it particularly suitable for hydrogenation reactions,⁷ since hydrogen has limited solubility in organic solvents.⁸ Furthermore, scCO₂ can easily gain access to the active centres in metal nanoparticles, due to its low viscosity and high diffusivity.⁹

In the last years, the preparation of metal nanoparticles in supercritical fluids (SCF) has significantly increased.¹⁰ Stabilisers such as dendritic polymers functionalized with perfluoroalkyl, perfluorooligoether, polysiloxane, non-fluorinated alkyl and oligoethylene glycol moieties have been used to prepare palladium and silver

RuNP and RhNP in catalytic arene hydrogenation in scCO₂

nanoparticles.^{10d} Silver nanocrystals ranging from 2 to 10 nm were prepared in scCO₂ using perfluorinated thiols as stabilisers.¹¹ In many examples, the nanoparticles were found stabilised by water-in-scCO₂ microemulsions.¹²

MNP-catalysed hydrogenation processes in supercritical fluids, especially in scCO₂, are scarce.¹³ Rh, Pd and Ru nanoparticles stabilised by surfactants in water/SCF mixtures¹⁴ or in water-in-scCO₂ microemulsions are frequently used.^{12a,15} However, the aqueous surfactant solutions present important drawbacks, mainly the low solubility of organic substrates, besides the difficulty to control the pH under these conditions. A further original approach to prepare MNP in scCO₂ has been described taking advantage of the swelling of the plastics in scCO₂, which act as stabilisers of Rh and Pd nanoparticles applied in hydrogenation catalytic reactions.¹⁶

In relation to the stabilisers used for the synthesis of MNP, a great variety of compounds (surfactants, polymers, macromolecules, dendrons and ligands) has been employed.¹⁷ In particular, molecular ligands become attractive as MNP stabilisers to be applied in catalysis, due to their coordination to the metallic surface allowing selectivity induction in the catalytic reaction, analogously to the behaviour of classical homogeneous catalysts. While P-donor ligands have been extensively used in hydrogenation processes catalysed by organometallic complexes, few reports are related to their catalytic applications concerning MNP. Therefore, Fujihara and co-workers reported BINAP-stabilised palladium nanoparticles (BINAP = 2,2-bis(diphenylphosphino)-1,10-binaphthyl), which led to high enantiomeric excess (*ee*) in the asymmetric hydrosilylation of styrene under mild conditions (*ee* up to 95%), inducing a high kinetic resolution for the starting racemic substrate.¹⁸ Also chiral xylofuranide diphosphites used to prepare PdNP have been highly enantioselective in the allylic alkylation reactions (up to 97% of *ee*).¹⁹

As mentioned in Chapter 1, the most studied reaction using MNP is the arene hydrogenation, which has an important industrial impact, being rhodium and ruthenium MNP the most employed catalysts. Concerning conventional solvents, Finke *et al.* have studied the real nature of the catalysts employed in this reaction and have developed systems under mild reaction conditions (22 °C, 3.7 H₂ atm) for anisole

hydrogenation.^{1d,20} Roucoux *et al.* have been developed catalytic systems for this kind of transformations by using Rh²¹ and Ir²² NP in water, with the advantage that these systems could be recycled. In relation to ionic liquids as reaction medium, Dupont *et al* have extensively studied these transformations using Ru,^{23a,b} Rh^{23c} and Ir^{23c} NP.

In this part of the Thesis, the preparation of new rhodium and ruthenium nanoparticles stabilized by phosphines containing fluorinated groups is described (ligands **1** and **2** in Figure 3.1), with the aim to increase the affinity of MNP to scCO₂. For comparative purposes, triphenylphosphine was also used as stabilizer. The catalytic behaviour of these new materials in the hydrogenation of different arenes in scCO₂ has been evaluated. THF has been also used for comparative purposes.

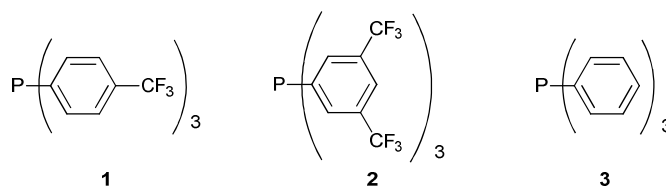


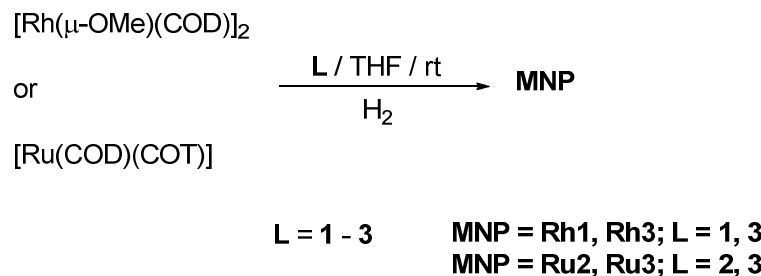
Figure 3.1. P-donor ligands (**1-3**) used to stabilize **RhL** and **RuL** nanoparticles.

3.2. Results and Discussion

3.2.1. Synthesis of rhodium and ruthenium nanoparticles

Metallic nanoparticles were prepared by decomposition of organometallic precursors under reductive atmosphere following the general methodology described in section 1.3.1.1 of this Thesis.²⁴ Therefore, [Rh(μ-OMe)(COD)]₂ or [Ru(COD)(COT)] (COD = 1,5-cyclooctadiene; COT = cyclooctatriene) dissolved in THF in the presence of the corresponding phosphine (**1-3**, Figure 3.1) was pressurized under hydrogen (3 bar) at room temperature (Scheme 3.2). MNP were precipitated with pentane giving black solids in moderate yields for RhNP (44 to 57 %) and good yields for RuNP (54 to 74%).

RuNP and RhNP in catalytic arene hydrogenation in scCO₂



Scheme 3.2. Synthesis of Rh and Ru nanoparticles stabilized by ligands **1 – 3**.

Triphenylphosphine acted as a good stabilizer for both metals (**Rh3** and **Ru3**), while the fluorinated phosphines **1** and **2** behaved differently depending on the metal nature, leading to the formation of rhodium **Rh1** (but not **Rh2**) and ruthenium **Ru2** (but not **Ru1**) nanoparticles. This behaviour could be related to the relative size of the nanoclusters (rhodium nanoparticles bigger than ruthenium ones, see Table 3.1). For small nanoparticles, the relative number of sites showing low coordination numbers (mainly vertexes and edges) is more important than that placed on faces (higher coordination number). Thus, the relative ratio of coordination sites (placed on vertexes, edges or faces), showing a preference for the less-sterically demanding ligand (**1**) when bigger rhodium particles are involved, even though its lower Lewis basicity compared with ligand **2**. It is important to note that RuNP were isolated starting from relative high metal concentration (10^{-3} mol L⁻¹) (Figure 3.3). However RhNP were obtained working at more diluted conditions ($[\text{Rh}] \leq 10^{-4}$ mol L⁻¹) (Figure 3.5), otherwise agglomerates were only observed.

Concerning the metal/ligand ratio (M/L), only the ratio M/L = 1/0.2 led to small and dispersed NP; for ratios M/L higher than 1/0.2 (up to 1/1), agglomerates were exclusively observed (Figure 3.2).

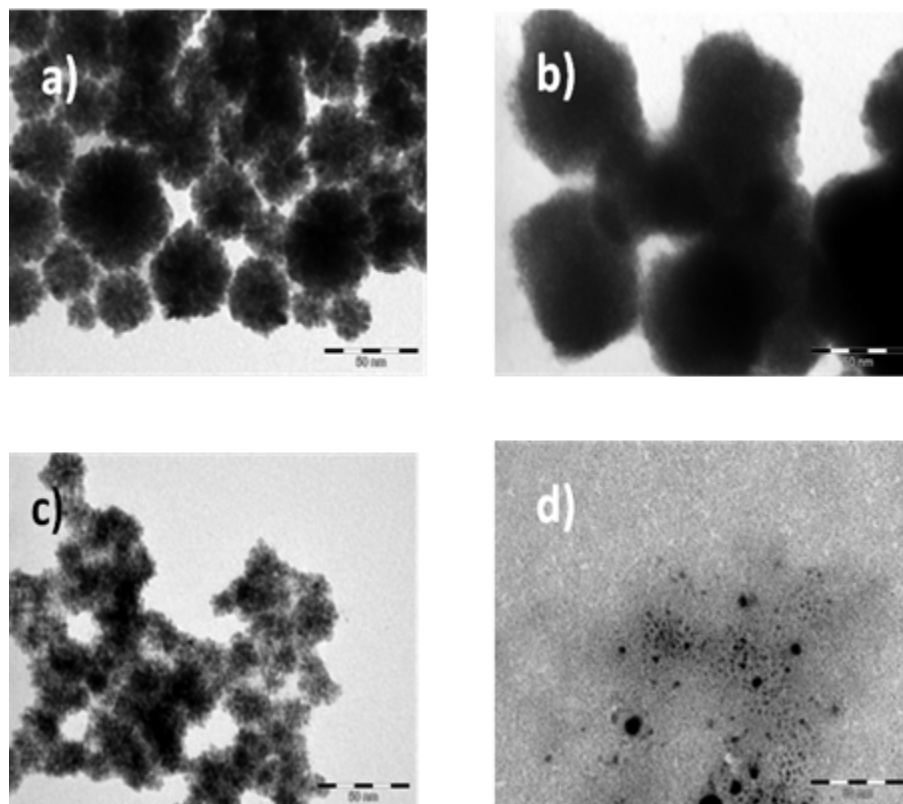


Figure 3.2. Metal nanoparticles synthesised at different M/L ratios; $[Ru] = 10^{-3}$ M, $[Rh] = 10^{-4}$ M. RhNP: a) $Rh/\mathbf{1} = 1/0.5$, b) $Rh/\mathbf{1} = 1/1$. RuNP: c) $Ru/\mathbf{2} = 1/0.5$, d) $Ru/\mathbf{2} = 1/1$.

Metal nanoparticles were analyzed by Transmission Electronic Microscopy (TEM) (Figures 3.3 and 3.5). The micrographs corresponding to RuNP, **Ru2** and **Ru3** (Figure 3.3), showed the formation of small nanoparticles (*ca.* mean diameter of 1.3 nm), reasonably homogenous in size and well dispersed on the grid.

The powder XRD analysis of **Ru2** showed the hexagonal cubic packing of the metallic core, analogously to that observed for the bulk metal (Figure 3.4).

In contrast, rhodium nanoparticles were bigger, exhibiting a tendency to agglomerate. In addition, the ligand nature induced significant size differences (Figure 3.5), being smaller (*ca.* 1.7 nm) and less dispersed in size with triphenylphosphine as a stabilizer than when fluorinated phosphine **1** was used (*ca.* 2.5 nm).

RuNP and RhNP in catalytic arene hydrogenation in scCO₂

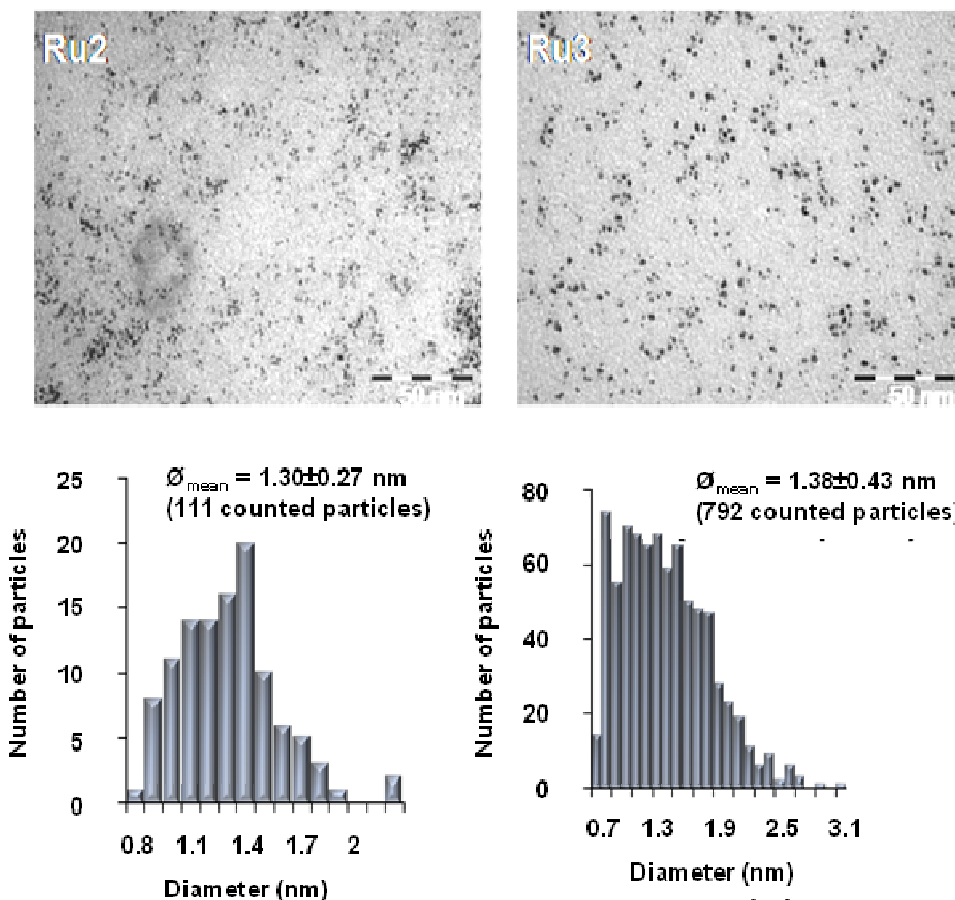


Figure 3.3. TEM micrographs of **Ru2** (left) and **Ru3** (right) with the corresponding size distribution diagram.

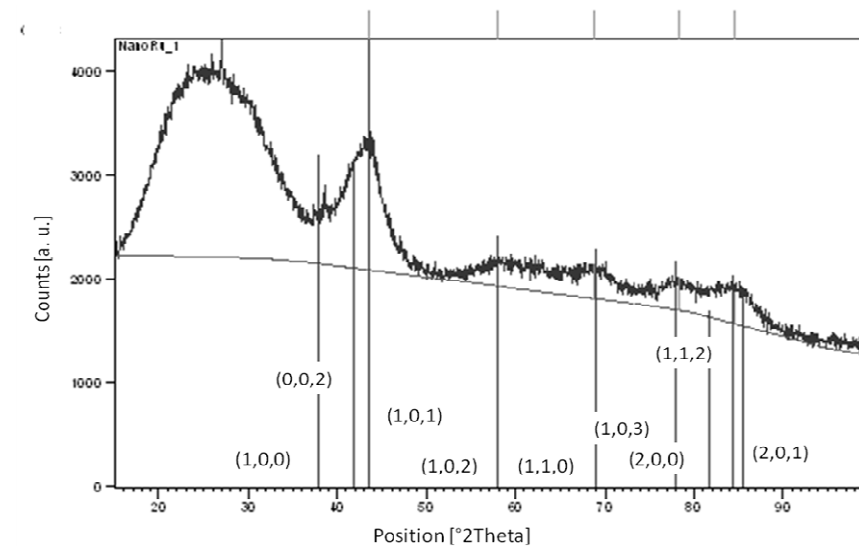


Figure 3.4. Powder XRD analysis of **Ru2**. The crystallographic planes for Ru showing hcp arrangement are shown. The large peak at ca. 25° is due to amorphous material (glass capillary).

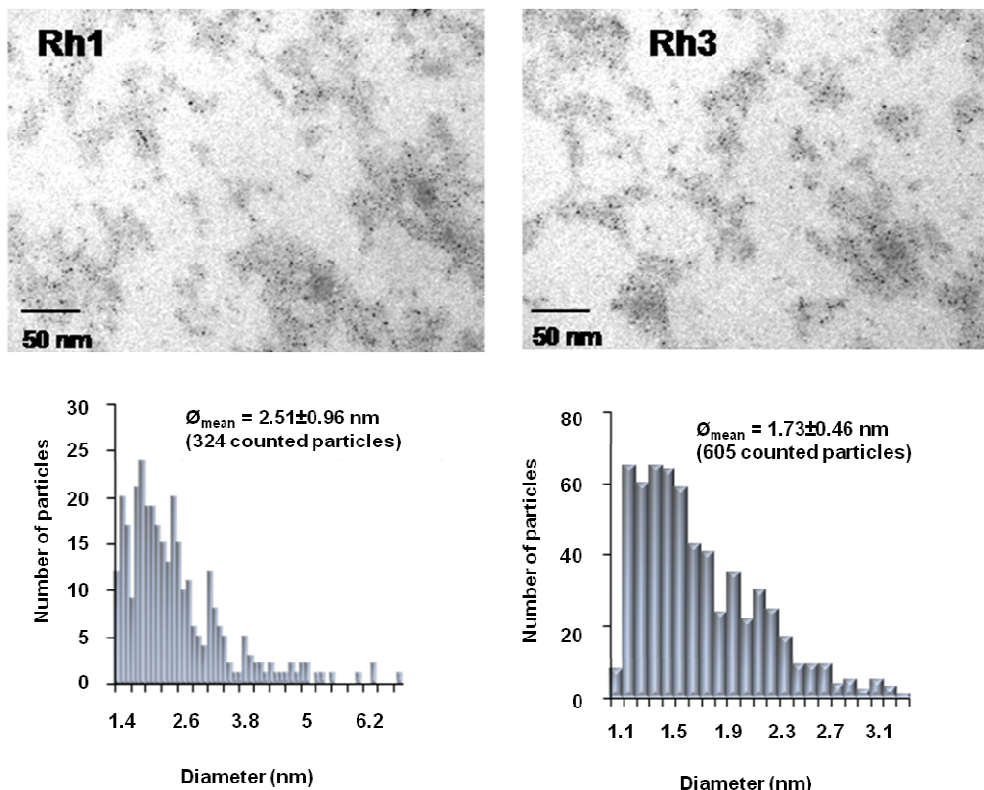


Figure 3.5. TEM micrographs of **Rh1** (left) and **Rh3** (right) with the corresponding size distribution diagram.

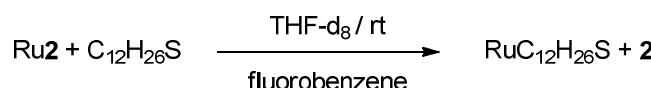
Raman spectra for RuNP allowed the $\text{Ru}^0\text{-P}$ stretching assignment (see Table 3.1), giving for **Ru1** 423 cm^{-1} and for **Ru3** 500 cm^{-1} . Infrared spectra of these materials analyzed as KBr pellets (recorded range: $4000\text{--}400 \text{ cm}^{-1}$), evidenced the presence of phosphine ligands and the absence of their oxide partners (no absorption bands at *ca.* 1300 cm^{-1} were observed in any case). The high energy shift observed for the C-P stretching absorption band for MNP (in the range of $798\text{--}804 \text{ cm}^{-1}$) compared to that corresponding to the free ligands ($701\text{--}745 \text{ cm}^{-1}$), points to a M(0)-P back-donation, strengthening C-P bond. This electronic density increase on the phosphine also induces an effect on the C-F stretching of the trifluoromethyl groups; actually, C-F bond is reinforced when placed at *para* position in relation to the phosphorous atom (**Rh1**: 1261 cm^{-1} *versus* 1164 cm^{-1}) and is weakened when placed at *meta* position (**Ru2**: 1063 cm^{-1} *versus* 1131 cm^{-1}).

Table 3.1. Characterization of MNP.

MNP	<i>d</i> (nm) ^a	IR data (cm ⁻¹) ^b	Calculated formula ^c
Rh1	2.51±0.96 (Rh ₅₉₅)	802(C–P st, w), 1261 (C–F st, w), [701 (C–P st, w), 1164 (C–F st, w)] ^d	Rh ₅ (1)(THF) ₁₅ (Rh ₅₉₅ (1) ₁₁₉ (THF) ₁₇₈₅)
Rh3	1.73±0.46 (Rh ₁₉₅)	802 (C–P st, w), [745 (C–P st, w)] ^d	Rh ₅ (3)(THF) ₃₀ (Rh ₁₉₅ (3) ₃₉ (THF) ₁₁₇₀)
Ru2	1.30±0.27 (Ru ₈₅)	798 (C–P st, w), 1063 (C–F st, w), [704 (C–P st, w), 1131 (C–F st, w)] ^d , 423 (Ru–P) ^e	Ru ₅ (2)(THF) ₂₀ (Ru ₈₅ (2) ₁₇ (THF) ₃₄₀)
Ru3	1.38±0.43 (Ru ₁₀₁)	804 (C–P st, w), [745 (C–P st, w)] ^d , 500 (Ru–P) ^e	Ru ₅ (3)(THF) ₃₀ (Ru ₁₀₁ (3) ₂₀ (THF) ₆₀₆)

^a Determined by TEM. In brackets, the estimated metallic composition considering a compact packing arrangement of spherical nanoparticles (hcp for Ru and fcc for Rh clusters). ^b Data in the range of 4000 – 400 cm⁻¹; samples prepared as KBr pellets; in brackets, the attribution and relative intensity of the bands. ^c From elemental analysis. In brackets, the proposed formula on the basis of the metallic nanocluster composition. ^d In square brackets, IR data for the corresponding free ligand. ^e Frequencies observed by Raman spectroscopy (range recorded: 4000-200cm⁻¹)

In order to check the stability of the ligand under the reductive synthetic conditions, we carried out an exchange ligand reaction between **Ru2** nanoparticles and dodecanethiol using fluorobenzene as an internal standard (Scheme 3.3).



Scheme 3.3. Ligand exchange reaction of **Ru2** with dodecanethiol.

The reaction was monitored by ¹⁹F (Figure 3.6) and ³¹P NMR. After 22 days, the phosphine displacement was estimated in 56%, without any sign of phosphine hydrogenation.

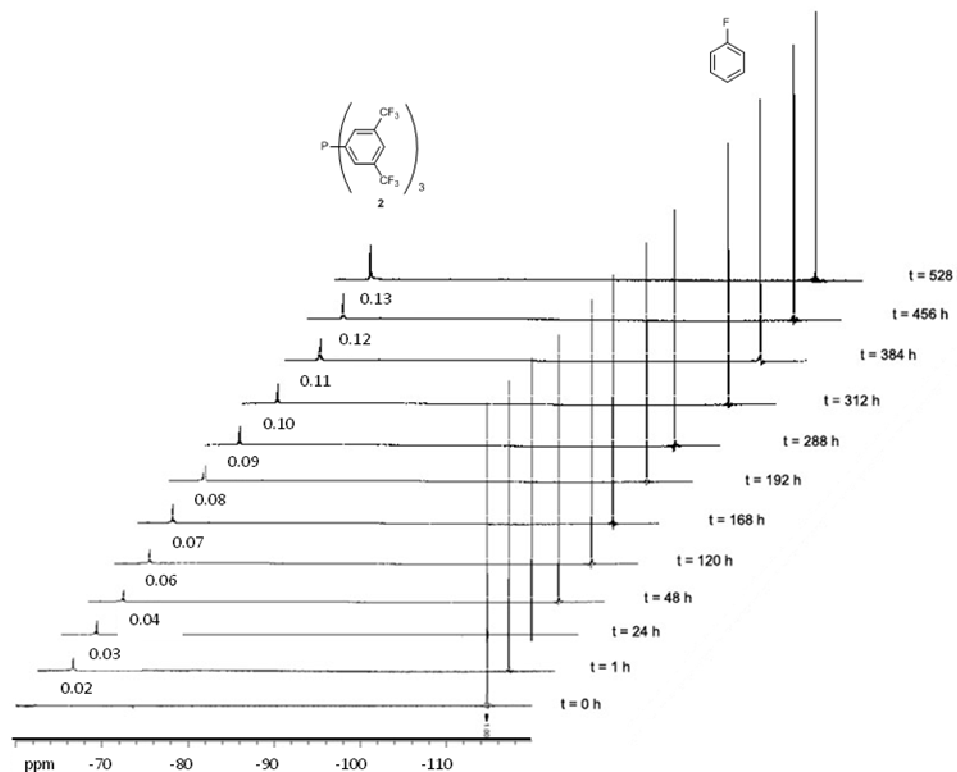
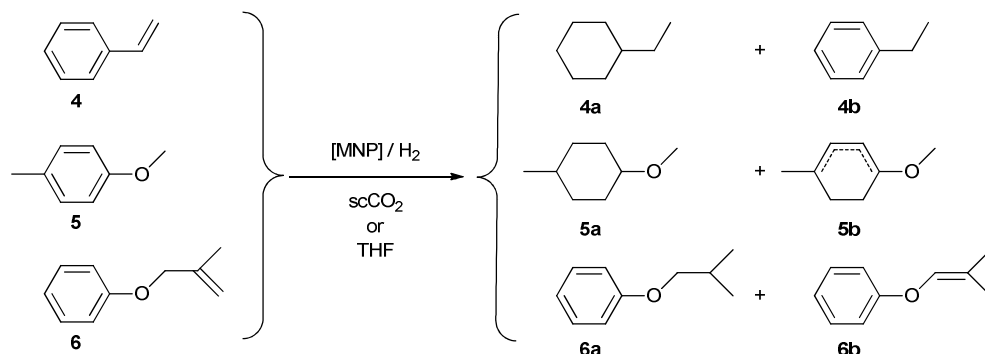


Figure 3.6. ^{19}F NMR monitoring (THF-d_8 , 298 K, 376.1 MHz) corresponding to the exchange reaction of **Ru2** nanoparticles with dodecanethiol (fluorobenzene as internal standard).

3.2.2. Catalytic reactivity of rhodium and ruthenium nanoparticles

Preformed MNP (**Rh1**, **Rh3**, **Ru2** and **Ru3**) were used as catalytic precursors for the hydrogenation reaction of styrene (**4**), *p*-methylanisole (**5**) and 2-methylprop-2-enoxybenzene (**6**) in THF and in scCO₂ (Scheme 3.4).



Scheme 3.4. Ruthenium- and rhodium- catalysed hydrogenation reactions.

RuNP and RhNP in catalytic arene hydrogenation in scCO₂

The rhodium systems were able to hydrogenate the substrate **4**, leading to a total styrene conversion in both solvents (entries 1–4, Table 3.2). In THF the product corresponds to the full hydrogenated compound (**4a**), while in scCO₂ medium, the major product corresponds to ethylbenzene (**4b**) (entries 1 and 3 *versus* 2 and 4, respectively, Table 3.2). On the contrary, **Rh1** and **Rh3** were inactive for the *p*-methylanisole hydrogenation in both solvents (entries 5–8, Table 3.2), being **Rh1** somewhat active in scCO₂ (entry 6, Table 3.2), favouring the fully hydrogenated product (**5a**).

Table 3.2. Metal catalysed hydrogenation of substrates **4** and **5** using preformed MNP (**Rh1** and **Rh3**) as catalytic precursors.^a

Entry	Catalytic precursor	Substrate	Solvent	%Conv ^b	Selectivity a:b ^c
1	Rh1	4	THF	100	100:0
2	Rh1	4	scCO ₂	100	40:60
3	Rh3	4	THF	100	99:1
4	Rh3	4	scCO ₂	100	30:70
5	Rh1	5	THF	0	-
6	Rh1	5	scCO ₂	21	85:15
7	Rh3	5	THF	4	nd
8	Rh3	5	scCO ₂	0	-

^a Catalytic conditions: T = 50 °C; t = 24h; M_{total}:S = 1:500; [M] = 4.5×10⁻⁴ M; gas pressure: in THF, P_{H₂} = 20 bar; in scCO₂, P_{H₂} = 20 bar, P_{total} = 200 bar. Results from duplicate experiments. ^b Determined by GC.

^c Determined by GC-MS.

Better activities were obtained for substrates **4** and **5** in both solvents using Ru nanocatalysts (entries 1–8, Table 3.3), than those observed for Rh ones, favouring in all the cases the formation of the fully hydrogenated product. It is important to note that **Ru2** and **Ru3** were less active for *p*-methylanisole than for styrene (entries 1–4 *versus* 5–8, Table 3.3), trend also observed for rhodium based catalysts.

Table 3.3. Metal catalysed hydrogenation of substrates **4** - **6** using preformed MNP (**Ru2** and **Ru3**) as catalytic precursors.^a

Entry	Catalytic precursor	Substrate	Solvent	%Conv ^b	Selectivity a:b ^c
1	Ru2	4	THF	100	100:0
2	Ru2	4	scCO ₂	100	100:0
3	Ru3	4	THF	100	78:22
4	Ru3	4	scCO ₂	100	100:0
5	Ru2	5	THF	100	100:0
6	Ru2	5	scCO ₂	52	91:9
7	Ru3	5	THF	73	98:2
8	Ru3	5	scCO ₂	24	94:6
9	Ru2	6	THF	44	90:10
10	Ru2	6	scCO ₂	18	92:8
11	Ru3	6	THF	41	96:4
12	Ru3	6	scCO ₂	23	63:37
13	Ru/C^d	4	THF	100	0:100
14	Ru/C^d	5	THF	10	80:20
15	Ru/C^d	6	THF	96	90:10

^a Catalytic conditions: T = 50 °C; t = 24h; M_{total}:S = 1:500; [M] = 4.5x10⁻⁴ M; gas pressure: in THF, P_{H2} = 20 bar; in scCO₂, P_{H2} = 20 bar, P_{total} = 200 bar. Results from duplicate experiments. ^b Determined by GC.

^c Determined by GC-MS. ^d Commercial Ru catalyst (Ru, 5%) on activated carbon.

TEM micrographs after styrene hydrogenation in scCO₂ showed that Ru nanoparticles remained well dispersed, in contrast to those reactions carried out in THF (Figure 3.7). However, using rhodium nanoparticles, agglomeration was observed in both solvents. This fact can be related to the lower activity of these systems in relation to those based on ruthenium due to the relative smaller metallic surface (Figure 3.8).⁴

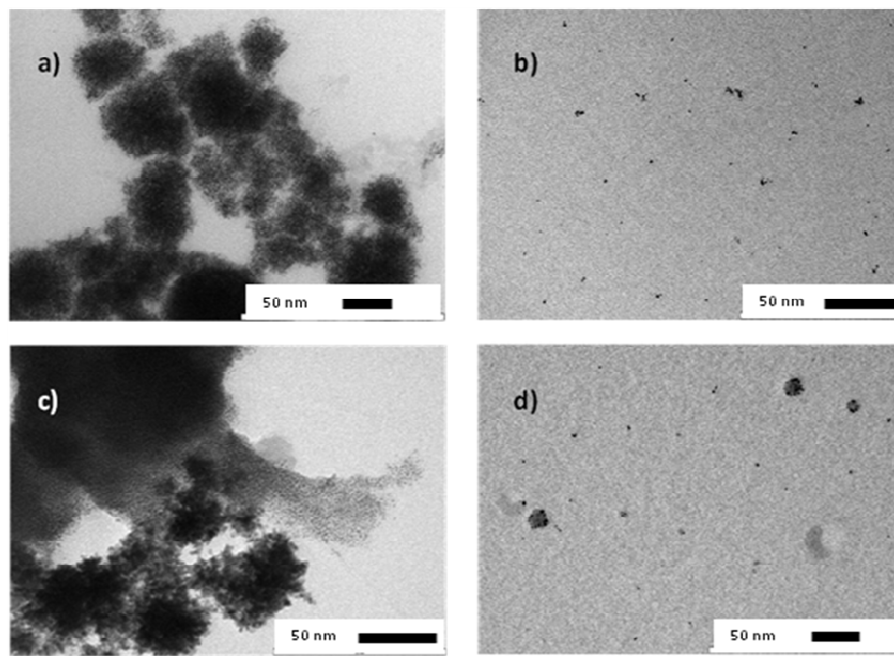


Figure 3.7. TEM micrographs of RuNP after styrene hydrogenation. Top: **Ru2** in a) THF and b) scCO₂. Bottom: **Ru3** in c) THF and d) scCO₂.

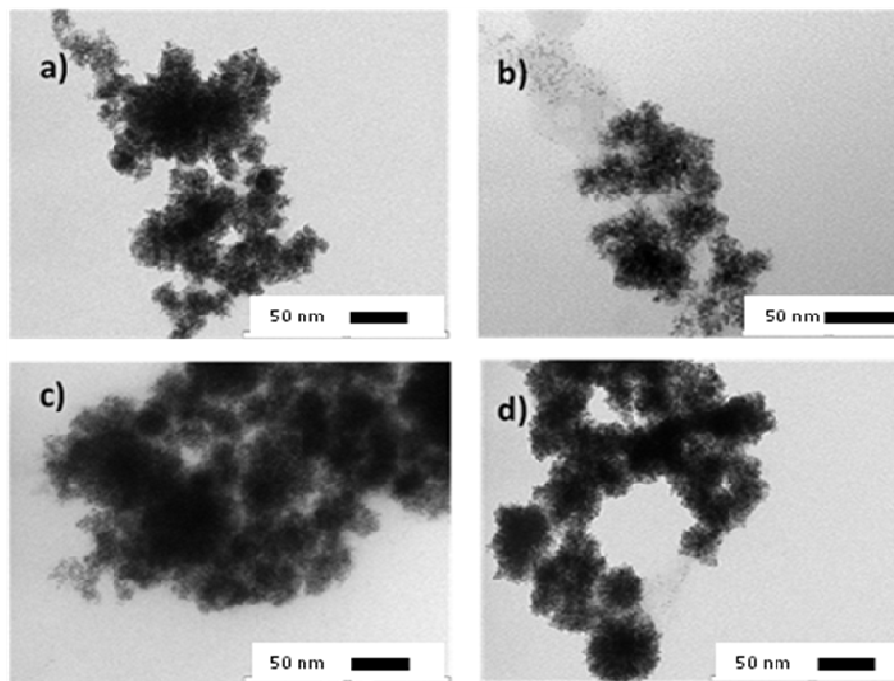


Figure 3.8. TEM micrographs of RhNP after styrene hydrogenation. Top: **Rh1** in a) THF and b) scCO₂. Bottom: **Rh3** in c) THF and d) scCO₂.

In order to avoid the steric hindrance induced by the methyl group on the substrate **5**, we tested the hydrogenation of **6** using the most active systems, **Ru2** and

Ru3. In THF, the systems were moderately active (up to 44% conversion, entries 9 and 11, Table 3.3), obtaining essentially the product corresponding to the hydrogenation of the exocyclic double bond (**6a**). Analogously to the behaviour observed for **5**, both catalytic systems were less active in scCO₂ (up to 23% substrate conversion, entries 10 and 12, Table 3.3); in addition, **Ru3** in scCO₂ favoured the isomerisation reaction (**6a:6b** = 63:37). When the commercial heterogeneous catalyst Ru/C was used, lower conversion towards the total hydrogenated product, were found than those obtained with the corresponding nanoparticle-based catalysts for substrates **4** and **5** (for **4**, entries 1 and 3 *versus* 13; for **5**, entries 5 and 7 *versus* 14, Table 3.3); but no significant differences were observed for **6** (entries 9 and 11 *versus* 15, Table 3.3). These results point to a strong interaction between the aromatic groups of the substrate and metallic surface, mainly for **4** and **5**, in agreement with the NMR study previously reported in our group.²⁵ Nevertheless, the conformation adopted by substrate **6** on the metallic surface probably favours the hydrogenation of the double bond instead of the aromatic ring.

3.3. Conclusions

New Ru and Rh nanoparticles have been prepared using phosphine ligands as stabilisers. Their preparation was highly dependent on the organometallic precursor and the ligand nature. While triphenylphosphine stabilised both kind of nanoparticles (**Ru3** and **Rh3**), ligands containing fluorinated groups, **1** and **2**, were appropriate stabilizers for rhodium (**Rh1**) and ruthenium (**Ru2**), respectively. These materials were fully characterised by TEM, IR, elemental analysis and XRD. The presence of the ligands at the metallic surface was mainly evidenced by vibrational spectroscopies and elemental analysis. In particular, the exchange ligand reaction between **Ru2** and dodecanethiol in THF showed the slow displacement of the phosphine **2** by the thiol (monitored by NMR), pointing to a strong interaction of the ligand with the metallic surface. These nanoparticles were used as catalytic precursors in hydrogenation reactions of substrates containing aromatic groups (substrates **4** – **6**). Substrate conversions obtained show that the catalytic systems are in general slower in scCO₂ than in THF, probably due to the different solubilities of the MNP in scCO₂ than in THF

even for the ligand **2** containing two fluorinated groups per aromatic ring. Ru nanoparticles remained dispersed after hydrogenation in scCO₂, in contrast to the agglomerates observed for RhNP. The relative higher metallic surface for Ru nanoparticles than that obtained for the rhodium ones agrees with the higher activity observed for Ru systems than that given for Rh ones. In addition, the selectivity observed points to a strong interaction between the phenyl groups of the substrates with the surface, mainly in the presence of oxygenated groups.

3.4. Experimental

MNP syntheses were performed using standard Schlenk techniques and Fisher–Porter bottle techniques under argon atmosphere. Organic solvents were dried following the procedures described in the literature.²⁶ Reagents and solvents were degassed by three vacuum–argon or vacuum–nitrogen cycles. Metallic nanoparticles were prepared by organometallic compound decomposition following the methodology described in the literature.²⁷ [Ru(COD)(COT)], 4-trifluoromethyltriphenylphosphine, 3,5 bistrifluoromethyl triphenylphosphine, triphenylphosphine, ruthenium 5% on activated carbon, styrene, 4-methyl anisole, dodecanethiol and fluorobenzene were purchased from Nanomeps, Alfa Aesar and Aldrich and used without further purification. [Rh(μ-OMe)(COD)]₂^{28,29} and 2-methylprop-2- enoxybenzene³⁰ were synthesised following the procedures described in the literature. Elemental analyses of Rh and Ru were carried out in a PerkinElmer Optima 3200 RL apparatus. Carbon and hydrogen analyses were done in a PerkinElmer 240 B apparatus. TEM and HR-TEM experiments were performed on a JEOL 200 CX-T electron microscope operating at 200 kV and a Philips CM12 electron microscope operating at 120 kV with respective resolutions of 4.5 and 5 Å . TEM analyses of the nanoparticles after catalysis were performed on a Zeiss 10 CA electron microscope at 100 kV with a resolution of 3 Å . Samples for TEM analysis were prepared by slow evaporation of a drop of colloidal solution deposited under argon onto holey carbon covered copper grids. Gas chromatography analyses (undecane used as an internal standard) were performed with a Hewlett- Packard 5890A instrument in an HP-5 (5% diphenylsilicone/95% dimethylsilicone column, 25 m x 0.2 mm), equipped with a

Hewlett-Packard HP3396 series II integrator. Catalytic experiments in scCO₂ were performed in a Parr autoclave (25 mL) with magnetic stirring. The autoclave was equipped with a liquid inlet, a gas inlet, a CO₂ inlet and a thermocouple. An electric heating mantle kept the temperature constant. Catalytic experiments in organic solvent were carried out in a Berghof autoclave (125 mL) with magnetic stirring and capacity of 100 atm of pressure equipped with gas and liquid inlet. An electric heating mantle kept the temperature constant.

3.4.1. Synthesis of metallic nanoparticles

3.4.1.1. General synthesis of Ru nanoparticles stabilized by phosphine ligands

In a typical experiment, 0.016 mmol of the appropriate ligand was introduced in a Fisher–Porter bottle and left under vacuum during 30 min. A solution of 25 mg of [Ru(COD)(COT)] (0.08 mmol) in 5 mL of neat THF, deoxygenated by freeze-pump cycles, was then added; and a total volume of 80 mL of THF was achieved. The bottle was then pressurized under 3 bar of H₂ pressure and stirred vigorously. After 18 h, a homogeneously brown solution was obtained and depressurized. Solvent was evaporated under vacuum up to approximately 10 mL. Deoxygenated pentane (10 mL) was then added and a brown precipitate was formed. After filtration, the precipitate was washed with deoxygenated pentane (2 × 10 mL) and dried under reduced pressure. The resulting black powder obtained was characterized by IR spectroscopy, TEM and elemental analysis; **Ru2** was also analysed by powder XRD.

Ru2. Mass: 19.6 mg. IR (KBr, pellet): 798 (C–P st, w), 1063 (C–F st, w), 423 (Ru–P) cm⁻¹. Elemental analysis: Ru = 19.73%, C = 45.36%, H = 7.16%. Calculated for Ru₅(**2**)(THF)₂₀: Ru = 19.3%, C = 47.7%; H = 6.5%. Mean diameter (TEM) = 1.3 ± 0.27 nm (111 particles). XRD: hcp.

Ru3. Mass: 21.4 mg. IR (KBr, pellet): 804 (C–P st, w), 500 (Ru–P) cm⁻¹. Elemental analysis: Ru = 16.6%, C = 51.45%, H = 8.46%. Calculated for Ru₅(**3**)(THF)₃₀: Ru = 17.3%, C = 56.6%; H = 8.7%. Mean diameter (TEM) = 1.38 ± 0.43 nm (792 particles).

3.4.1.2. General synthesis of Rh nanoparticles stabilized by phosphine ligands

In a typical experiment, 3.87 mg of [Rh(μ-OMe)(COD)]₂ (0.008 mmol) and 0.0032 mmol of the appropriate ligand were introduced in a Fisher–Porter bottle and left under vacuum during 30 min. 80 mL of neat THF, deoxygenated by freeze-pump cycles, was then added. The bottle was pressurized under 3 bar of hydrogen and stirred vigorously. After 18 h, a homogeneous grey solution was obtained and depressurized. Solvent was evaporated under vacuum up to approximately 10 mL. Deoxygenated pentane (10 mL) was then added and a black precipitate was formed. After filtration, the precipitate was washed with deoxygenated pentane (2 – 10 mL) and dried under reduced pressure. The resulting black powder obtained was characterized by IR spectroscopy, TEM and elemental analysis.

Rh1. Mass: 3.1 mg. IR (KBr, pellet): 802 (C–P st, w), 1261 (C–F st, w) cm⁻¹. Elemental analysis: Rh = 27.1%, C = 47.72%, H = 6.61%. Calculated for Rh₅(1)(THF)₁₅: Rh = 25.0%, C = 47.2%; H = 6.4%. Mean diameter (TEM) = 2.51 ± 0.42 nm.

Rh3. Mass: 3.3 mg. IR (KBr, pellet): 802 (C–P st, w) cm⁻¹. Elemental analysis: Rh = 17.2%, C = 56.26%, H = 7.73%. Calculated for Rh₅(3)(THF)₃₀: Rh = 17.5%, C = 56.4%; H = 8.7%. Mean diameter (TEM) = 1.73 ± 0.46 nm.

3.4.2. Catalytic reactions

3.4.2.1. Hydrogenation of arenes with metallic nanoparticles in THF

As a general procedure for preformed MNP, the Berghof autoclave was introduced in a glove box, 0.009 mmol of MNP were introduced and then the autoclave closed to ensure the inert atmosphere inside. Then 4.5 mmol of substrate and 20 mL of neat and deoxygenated THF were added. The autoclave was pressurized at 20 atm of H₂, stirred and heated at 50 °C during 24 h. After cooling to 0 °C the autoclave was depressurized and, if necessary a TEM grid was prepared and the reaction mixture was then filtered through a celite column.

3.4.2.2. Hydrogenation of arenes with metallic nanoparticles in scCO₂

As a general procedure for preformed MNP, the Parr autoclave was introduced in a glove box, 0.011 mmol of MNP were introduced and then the autoclave closed to ensure the inert atmosphere inside. Then 5.6 mmol of substrate were added. The autoclave was pressurized at 20 atm of H₂ and pressurized with CO₂ at 200 atm of total pressure. The autoclave was then stirred and heated at 50 °C during 24 h. After this time, the autoclave was cooled at 0 °C and slowly depressurized through a cold trap. The reaction mixture was extracted with diethylether and, when specified a TEM grid was prepared and the reaction mixture was then filtered through a celite column.

3.4.3. Ligand exchange reaction monitored by NMR

10 mg of **Ru2** nanoparticles, 0.7 mL of THF-d₈ and 0.03 mL (0.3 mmol) of fluorobenzene as an internal standard were introduced in a NMR Young joint tube. After ¹⁹F and ³¹P NMR spectra recording, 0.1 mL of dodecanethiol (0.4 mol) was added and the tube was gently stirred at 298 K to homogenate the solution. ¹⁹F and ³¹P NMR spectra were recorded on time.

3.5. References

- ¹ a) A. Roucoux, A. Nowicki and K. Philippot in: D. Astruc (Ed.), *Nanoparticles and Catalysis*, Wiley-VCH, Weinheim, **2008**, p. 349 (Chapter 11). b) A. Roucoux and K. Philippot in: J.G. de Vries, C.J. Elsevier (Eds.). *The Handbook of Homogeneous Hydrogenation*, Wiley-VCH, Weinheim, **2007**, p. 217. c) D. Astruc, F. Lu and J.R. Aranzaes. *Angew. Chem. Int. Ed.* **2005**, 44, 7852. d) J.A. Widgren and R.G. Finke. *J. Mol. Catal. A: Chem.* **2003**, 191, 187. e) J.D. Aiken III and R.G. Finke. *J. Mol. Catal. A: Chem.* **1999**, 145, 1.
- ² a) H.U. Blaser, C. Malan, B. Pugin, F. Spindler, H. Steiner and M. Studer. *Adv. Synth. Catal.* **2003**, 345, 103. b) J.G. de Vries and C.J. Elsevier (Eds.). *The Handbook of Homogeneous Hydrogenation*, Wiley-VCH, Weinheim, **2007**.
- ³ K. Weissermel and H.-J. Arpe. *Industrial Organic Chemistry*, VCH, New York, **1993**
- ⁴ J. Durand, E. Teuma and M. Gómez. *Eur. J. Inorg. Chem.* **2008**, 3577.
- ⁵ P.T. Anastas and J.C. Warner. *Green Chemistry: Theory and Practice*, Oxford University Press, Oxford, **1998**.
- ⁶ W. Leitner. *Acc. Chem. Res.* **2002**, 35, 746.
- ⁷ a) P.G. Jessop, T. Ikariya and R. Noyori. *Chem. Rev.* **1999**, 99, 475. b) A. Baiker. *Chem. Rev.* **1999**, 99, 453.
- ⁸ C.L. Young (Ed.). *IUPAC Solubility Data Series: Hydrogen and Deuterium*, vol. 5/6, Pergamon, New York, **1981**.
- ⁹ D.J. Cole-Hamilton. *Science*. **2003**, 299, 1702.
- ¹⁰ a) F. Cansell and C. Aymonier. *J. Supercrit. Fluids*. **2009**, 47, 508. b) E. Reverchon and R. Adami. *J. Supercrit. Fluids*. **2006**, 37, 1. c) Q. Xu and W. Ni. *Prog. Chem.* **2007**, 19, 1419. d) S. Moisan, V. Martinez, P. Weisbecker, F. Cansell, S. Mecking and C. Aymonier. *J. Am. Chem. Soc.* **2007**, 129, 10602. e) A. Kameo, T. Yoshimura and K. Esumi. *Colloids Surf. A: Physicochem. Eng. Aspects*. **2003**, 215, 181. f) M.C. McLeod, R.S. McHenry, E.J. Beckman and C.B. Roberts. *J. Phys. Chem. B*. **2003**, 107, 2693.
- ¹¹ a) P.S. Shah, J.D. Holmes, R.C. Doty, K.P. Johnston and B.A. Korgel. *J. Am. Chem. Soc.* **2000**, 122, 4245. b) P.S. Shah, S. Husain, K.P. Johnston and B.A. Korgel. *J. Phys. Chem. B*. **2002**, 106, 12178.

- ¹² a) J.L. Zhang and B.X. Han. *J. Supercrit. Fluids.* **2009**, 47, 531. b) C.A. Fernandez and C.M. Wai. *Small.* **2006**, 2, 1266. c) J. Eastoe and S. Gold. *Phys. Chem. Chem. Phys.* **2005**, 7, 1352.
- ¹³ N. Yan, C. Xiao, Y. Kou. *Coord. Chem. Rev.* **2010**, 254, 1179.
- ¹⁴ a) R.J. Bonilla, B.R. James and P.G. Jessop. *Chem. Commun.* **2000**, 941. b) K.M.K. Yu, P. Meric and S.C. Tsang. *Catal. Today.* **2006**, 114, 428.
- ¹⁵ a) M. Ohde, H. Ohde and C. M. Wai. *ACS Symp. Ser.* **2003**, 860, 419. b) P. Meric, K. M. K. Yu, A. T. S. Kong and S. C. Tsang. *J. Catal.* **2006**, 237, 330. c) M. Ohde, H. Ohde and C. M. Wai. *Chem. Commun.* **2002**, 2388.
- ¹⁶ H. Ohde, M. Ohde and C.M. Wai. *Chem. Commun.* **2004**, 930.
- ¹⁷ L. S. Ott and R.G. Finke. *Coord. Chem. Rev.* **2007**, 251, 1075.
- ¹⁸ M. Tamura and H. Fujihara. *J. Am. Chem. Soc.* **2003**, 125, 15742.
- ¹⁹ a) S. Jansat, M. Gómez, K. Philippot, G. Muller, E. Guiu, C. Claver, S. Castillón and B. Chaudret. *J. Am. Chem. Soc.* **2004**, 126, 1592. b) I; Favier, M. Gómez, G. Muller, M. R. Axet, S. Castellón, C. Claver, S. Jansat, B. Chaudret and K. Philippot. *Adv. Synth. Catal.* **2007**, 349, 2459.
- ²⁰ J. A. Widegren and R. G. Finke. *Inorg. Chem.* **2002**, 41, 1558.
- ²¹ a) A. Roucoux, J. Schulz and H. Patin. *Adv. Synth. Catal.* **2002**, 345, 222. b) A. Roucoux, J. Schulz and H. Patin. *Chem. Eur. J.* **2000**, 6, 618. c) C. Hubert, A. Denicourt, N. Nowicki, P. Beaunier and A. Roucoux, *Green Chem.* **2010**, 12, 1167.
- ²² V. Mévellec, A. Roucoux, E. Ramirez, K. Philippot and B. Chaudret. *Adv. Synth. Catal.* **2004**, 346, 72.
- ²³ a) M. H. G. Prechtl, M. Scariot, J. D. Scholten, G. Machado, S. R. Teixeira and J. Dupont. *Inorg. Chem.* **2008**, 47, 8995. b) L. M. Rossi, J. Dupont, G. Machado, P. F. P. Fichtner, C. Radtke, I. J. R. Baumvol and S. R. Teixeira. *J. Braz. Chem. Soc.* **2004**, 15, 904. c) G. S. Fonseca, A. P. Umpierre, P. F. P. Fichtner, S. R. Teixeira and J. Dupont. *Chem. Eur. J.* **2003**, 9, 3263.
- ²⁴ B. Chaudret. *Top. Organomet. Chem.* **2005**, 16, 233.
- ²⁵ I. Favier, S. Massou, E. Teuma, K. Philippot, B. Chaudret and M. Gómez. *Chem. Commun.* **2008**, 3296.

- ²⁶ D. D. Perrin and W. L. F. Armarego. *Purification of Laboratory Chemicals*. 3^a Ed. Pergamon Press, Oxford, **1988**.
- ²⁷ K. Philippot and B. Chaudret. *C. R. Chimie*. **2003**, 6, 1019
- ²⁸ J. Chatt and L. M. Venanzi. *J. Chem. Soc.* **1957**, 4735.
- ²⁹ R. Usón, L. A. Oro and J. Cabeza. *Inorg. Synth.* **1985**, 23, 126.
- ³⁰ A. T. Shulgin and A. W. Baker. *J. Org. Chem.* **1963**, 28, 2468.

Chapter 4

New Bicyclic P-
donor Ligands:
Synthesis,
Structure and
Applications in
Pd-Catalysed C-C
Bond Formation
in Ionic Liquids

UNIVERSITAT ROVIRA I VIRGILI
ORGANOMETALLIC COMPOUNDS AND METAL NANOPARTICLES AS CATALYSTS IN LOW ENVIRONMENTAL IMPACT SOLVENTS
Martha Verónica Escárcega Bobadilla
ISBN:978-84-694-1249-7/DL:T-324-2011

4.1. Introduction

In the field of enantioselective catalysis, a large variety of chiral phosphorous-based ligands has been developed since the pioneering works of Knowles,¹ Horner² and Kagan.³ Looking for high asymmetric inductions, rigid and well-defined coordination environments around the metallic centres besides electronic effects appeared beneficial to achieve high enantiomeric excesses.⁴ Therefore, phosphorous atom placed on a heterocycle can play a crucial role in the asymmetric induction.⁵ The noteworthy contribution of Burk and co-workers developing the efficient phospholane DuPhos (Chart 4.1) which gave excellent enantioselectivities especially in asymmetric hydrogenation,⁶ stimulated the catalytic applications of five-membered phosphacycle-based chiral ligands.

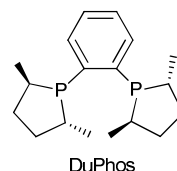


Chart 4.1. DuPhos ligand

In addition to saturated heterocyclic phospholanes, other five-membered P-cyclic ligands such as phospholes,⁷ 2- and 3-phospholenes⁸ and phosphaferrocenes⁹ (Figure 4.1) have been also applied in metal-catalysed organic processes, including bicyclic backbones, such as phosphanorbornadiene and phosphanorbornene structures described by Mathey and co-workers.¹⁰

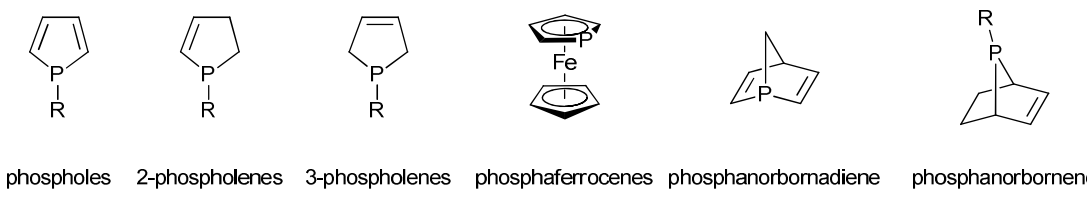


Figure 4.1. Skeletons of phosphorus-containing unsaturated heterocycles.

However, P-donor ligands based on fused saturated five-membered bicyclic structures have been less commonly applied in catalysis (Figure 4.2). The first work

New bicyclic P-donor ligands: synthesis, structure and catalytic applications in ILs

was reported by Vedejs *et al.* preparing P,C-sterogenic phosphabicyclo[3.3.0]octanes used in organocatalysis, in particular in enantioselective acylations (**A** in Figure 4.2).¹¹ Some years later, Pietrusiewicz and co-workers developed related phospholane and also phospholene (**B** in Figure 4.2) ligands to be employed in Pd-catalysed C-C bond formation reactions.¹² RajanBabu *et al.* described the applications in Pd-catalysed asymmetric allylic alkylations of mono- and bis-phospholanes synthesised from D-mannitol (**C** in Figure 4.2).¹³ In addition, Buono *et al.* described a diamidophosphite derived from 1,3-diaza-2-phosphabicyclo[3.3.0]octane and its further catalytic uses (Cu-catalysed enantioselective conjugate addition of diethylzinc to enones and Pd-catalysed allylic substitutions) (**D** in Figure 4.2).¹⁴ Other groups, have employed this kind of bicyclic diamidophosphites in asymmetric catalytic processes.¹⁵ Chiral bicyclic phosphoramidites (**E** in Figure 4.2) gave high enantiomeric excesses in Rh-catalysed olefin hydrogenation reactions.¹⁶

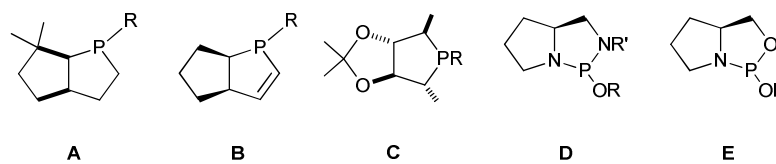


Figure 4.2. P-heterocyclic ligands containing saturated five-membered bicyclic structures.

In this context, azadioxaphosphabicyclo[3.3.0]octane compounds (**1** and **2** in Figure 4.3) represent a new class of ligands containing two fused five-membered rings derived from tartaric acid. Few reports are described in the literature concerning the synthesis of *trans* fused five-membered heterocycles^{13,17} and for the best of our knowledge, only one crystal structure has been described.¹⁸

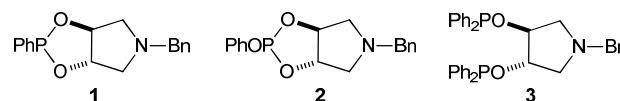


Figure 4.3. Azaphosphabicyclo[3.3.0]octane ligands **1** and **2**, and the diphosphinite **3**.

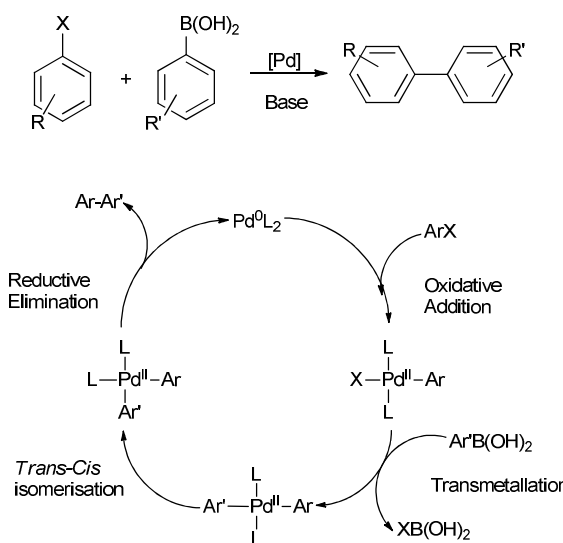
Since its discovery in 1979,¹⁹ the Suzuki–Miyaura reaction allows the cross-coupling of aryl halides with boron compounds in the presence of a base. This reaction has proved over the years to be one of the most popular reactions for carbon–carbon bond formation through palladium catalysis.²⁰ The impressive development of this reaction in both academic and industrial laboratories can be explained for several reasons: i) Due to the mild reaction conditions, a wide range of functional groups are tolerated, ii) boronic acids are readily available, stable and considered of low toxicity, iii) generally dry solvents are not required, and iv) wide range of substrates can be used. Usual catalytic systems rely on homogeneous palladium catalysts associated with an appropriate ligand in conventional organic or biphasic media.

Concerning to the Suzuki reaction, aryl halides or triflates derivatives are often used as substrates and coupled with aryl boronic acids in the presence of a base and palladium catalyst to obtain the corresponding biaryl products (Scheme 4.1), which have a wide range applications such as pharmaceuticals,²¹ liquid crystal technology²² and fire resistant synthetic fibers.²³

In relation with the mechanism (Scheme 4.1) the generally accepted cycle involves an oxidative addition of the aryl halide to the palladium(0) species, transmetallation involving boronic acid to form a *trans*-diarylpalladium(II) species, isomerization of the *trans* isomer to the *cis* one, and reductive elimination of the biaryl, regenerating the Pd(0) active species.²⁴

A number of remarkable results have been reported concerning the cross-coupling of boronic compounds with aryl or vinyl iodide, bromide and even demanding chloride substrates under mild conditions.²⁵

In relation to the solvents, as discussed in Chapter 1, ILs are often used to immobilize the palladium catalyst in an ionic phase of a biphasic system, bridging the gap between homogeneous and heterogeneous catalysis, allowing an easy recovery of the catalysts. Ionic liquids present different advantages in front of conventional organic solvents such as the catalyst recovery for further recycling, especially interesting in asymmetric catalysis.²⁶ Recently, a lot of studies have been carried out concerning this reaction by using ionic liquid under biphasic conditions.²⁷



Scheme 4.1. General reaction and proposed catalytic cycle for Pd-catalysed Suzuki C-C cross coupling.

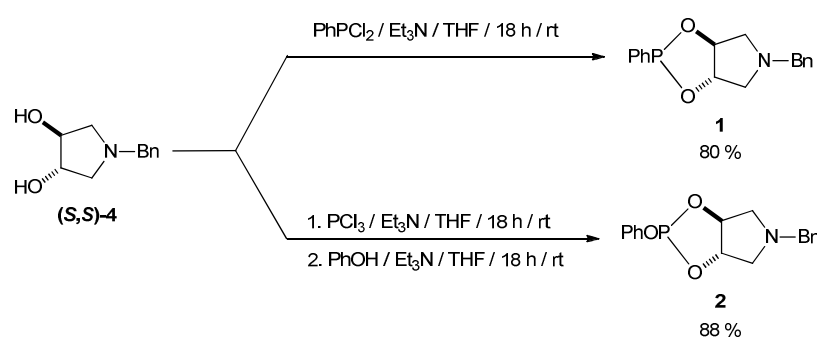
In this part of the Thesis, the synthesis of phosphonite **1** and phosphite **2** derived from natural tartaric acid and their applications in Pd-catalysed C-C bond formation processes in organic and ionic liquid solvents have been developed. Bis(phosphinite) **3** was also studied in order to compare the effect of the rigidity in bicyclic ligands. The robustness of these ligands in [BMI][PF₆] (BMI = 1-butyl-3-methyl imidazolium) under catalytic conditions has been proven, in contrast to the low stability observed in toluene. In order to evidence the coordination ability of these ligands, two complexes containing ligands **1** and **2**, **Pd1** and **Pd2** respectively, have been synthesised and fully characterised. A conformational study of the new azadioxaphosphane bicyclo[3.3.0]octane ligands **1** and **2** has been also carried out.

The choice of N-containing ligands was made with the aim of study the possibility of quaternisation of this group to increase the affinity for the ionic liquid medium. Unfortunately all attempts tested were unsuccessful.

4.2. Results and Discussion

4.2.1. Synthesis and characterization of azadioxaphosphabicyclo [3.3.0]octane compounds

Ligand **1** has been prepared following the methodology reported for related phosphonite compounds,²⁸ starting from the optically pure (*S,S*)-**4** diol by reaction with phenyl dichlorophosphine, giving a white solid in a good yield (80%) after filtration through anhydrous basic alumina under argon atmosphere, in order to remove the acidic by-products derived from the PhPCl₂ (Scheme 4.2).



Scheme 4.2. Synthesis of chiral oxyphosphanes **1** and **2**.

³¹P{¹H} NMR spectrum of **1** exhibited two singlet signals pointing to a mixture of isomers (Figure 4.4b). In fact, the ¹H NMR spectrum (Figure 4.4a) showed three species with an invariable ratio (1/0.63/0.46) in the studied temperature range (298 – 193 K). The three isomers could be only distinguished by the signals of the methylene of the benzyl group. The 2D-HSQC experiment confirmed the presence of these three isomers. In order to corroborate this structural behaviour, the new related ligand **2** was prepared following the two-step synthetic methodology for phosphites described elsewhere (Scheme 4.2).²⁹ An analogous isomeric behaviour in solution was found by ¹H NMR (isomeric ratio 1/0.9/0.6), but in this case the ³¹P{¹H} NMR spectrum showed three singlet signals (Figures 4.4c and 4.4d).

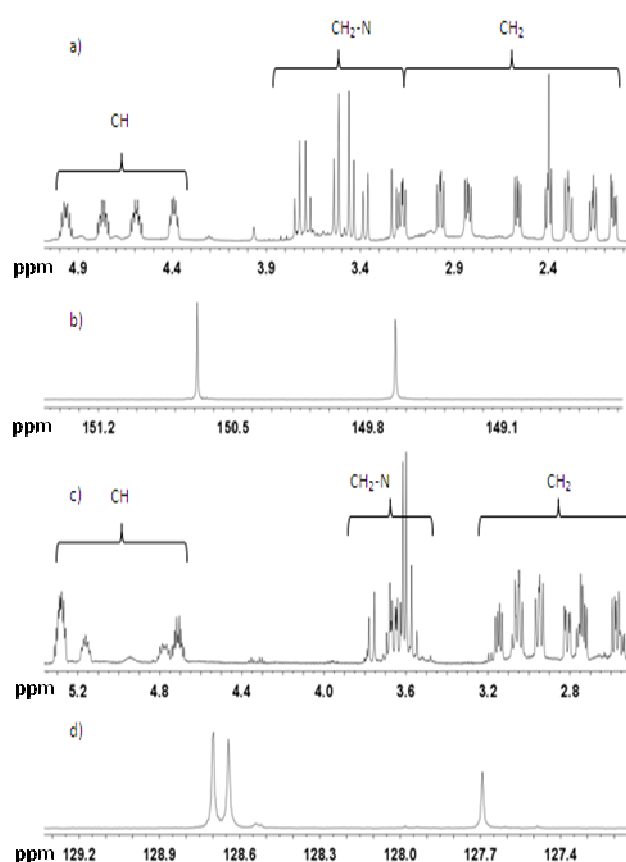


Figure 4.4. ^1H (500.13 MHz) and $^{31}\text{P}\{^1\text{H}\}$ (202.5 MHz) NMR spectra for phosphonite **1** (a, b) and phosphite **2** (c, d) in CD_2Cl_2 and CDCl_3 respectively at 298 K. For ^1H NMR spectra, only the methylene and methinic proton region is exhibited.

For both compounds, NOESY experiments at 323 K and 298 K (Figure 4.5) did not reveal exchange between the different conformations (all signals showed opposite sign in relation to the diagonal).

With the aim to understand the nature of these isomers, a modelling study was carried out. Concerning the two five-membered fused rings, a *trans* arrangement is imposed due to the controlled stereochemistry of the two bridge carbon atoms. Because of the substituents on P (phenyl and phenoxide for **1** and **2** respectively) and N (benzyl for both ligands) atoms, two conformations could be possible, *syn* and *anti*, if both groups point to the same or opposite direction respectively (Figure 4.6). Taking into account that the three isomers are only differentiated by the CH_2 group of the benzyl substituent on the nitrogen, they might arise from the different relative spatial disposition of this group in the ligand structure (R' in Figure 4.6).

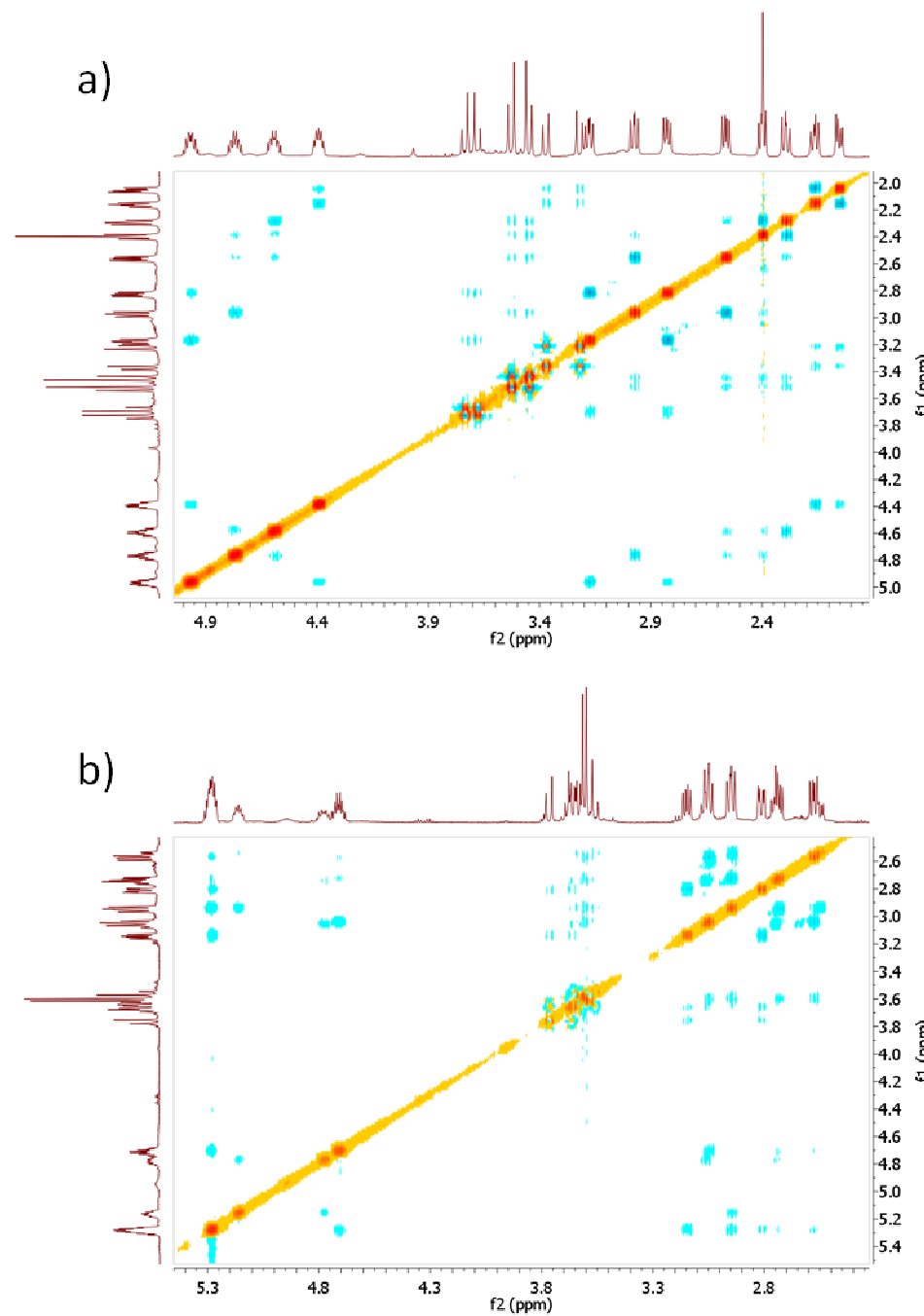


Figure 4.5. NOESY ^1H - ^1H NMR experiments at 298 K of a) **1** and b) **2**.

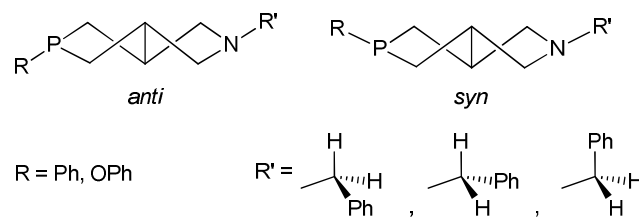


Figure 4.6. *Syn* and *anti* conformations for *trans* fused five-membered heterocycles.

This fact generates three possible isomers for each *syn* and *anti* conformation. The structures of the six conformations were modelled at semi-empirical PM3 level and their energies calculated by density functional theory (DFT B3LYP) using 6-31G* polarization basis set and pseudopotentials (Figure 4.7).

For each compound, two conformations exhibited high energy (more than 2.2 kcal/mol in relation to the most stable conformation) and were not considered. The other four conformations of close energy (between 0.01 and 0.36 kcal/mol in relation to the most stable conformation) led to a Boltzmann distribution at 298 K of *ca.* 1/0.75/0.6/0.5 and 1/1/0.9/0.6 for **1** and **2** respectively (Figure 4.7). Conformers *anti*-**1a** and *syn*-**1b** (Figure 4.7) cannot probably be discriminated by NMR. In this case, the three conformers (*anti*-**1a** or *syn*-**1b**/*anti*-**1c**/*syn*-**1d**) would be in a relative ratio of 1/0.74/0.53. In the case of **2**, conformers with *anti* arrangement could not be distinguished by NMR, leading to a ratio 1/0.88/0.6 (*anti*-**2**/*syn*-**2c**/*syn*-**2d**) (Figure 4.8). These data are in agreement with the experimental observations (see above). It is important to note that the rotation around the N-Bn bond leads to conformations of different energy, as demonstrated by the corresponding energy calculations (Figure 4.9), in agreement with the interchange lack stated by NMR between the different conformers at room temperature (see above).

In order to study the stability of ligands **1-3** under catalytic conditions, a $^{31}\text{P}\{\text{H}\}$ NMR monitoring study was carried out in toluene and [BMI][PF₆] under basic conditions. It is well known that P-O bonds in oxyphosphane ligands can be easily hydrolysed to form the corresponding phosphonic acid derivatives.³⁰ Ligands **1**, **2** and **3** dissolved in [BMI][PF₆] in the presence of an aqueous solution of sodium carbonate at 60 °C (conditions used for the catalytic reactions, see below), proved to be stable, without showing any sign of degradation (Figure 4.10).

On the contrary, the three ligands quickly decomposed using toluene or [EMI][PH(O)OMe] (EMI = 1-ethyl-3-methyl imidazolium) as solvent, probably due to the basic character of this anion that favours the ligand hydrolysis.

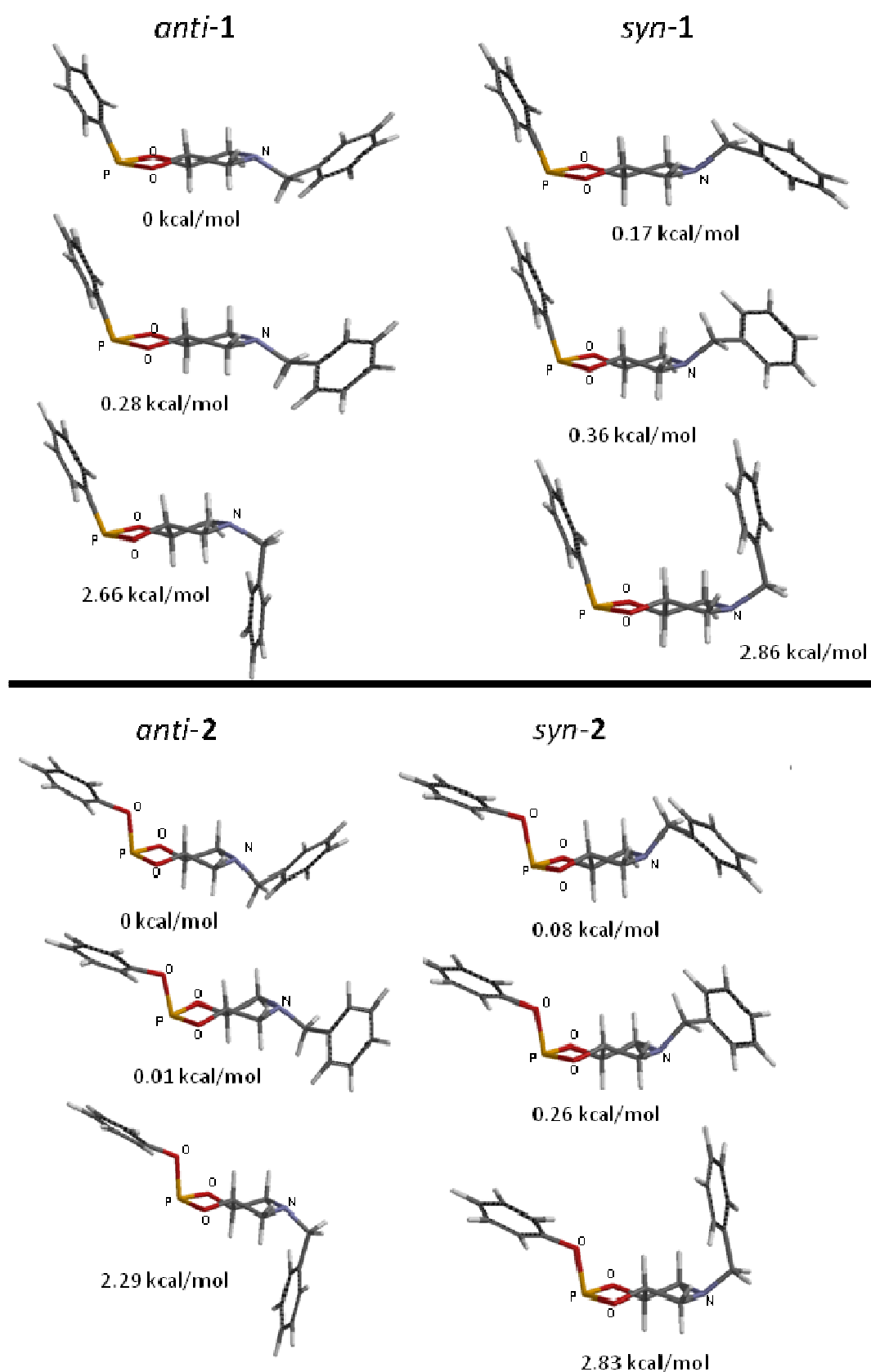


Figure 4.7. Modelled structures (PM3(tm)) for the six conformations for phosphonite **1** (above) and phosphite **2** (below). Relative energies calculated by DFT.

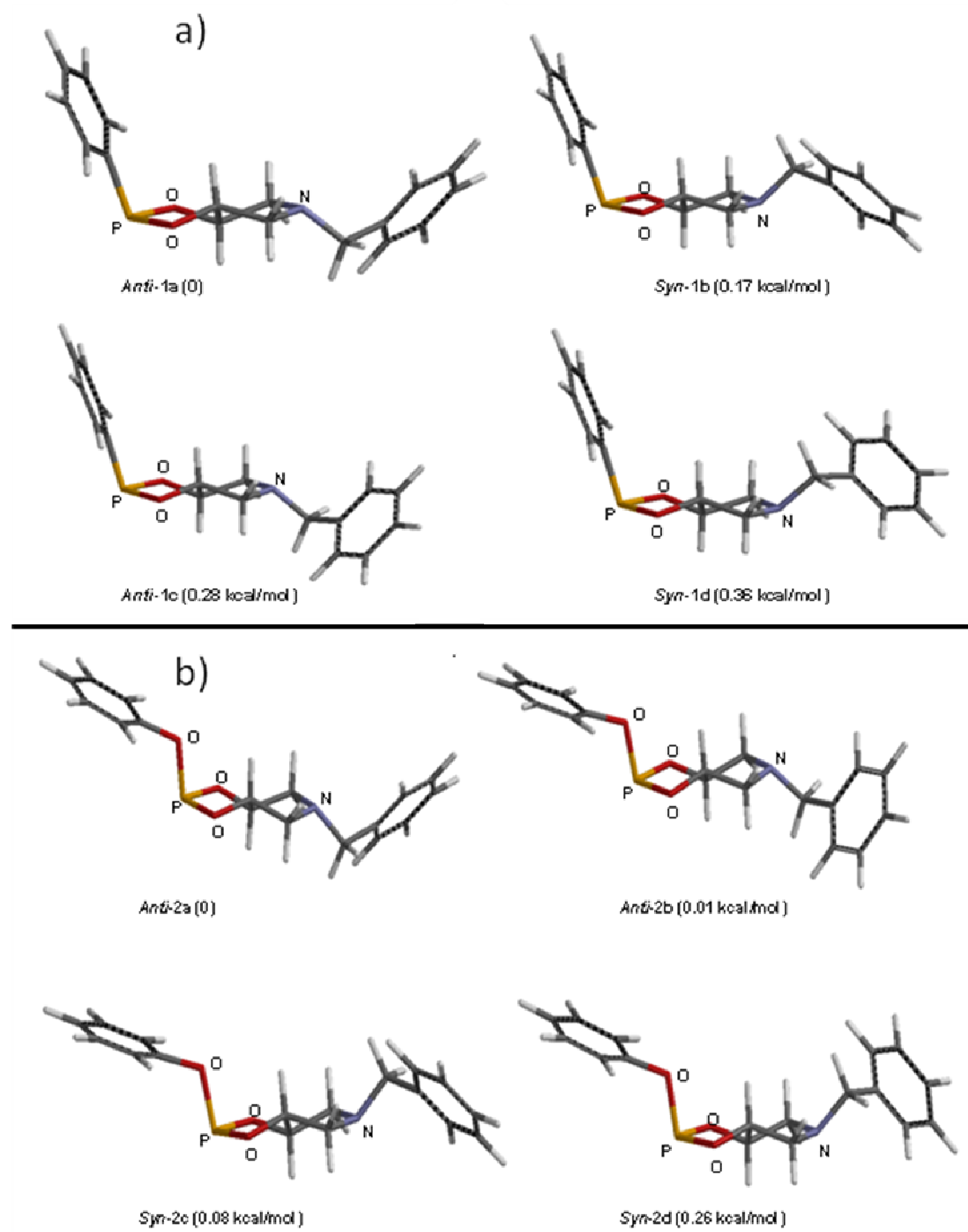


Figure 4.8. Modelled structures (PM3(tm)) for the four more stable conformations for:

a) **1** and b) **2**. In brackets, relative energies calculated by DFT.

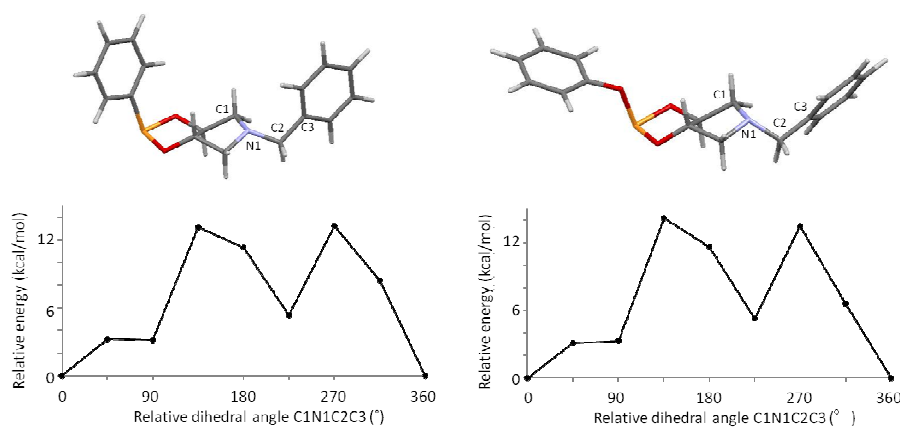


Figure 4.9. Calculated energy (DFT) by changing the dihedral angle around the N1-C2 bond for the most stable conformation of **1** (left) and **2** (right). For **1**, this angle is to 66° and for **2** to 67° (for comparation, this angle is taken as 0°).

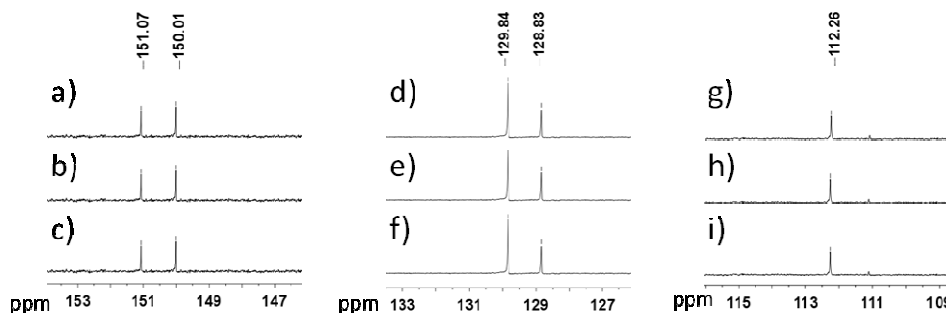
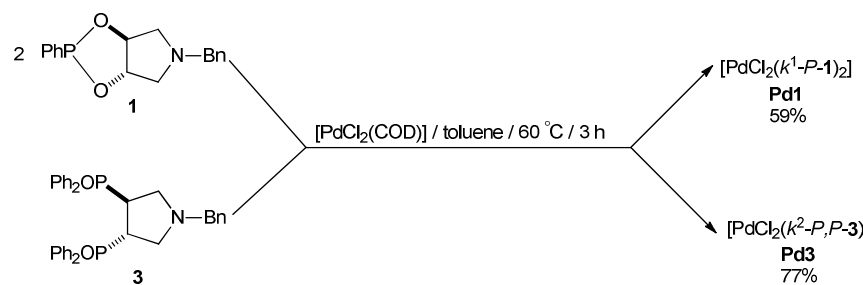


Figure 4.10. $^{31}\text{P}\{\text{H}\}$ NMR (121.5 MHz, 298 K, CDCl_3) spectra of ligands **1** (a, b, c), **2** (d, e, f) and **3** (g, h, i): in [BMI][PF_6] (a, d, g); in [BMI][PF_6] in the presence of Na_2CO_3 (aq) at 298 K (b, e, h) and after heating at 60 °C for 1h (c, f, i).

4.2.2. Preparation of palladium complexes

With the aim to prove the coordination ability of mono- and bidentated oxaphosphane ligands, palladium complexes $[\text{PdCl}_2(\kappa^1-\text{P}-\mathbf{1})_2]$ and $[\text{PdCl}_2(\kappa^2-\text{P},\text{P}-\mathbf{3})]$ were prepared from $[\text{PdCl}_2(\text{COD})]$ in toluene at 60 °C in the presence of the appropriate ligand, **1** and **3** respectively (Scheme 4.3).



Scheme 4.3. Synthesis of complexes **Pd1** and **Pd2**.

In the case of **Pd1** containing **1**, one singlet at +130 ppm was observed in the $^{31}\text{P}\{\text{H}\}$ NMR spectrum in agreement with Pd(II) related complexes.³¹ ^1H and ^{13}C NMR spectra showed signals corresponding to only one isomer in the studied temperature range (298-173 K), indicating that the different ligand conformations are undistinguished upon coordination, in contrast to the free ligand which exhibits three isomers in solution (Figure 4.11).

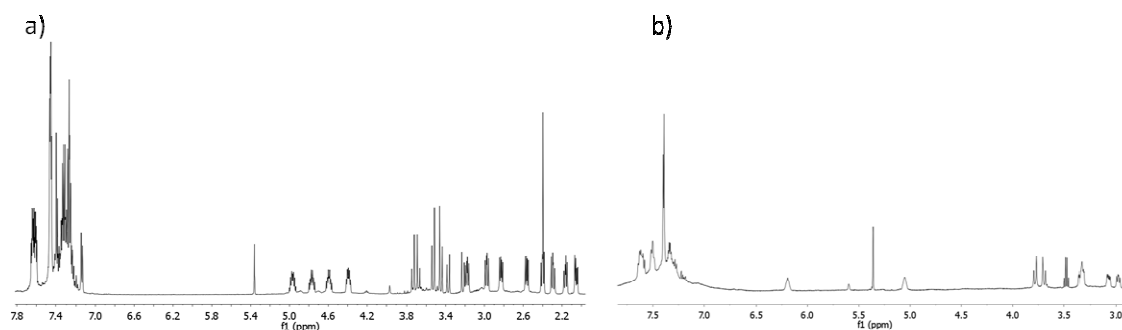


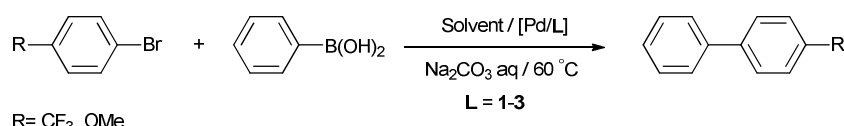
Figure 4.11. ^1H NMR (500.13 MHz, CD_2Cl_2 , 298 K) spectra of a) free ligand **1** and b) $[\text{PdCl}_2(\kappa^1-\text{P}-\mathbf{1})_2]$ complex.

The $^{31}\text{P}\{\text{H}\}$ NMR spectrum of **Pd3**, containing a seven-membered metallacycle, showed one singlet at +122 ppm, characteristic for Pd complexes coordinated to bidentated phosphinites.³² The ^1H NMR spectrum of **Pd3** was similar to that observed for the free ligand, exhibiting slight changes in the chemical shifts.

4.2.3. Catalytic results

4.2.3.1. Suzuki C-C cross-couplings

Reaction between 4-R-bromobenzene derivatives ($\text{R} = \text{CF}_3, \text{OCH}_3$) and phenylboronic acid under basic biphasic conditions, solvent- H_2O ,³³ was carried out using palladium catalysts containing oxyphosphane ligands **1-3** (Scheme 4.4). Water was necessary to favour the solubility of sodium carbonate. Catalytic precursors were generated *in situ* from $[\text{PdCl}_2(\text{COD})]$ and the appropriate ligand. Toluene and ionic liquids ($[\text{BMI}][\text{PF}_6]$ and $[\text{EMI}][\text{PH(OOMe)}]$) were used as a reaction medium. The catalytic results are summarised in Table 4.1.



Scheme 4.4. Palladium-catalysed Suzuki C-C cross coupling between 4-R-bromobenzene derivatives and phenylboronic acid.

The three catalytic systems, Pd/**1**, Pd/**2** and Pd/**3**, were active in [BMI][PF₆] and in toluene for both substrates 1-bromo-4-trifluorobenzene and 1-bromo-4-methoxybenzene. Higher conversions were obtained for 1-bromo-4-trifluorobenzene (entries 1, 3, 5, 6 and 8 in Table 4.1) than for 1-bromo-4-methoxybenzene (entries 2, 4, 7 and 9 in Table 4.1) as expected by the induced activation when electron-withdrawing substituents are involved.³⁴ In both catalytic reactions, an excellent chemoselectivity was observed, only giving the expected cross-coupling product. Catalytic system Pd/**3** was more active than Pd/**1** in both toluene and [BMI][PF₆] (entries 6-9 versus 1-4 in Table 4.1). Catalytic system Pd/**2** gave similar conversion than Pd/**3** in [BMI][PF₆] (entry 5, Table 4.1).

In order to check the positive influence of the P-donor ligands employed, we evaluated the catalytic behaviour of the Pd system with diol (*S,S*)-**4** (Scheme 4.2). This compound is one of the plausible by-products formed by hydrolysis of P-O bonds in oxaphosphane ligands. For the most active substrate, 1-bromo-4-trifluorobenzene, in [BMI][PF₆], Pd/**4** system provided *ca.* 80% conversion (entry 10 in Table 4.1) lower than for Pd/**3** (entry 6 in Table 4.1) but close to that obtained using Pd/**1** catalyst (entry 1 in Table 4.1). However, for Pd/**4**, *ca.* 23% of the product corresponded to the dehalogenated compound, trifluoromethylbenzene. Furthermore, the catalytic mixture became black after catalysis in contrast to yellow solutions obtained using P-donor ligands. TEM analysis of the post-catalytic ionic liquid suspension for Pd/**4** system, showed the presence of small palladium nanoparticles (PdNP) with a mean diameter of 2.10 nm, although they tend to be agglomerated (Figure 4.12). Their formation was probably due to the absence of good donor ligands (such as **1-3**), which avoids the formation of more active and selective catalytic molecular species. The surface reactivity of the *in situ* generated PdNP could be responsible of the dehalogenation reaction, favoured using heterogeneous catalysts.³⁵ Similar result was obtained in the

New bicyclic P-donor ligands: synthesis, structure and catalytic applications in ILs

absence of any ligand (entry 11 in Table 4.1). In toluene, only 12% substrate conversion was afforded in the absence of any ligand, mainly giving the corresponding homocoupling product coming from the substrate (4,4'-CF₃-1,1'-biphenyl).

Table 4.1. Suzuki C–C couplings between 4-R-bromobenzene derivatives (R = CF₃, OCH₃) and phenylboronic acid catalysed by Pd/L systems (L = **1–3**).^a

Entry	Ligand	Solvent	R	t [h]	Conv [%]
1	1	[BMI][PF ₆]	CF ₃	1	80 ^b
2	1	[BMI][PF ₆]	OMe	15	24 ^c
3	1	Toluene	CF ₃	1	66 ^b
4	1	Toluene	OMe	15	20 ^c
5	2	[BMI][PF ₆]	CF ₃	1	98 ^b
6	3	[BMI][PF ₆]	CF ₃	1	91 ^b
7	3	[BMI][PF ₆]	OMe	15	32 ^c
8	3	Toluene	CF ₃	1	94 ^b
9	3	Toluene	OMe	15	65 ^c
10	4	[BMI][PF ₆]	CF ₃	1	79 ^{b,d}
11	-	[BMI][PF ₆]	CF ₃	1	77 ^{b,e}
12	3	[EMI][PH(O)OMe]	CF ₃	1	36 ^b
13	3	[EMI][PH(O)OMe]	CF ₃	1	5 ^{b,f}
14	3	[EMI][PH(O)OMe]	CF ₃	1	0 ^{b,g}

^a Reaction conditions: Pd:L:aryl bromide:phenylboronic acid:sodium carbonate = 1:1.2:100:120:250 mmol in 1 mL of [BMI][PF₆] or toluene or [EMI][PH(O)OMe] and 2 mL of water at 60 °C; results obtained from duplicate experiments. ^b Determined by ¹⁹F NMR and GC-MS. ^c Determined by ¹H NMR and GC-MS. ^d Cross-coupling product:dehalogenated product = 73:26 (in [BMI][PF₆]). ^e Cross-coupling product:dehalogenated product = 85:15. ^f Without base. ^g Without base and water.

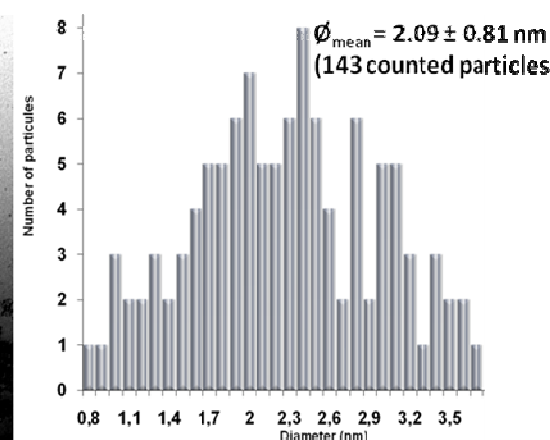
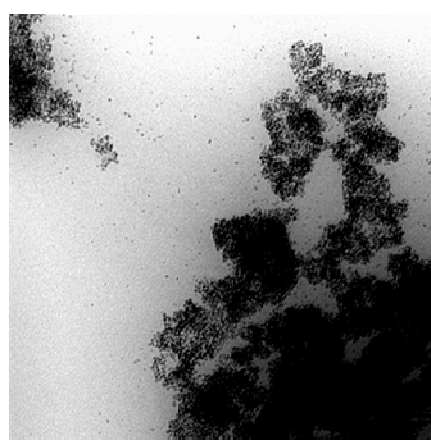
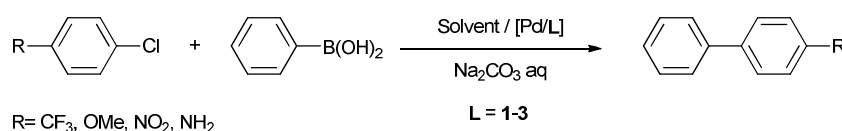


Figure 4.12. Transmission electronic microscopy (TEM) micrograph of the post-catalytic ionic liquid suspension for Pd/**4** system.

With the aim to avoid the addition of a external base, we used [EMI][PH(O)OMe] as solvent, which contains a basic anion, following the encouraging results previously obtained for Heck coupling reactions.³⁶ In this solvent, Pd/**3** catalytic system using 1-bromo-4-trifluorobenzene as substrate was inactive even in the presence of water (entries 13 and 14 in Table 4.1) and poorly active under aqueous basic conditions (entry 12 in Table 4.1). This behaviour could be probably due to the decomposition of ligand **3** in this solvent (see above).

After these promising results where activation of 1-bromo-4-methoxybenzene was achieved in both toluene and [BMI][PF₆], we evaluated the catalytic behaviour of Pd/L systems using less reactive chloroaryl substrates (Scheme 4.5 and Table 4.2).



Scheme 4.5. Palladium-catalysed Suzuki C-C cross coupling between 4-R-chlorobenzene derivatives and phenylboronic acid.

As expected, in relation to the analogous bromo derivatives, the chloroaryl substrates required higher reaction times to achieve high conversions (more than 90% for 1-chloro-4-trifluorobenzene after 15 h of reaction at 60 °C entries 1, 5 and 7 in Table 4.2). For 1-chloro-4-methoxybenzene, from moderate (31-55% conversion, entries 8 and 10 in Table 2) to excellent conversions (up to 91%, entries 2 and 4 in Table 4.2) at 100 °C and after two days of reaction, were obtained. In general for both catalysts, Pd/**1** and Pd/**3**, higher activities were achieved in [BMI][PF₆] than those obtained in toluene, in particular for Pd/**1** (for Pd/**1**, see entries 1-2 *versus* 3-4; for Pd/**3**, see entries 7 *versus* 9 in Table 4.2). This behaviour could be due to the ligand degradation in toluene under basic conditions (see above), especially noteworthy at long times and high temperatures. Surprisingly for chloro-substrates, Pd/**1** catalytic system exhibited higher activity than Pd/**3** (entries 1-4 *versus* 7-10 in Table 4.2), in contrast to that observed for bromo-substrates (entries 1-8 in Table 4.1). Pd/**2** gave similar results than Pd/**3** in [BMI][PF₆] (entries 5-6 *versus* 7-8, Table 4.2).

Table 4.2. Suzuki C–C couplings between 4-R-chlorobenzene derivatives (R = CF₃, OCH₃, NO₂, NH₂) and phenylboronic acid catalysed by Pd/L systems (L = **1–3**).^a

Entry	L	Solvent	R	t [h]	Conv [%]
1	1	[BMI][PF ₆]	CF ₃	15	99 ^c
2	1	[BMI][PF ₆]	OMe	48 ^b	91 ^d
3	1	Toluene	CF ₃	15	82 ^c
4	1	Toluene	OMe	48 ^b	85 ^d
5	2	[BMI][PF ₆]	CF ₃	15	90 ^c
6	2	[BMI][PF ₆]	OMe	48 ^b	26 ^d
7	3	[BMI][PF ₆]	CF ₃	15	96 ^c
8	3	[BMI][PF ₆]	OMe	48 ^b	31 ^d
9	3	Toluene	CF ₃	15	18 ^c
10	3	Toluene	OMe	48 ^b	55 ^d
11	1	[BMI][PF ₆]	NO ₂	15	41 ^d
12	1	[BMI][PF ₆]	NH ₂	48 ^b	29 ^d
13	3	[BMI][PF ₆]	NO ₂	15	35 ^d
14	3	[BMI][PF ₆]	NH ₂	48 ^b	26 ^d

^a Reaction conditions: Pd:L:arylchloride:phenylboronic acid:sodium carbonate = 1: 1.2:100:120:250 mmol in 1 mL of [BMI][PF₆] or toluene and 2 mL of water at 60 °C; results obtained from duplicate experiments. ^b T = 100 °C. ^c Determined by ¹⁹F NMR and GC-MS. ^d Determined by ¹H NMR and GC-MS.

Similar catalytic behaviour was observed using Pd/**1** and Pd/**3** systems in [BMI][PF₆] for activated 1-chloro-4-nitrobenzene (entries 11 and 13, Table 4.2) and for deactivated 4-chloro-aniline (entries 12 and 14, Table 4.2).

4.2.3.2. Recycling experiments

Taking into account the stability of Pd/**3** catalytic system under biphasic [BMI][PF₆]/water conditions, we evaluated the recyclability for the cross-coupling reaction between 1-bromo-4-trifluorobenzene and phenylboronic acid. Reaction carried out under the catalytic conditions described in entry 1 of Table 4.1, was repeated and the product extracted from the [BMI][PF₆]/water mixture, with diethyl ether each time. The ionic liquid catalytic phase could be reused up to ten times without loss of activity (95-99% conversion), and preserving the chemoselectivity towards the cross-coupling product (Figure 4.13).

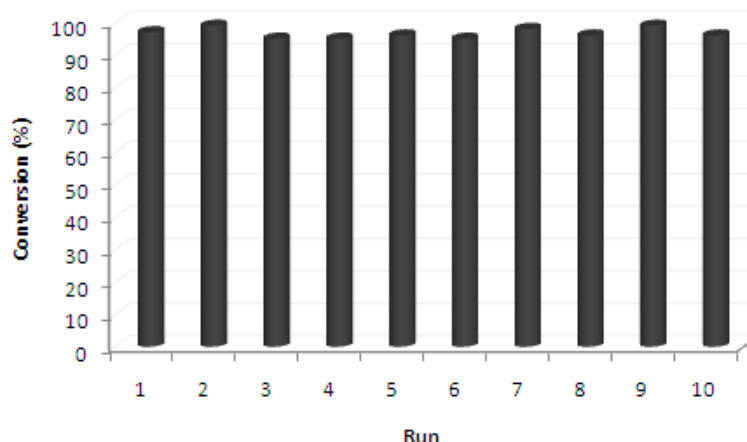
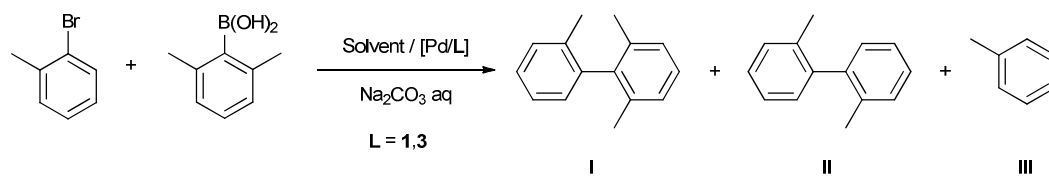


Figure 4.13. Histogram representing 1-bromo-4-trifluorobenzene conversion towards the formation of 4-(trifluoromethyl)-1,1'-biphenyl after each run of recycling, using Pd/**3** catalytic system.

4.2.3.3. Asymmetric Suzuki C–C cross-coupling

In an attempt of performing the asymmetric version of the reaction, several reactants (*ortho* and *diortho* substituted iodides and bromides: 1-bromo-2-methylbenzene, 2-bromo-1,3-dimethylbenzene, 1-iodo-2-methylbenzene, 2-iodo-1,3-dimethylbenzene, 1-bromo-2-methylnaphthalene and 1-bromo-2-methoxynaphthalene); as well as *ortho* and *diortho* substituted boronic acids: *o*-tolylboronic acid, (2,6-dimethylphenyl)boronic acid, (2-methylnaphthalen-1-yl)boronic acid and (2-methoxynaphthalen-1-yl)boronic acid) under different reaction conditions, were tested. Unfortunately, in all cases only the deboronated or dehalogenated products were mainly obtained (Scheme 4.6 and Table 4.3).



Scheme 4.6. Palladium-catalysed asymmetric Suzuki C–C couplings between 1-bromo-2-methylbenzene and 2,6-dimethylphenylboronic acid.

Table 4.3. Asymmetric Suzuki C–C couplings between 2-bromotoluene and 2,6-dimethylphenylboronic acid catalysed by Pd/L systems (L = **1**, **3**).^a

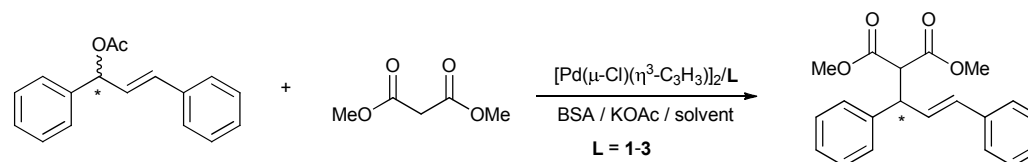
Entry	L	Solvent	Conv. [%] ^c	Selectivity I:II:III [%] ^c
1	1	[BMI][PF ₆]	100	0:0:100
2	1	Toluene	28	82:8:18
3	3	[BMI][PF ₆]	100	0:0:100
4	3	Toluene	100	3:97:0

^a Reaction conditions: Pd:L:1-methylbromide: (2,6-dimethylphenyl)boronic acid:sodium carbonate = 1:1.2:100:120:250 mmol in 1 mL of [BMI][PF₆] or toluene and 2 mL of water at 100 °C for 24 h; results obtained from duplicate experiments. ^b T = 60 °C. ^c Conversion determined by GC-MS.

In the case of the catalytic system Pd/**1** in toluene, the desired cross-coupling compound was the main product, but the conversion was low (entry 2 in Table 4.3). In [BMI][PF₆], only the dehalogenated product was obtained (entry 1, Table 4.3). Pd/**3** catalytic system mainly gave the dehalogenated and homo-coupling product in [BMI][PF₆] and toluene, respectively (entries 3 and 4, Table 4.3). At lower temperatures, the catalytic systems were inactive.

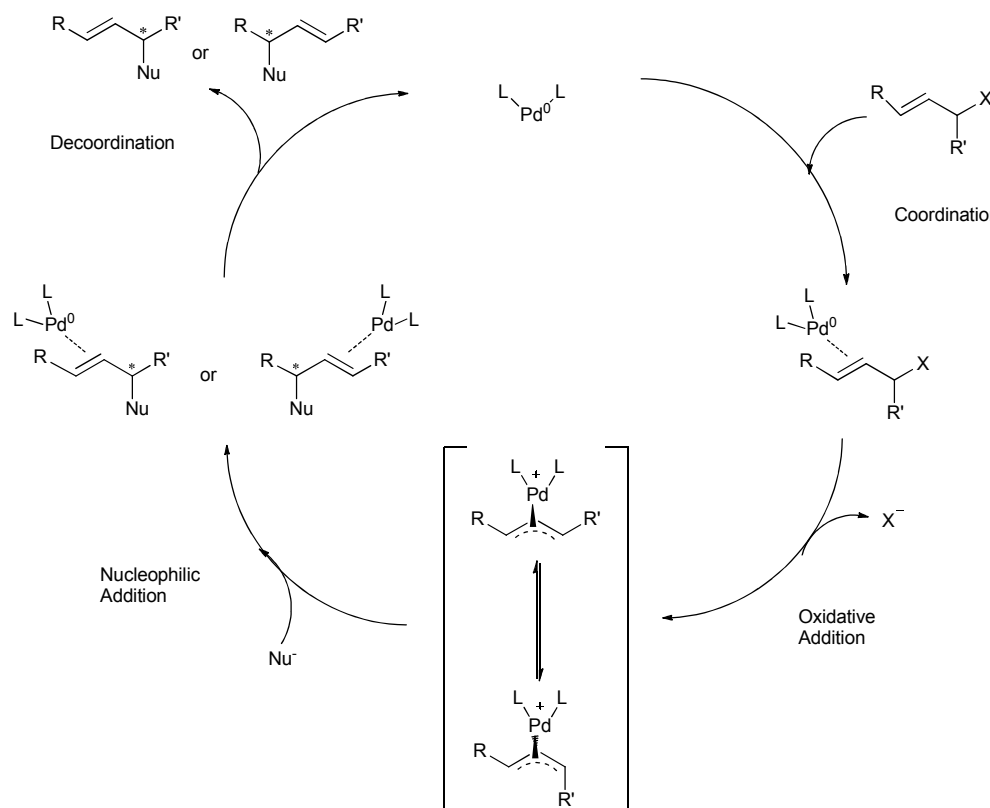
4.2.3.4. Asymmetric allylic alkylation

Palladium/L systems were tested in the benchmark allylic alkylation reaction starting from the racemic substrate 3-acetoxy-1,3-diphenyl-1-propene and dimethyl malonate as nucleophile, under basic Trost conditions (Scheme 4.7).³⁷



Scheme 4.7. Pd-catalysed asymmetric allylic alkylation.

The general catalytic cycle of the Pd-catalysed asymmetric allylic alkylation reaction using soft nucleophiles involves olefin complexation, subsequent oxidative addition, and then external nucleophilic attack and decoordination (Scheme 4.8).³⁸



Scheme 4.8. Catalytic cycle for Pd-catalysed asymmetric allylic alkylation using soft nucleophiles.

The catalytic results are summarized in Table 4.4. The catalytic precursor was generated *in situ* from $[\text{Pd}(\mu\text{-Cl})(\text{C}_3\text{H}_5)]_2$ and the appropriate ligand (**1-3**). Pd/**1** was the most active catalytic system in organic solvent, giving full conversion towards the expected product after 1h of reaction (entry 1 *versus* 2 and 3 in Table 4.4). This system led to the best asymmetric induction, however only a 26% of enantiomeric excess was achieved. Pd/**1** was also used in $[\text{BMI}][\text{PF}_6]$. The system was slower than in dichloromethane (entry 4 *versus* 1 in Table 4.4), giving also a lower enantioselectivity but towards the opposite enantiomer than that obtained in dichloromethane. The reversal of product configuration depending on the solvent nature (ionic liquid *versus* dichloromethane) has been also previously reported for copper catalysed Diels-Alder reactions.³⁹ This effect can be due to the influence of the anion nature in the catalytic intermediates.

Table 4.4. Asymmetric allylic alkylation catalysed by Pd/L systems (**L = 1-3**).^a

Entry	Ligand	Solvent	t (h)	Conv. (%) ^b	% ee ^c
1	1	CH ₂ Cl ₂	1	100	26 (<i>S</i>)
2	2	CH ₂ Cl ₂	4	100	0
3	3	CH ₂ Cl ₂	4	100	10 (<i>R</i>)
4	1	[BMI][PF ₆]	24	74	11 (<i>R</i>)

^a Reaction conditions: Pd : **1,2** = 2.5, **3** = 1.25; Pd : substrate = 50, 4 mL of CH₂Cl₂ or 1 mL [BMI][PF₆] at room temperature; results obtained from duplicate experiments. ^b Conversion determined by ¹H NMR.

^c Enantiomeric excess determined by HPLC on a Chiralcel OJ-H column.

4.3. Conclusions

New azadioxaphosphane bicyclo[3.3.0]octane ligands **1** and **2** derived from natural tartaric acid were prepared and characterized. NMR studies revealed that at least three conformers are present in solution due to the relative spatial disposition of benzyl and phosphorus substituents in both *syn* and *anti* arrangements. Modelling studies are in good agreement with the isomeric ratios observed by NMR spectroscopy. Nevertheless upon palladium coordination to give [PdCl₂(κ^1 -P-**1**)₂], the conformers are not thus far distinguished.

The catalytic systems Pd/**1-3** were highly active and selective in Suzuki C-C cross-couplings with substrates bearing both electron-donor and electron-withdrawing groups for 4-R-bromobenzene and 4-R-chlorobenzene derivatives. Using [BMI][PF₆] as solvent, the systems are active without formation of by-products allowing the activation of C-Cl bonds for substrates containing electron-donor substituents.

It is noteworthy that ligands **1-3** showed higher stability under catalytic basic biphasic conditions in [BMI][PF₆] than that observed in toluene and [EMI][PH(O)OMe]. This behaviour allowed the recycling of the catalytic phase in [BMI][PF₆] up to ten cycles without loss of activity.

Unfortunately, asymmetric Suzuki reactions were not selective towards the desired cross-coupling product, only giving the expected product in a very low yield and chemoselectivity (substrate conversion less than 30% using Pd/**1** catalytic system

in toluene). The catalytic evaluation of these chiral ligands in the Pd-catalysed asymmetric allylic alkylation model reaction gave low enantioselectivities.

4.4. Experimental

Syntheses were performed using standard Schlenk techniques under nitrogen or argon atmosphere. Organic solvents were dried following the procedures described in literature.⁴⁰ (2-methylnaphthalen-1-yl)boronic acid and (rac-3-acethoxy-1,3-diphenyl-1-propene) were synthesised following the methodology described in the literature⁴¹. PhPCl₂, Ph₂PCl, substrates, boronic acids, dimethylmalonate, potassium acetate, *N,O*-bis(trimethylsilyl)acetamide (BSA), [Pd(μ -Cl)(η^3 -C₃H₅)]₂ and [PdCl₂(COD)] were purchased from Sigma-Aldrich, Acros and Strem chemicals and used without further purification. [BMI][PF₆] and [EMI][PH(O)OMe] (99.5%) were purchased from Solvionic and treated under reduced pressure at 60 °C for 48 h prior to use. ¹H, ¹³C and ³¹P NMR spectra were recorded on a Bruker AV-300 spectrometer (300.13 MHz for ¹H) or a Brucker AV-400 (400.16 MHz for ¹H) or a Brucker AV-500 (500.13 MHz for ¹H). Chemical shifts are expressed in ppm upfield from SiMe₄. NOESY, ¹H and ¹³C correlation spectra were obtained using standard procedures. TEM experiments were performed on a Philips CM12 electron microscope operating at 120 kV with resolution of 4.5 Å. The images of particles dispersed in [BMI][PF₆] were obtained from a transmission electron microscope running at 120 kV. A drop of solution was deposited on a holey carbon grid and the excess of [BMI][PF₆] was removed in order to obtain a film as thin as possible. Images were recorded on the film of IL lying on the holes of the grid. IR spectra were recorded on a FTIR Nicolet Impact 400 spectrometer. Optical rotations were measured in a Perkin Elmer 241MC polarimeter.

4.4.1. Synthesis of P-donor ligands

4.4.1.1. (3*S*,4*S*)-1-benzylpyrrolidine-3,4-diol, 4

This compound was synthesised following the procedure described in the literature.⁴²

4.4.1.2. (3*S*,4*S*)-1-benzyl-3,4-bis(diphenylphosphinoxy)pyrrolidine, 3

This ligand was synthesised following the procedure described in the literature.⁴³.

4.4.1.3. (3*aS*,6*aS*)-5-benzyl-2-phenyltetrahydro-3*aH*-[1,3,2]dioxaphospholo[4,5-*c*]-pyrrole, 1

A solution of 100 mg (0.5 mmol) of **4** and 0.72 mL of Et₃N in 6.6 mL of THF were added dropwise to a solution of 0.07 mL of PhPCl₂ (0.5 mmol) in 1 mL of toluene at room temperature. The reaction mixture was stirred overnight affording a white suspension. The suspension was filtered through anhydrous basic alumina under argon atmosphere and solvent was evaporated obtaining the monophosphonite as a white powder (120 mg, 80%). $[\alpha]_D^{25} = +46.7^\circ$ (*c* 0.97 in CH₂Cl₂) ν_{max} (IR, KBr, pellet)/cm⁻¹ 1104 (P-O-C, st, s), 746 (P-O-C, st, w), 828 (P-C, st, w) HRMS (CI-CH₄) *m/z*: 299.1081 [M]⁺. C₁₇H₁₈NO₂P requires 299.1075.

Isomer "A" (48%): ¹H NMR (500.13 MHz, CD₂Cl₂, 298 K): δ = 2.30 (m, 1H, CH₂CH), 2.40 (m, 1H, CH₂CH), 2.57 (m, 1H, CH₂CH), 2.98 (m, 1H CH₂CH), 3.53 (d, 1H, CHHBn), 3.45 (d, 1H, CHHBn), 4.59 (m, 1H, CH), 4.77 (m, 1H, CH), 7.13-7.65 (m, 10 CChar). ¹³C NMR (125.5 MHz, CD₂Cl₂, rt): δ = 58.5 (CH₂CH, *J*_{CP} = 3.8 Hz), 58.9 (CH₂CH, *J*_{CP} = 3.8 Hz), 59.8 (CH₂Bn), 79.3 (CH, *J*_{CP} = 11.3 Hz), 84.1 (CH, *J*_{CP} = 8.8 Hz), 127 (CH_{ar}), 128.1 (CH_{ar}), 128.3 (CH_{ar}P, *J*_{CP} = 8.8 Hz), 128.3 (CH_{ar}), 128.5 (CH_{ar}), 128.6 (CH_{ar}), 130 (CH_{ar}P, *J*_{CP} = 21.3 Hz), 130.2 (CH_{ar}), 138.2 (C_{ipso}Bn), 140.1 (C_{ipso}P, *J*_{CP} = 23.8 Hz). ³¹P NMR (121.4 MHz, CD₂Cl₂, rt): δ = 149.66.

Isomer "B" (30%): ¹H NMR (500.13 MHz, CD₂Cl₂, 298 K): δ = 2.83 (m, 2H, CH₂CH), 3.18 (m, 2H, CH₂CH), 3.74 (d, 1H, CHHBn), 3.68 (d, 1H, CHHBn), 4.39 (m, 1H, CH), 4.97 (m, 1H, CH), 7.13-7.65 (m, 10 CChar). ¹³C NMR (125.5 MHz, CD₂Cl₂, rt): δ = 58.0 (CH₂CH, *J*_{CP} = 2.5 Hz), 59.8 (CH₂CH), 60.3 (CH₂Bn), 78.1 (CH, *J*_{CP} = 11.3 Hz), 84.7 (CH, *J*_{CP} = 16.3 Hz), 127.1 (CH_{ar}), 128.2 (CH_{ar}), 128.3 (CH_{ar}P, *J*_{CP} = 8.8 Hz), 128.6 (CH_{ar}P), 128.8 (CH_{ar}), 130 (CH_{ar}P, *J*_{CP} = 21.3 Hz), 130.3 (CH_{ar}), 138.3 (C_{ipso}Bn), 140.5 (C_{ipso}P, *J*_{CP} = 23.8 Hz). ³¹P NMR (121.4 MHz, CD₂Cl₂, rt): δ = 150.69.

Isomer "C" (22%): ^1H NMR (500.13 MHz, CD_2Cl_2 , 298 K): δ = 2.06 (m, 2H, CH_2CH), 2.17 (m, 2H, CH_2CH), 3.37 (d, 1H, CHHBn), 3.22 (d, 1H, CHHBn), 4.39 (m, 1H, CH), 4.97 (m, 1H, CH), 7.13-7.65 (m, 10 CChar). ^{13}C NMR (125.5 MHz, CD_2Cl_2 , rt): δ = 58.0 (CH_2CH , $J_{\text{CP}} = 2.5$ Hz), 59.5 (CH_2Bn), 59.8 (CH_2CH), 78.1 (CH, $J_{\text{CP}} = 11.3$ Hz), 84.7 (CH, $J_{\text{CP}} = 16.3$ Hz), 126.9 (CH_{ar}), 128.2 (CH_{ar}), 128.3 (CH_{arP} , $J_{\text{CP}} = 8.8$ Hz), 128.6 (CH_{ar}), 128.8 (CH_{ar}), 130 (CH_{arP} , $J_{\text{CP}} = 21.3$ Hz), 130.3 (CH_{ar}), 138.2 (C_{ipsoBn}), 140.5 (C_{ipsoP} , $J_{\text{CP}} = 23.8$). ^{31}P NMR (121.4 MHz, CD_2Cl_2 , rt): δ = 150.69.

4.4.1.4. (3a*S*,6a*S*)-5-benzyl-2-phenoxytetrahydro-3a*H*-[1,3,2]dioxaphospholo[4,5-*c*]-pyrrole, 2

0.023 mL (0.26 mmol) of PCl_3 were dropwise added to a solution of 50 mg (0.26 mmol) of **4** and 0.072 mL of Et_3N in 20 mL of THF at -110 °C and stirred at 70 °C for 5 h. Then the solvent was removed under reduced pressure and 20 mL of THF were added and mixture cooled at -110 °C, after 24 mg of phenol in 20 mL of THF and 0.036 mL of Et_3N were dropwise added over a period of 15 min. The reaction mixture was stirred 3 h affording a white suspension. The suspension was filtered through anhydrous basic alumina under argon atmosphere and solvent was evaporated obtaining the monophosphite as a white powder (73 mg, 88%). $[\alpha]_D^{25} = +51.5^\circ$, (c 1.1 in CH_2Cl_2) ν_{max} (IR, KBr, pellet)/cm⁻¹ 1099 (P-O-Car, st, w), 838 (P-O, st, s), 744 (P-O-C, st, w). HRMS (Cl-CH₄) *m/z*: 316.1102 ([M]⁺H) $\text{C}_{17}\text{H}_{19}\text{NO}_3\text{P}$ requires 316.1103.

Isomer "A" (40%): ^1H NMR (500.13 MHz, CDCl_3 , 298 K): δ = 2.58 (m, 1H, CHHCH), 2.73 (m, 1H, CHHCH), 2.95 (m, 1H, CHHCH), 3.06 (m, 1H, CHHCH), 3.63 (d, 1H, CHHBn), 3.59 (d, 1H, CHHBn), 5.28 (m, 1H, CH), 4.71 (m, 1H, CH), 7.01-7.36 (m, 10 CChar). ^{13}C NMR (125.5 MHz, CDCl_3): δ = 58.3 (CH_2CH , $J_{\text{CP}} = 5$ Hz), 59.6 (CH_2CH), 59.9 (CH_2Bn), 78.4 (CH, $J_{\text{CP}} = 2.5$ Hz), 78.6 (CH, $J_{\text{CP}} = 20.1$ Hz), 119.6-129.7 (CH_{ar}), 133.9 (C_{ipsoBn}), 152.4 (C_{ipsoP} , $J_{\text{CP}} = 8.8$ Hz). ^{31}P NMR (202.5 MHz, CDCl_3): δ = 128.7.

Isomer "B" (36%): ^1H NMR (500.13 MHz, CDCl_3 , 298 K): δ = 2.55 (m, 1H, CHHCH), 2.75 (m, 1H, CHHCH), 2.95 (m, 1H, CHHCH), 3.058 (m, 1H, CHHCH), 3.77 (d, 1H, CHHBn), 3.67 (d, 1H, CHHBn), 4.78 (m, 1H, CH), 5.16 (m, 1H, CH), 7.01-7.36 (m, 10 CChar). ^{13}C NMR (125.5 MHz, CDCl_3 , rt): δ = 58.2 (CH_2CH , $J_{\text{CP}} = 2.5$ Hz), 59.7 (CH_2CH), 60.1 (CH_2Bn),

76.5 (CH, J_{CP} = 6.3 Hz), 77.4, 119.5-129.7 (CH_{ar}), 138.2 (C_{ipso}Bn), 152 (C_{ipso}P, J_{CP} = 6.3 Hz).
³¹P NMR (202.5 MHz, CDCl₃, rt): δ = 128.64.

Isomer “C” (24%): ¹H NMR (500 MHz, CDCl₃, 298 K): δ = 2.81 (m, 2H, CH₂CH), 3.14 (m, 2H, CH₂CH), 3.60 (d, 1H, CHHBn), 3.64 (d, 1H, CHHBn), 5.36 (m, 2H, CH), 7.01-7.36 (m, 10 CHar). ¹³C NMR (125.5 MHz, CDCl₃, rt): δ = 59.4 (CH₂CH, J_{CP} = 2.5 Hz), 60.2 (CH₂Bn), 75.5 (CH, J_{CP} = 6.3 Hz), 119.6-129.7 (CH_{ar}), 137.7 (C_{ipso}Bn), 152 (C_{ipso}P, J_{CP} = 5).
³¹P NMR (202.5 MHz, CDCl₃, rt): δ = 127.69.

4.4.2. Synthesis of Pd complexes

4.4.2.1. Dichloro- κ^1 -P-bis-{(3a*S*,6*aS*)-5-benzyl-2-phenyltetrahydro-3*aH*-[1,3,2]dioxaphospholo[4,5-*c*]pyrrole}palladium(II), Pd1

To a solution of 0.046 g (0.154 mmol) of ligand **1** in 20 mL of anhydrous and deoxygenated toluene it was added 0.027 g (0.077 mmol) of the palladium precursor [PdCl₂(COD)]. The reaction mixture was then heated at 50 °C and stirred during 2 h. Then the solvent was evaporated under reduced pressure and the precipitate washed with ethyl ether. The complex was obtained as a yellowish powder (0.070 g, 59%). δ_H ¹H NMR (400.16 MHz, CD₂Cl₂, 213 K): δ 3.05 (m, 4H, CH₂CH), 3.16 (m, 4H, CH₂CH), 3.70 (d, 2H, CH₂Bn), 3.78 (d, 2H, CH₂Bn), 5.04 (bs, 2H, CH), 6.14 (m, 2H, CH), 7.27-7.63 (m, 20H, ar) ¹³C NMR (125.47 MHz, CD₂Cl₂, rt): δ = 57.5 (pt, J_{CP} = 5 Hz, CH₂CH), 58.3 (pt, J_{CP} = 5 Hz, CH₂CH), 59.3 CH₂Bn, 83 (pt, J_{CP} = 2.5 Hz, CH), 83.1 (pt, J_{CP} = 2.5 Hz, CH), 127.5 CH_{ar}, 127.6 (pt, J_{CP} = 7 Hz, CH_{ar}P), 128.5 CH_{ar}, 128.7 CH_{ar}, 130.8 (pt, J_{CP} = 5.7 Hz, CH_{ar}P), 132.2 CH_{ar}, 134.0 (d, J_{CP} = 96 Hz, C_{ipso}P), 137.5 C_{ipso}Bn. ³¹P NMR (121.50 MHz, CD₂Cl₂, rt): δ = 130.44. ν_{max} (IR, KBr, pellet)/cm⁻¹ 749 (P-C, st, w), 1022 (P-O-Cal, st), 1437 (C-N, st,w), 2961 (C=C, st,w). EA C 52.69, H 4.72, N 3.57. C₃₄H₃₆Cl₂N₂O₄P₂Pd requires C 52.63, H 4.68, N 3.61. HRMS (ESI) *m/z*: 737.0886 [M]⁺-Cl. C₃₄H₃₆N₂O₄ClPd requires 737.0879.

4.4.2.2. *Dichloro- κ^2 -P,P-(3S,4S)-1-benzyl-3,4-bis(diphenylphosphinoxy)pyrrolidine]-palladium(II), Pd3*

To a solution of 0.043 g (0.077 mmol) of ligand **3** in 20 mL of anhydrous and deoxygenated toluene it was added 0.027 g (0.077 mmol) of the palladium precursor [PdCl₂(COD)]. The reaction mixture was then heated at 50 °C and stirred during 2 h. Then the solvent was evaporated under reduced pressure and the precipitate washed with ethyl ether. The complex was obtained as a yellowish powder. (44 mg, 77%). ¹H NMR (300.13 MHz, CD₂Cl₂, 298 K): δ = 2.59 (m, 2H, CH₂CH), 2.85 (m, 2H, CH₂CH), 3.40 (d, 1H, CH₂Bn), 3.64 (d, 1H, CH₂Bn), 4.81 (2H, m, 2CH), 7.055-8.1 (25H, m, ar); ¹³C NMR (75.47 MHz, CD₂Cl₂, rt): δ = 57.3 (pt, J_{CP} = 3.5, 3.5 Hz, CH₂), 59.8 (CH₂), 77.2 (CH₂Bn), 80.6 (2CH), 127.5 (CH_{ar}), 127.9 (pt, J_{CP} = 6 Hz, CH_{ar}P), 128.4 (CH_{ar}), 128.7 (CH_{ar}), 128.8 (pt, J_{CP} = 6 Hz, CH_{ar}P), 130.8 (dd, J_{CP} = 27.8, 27 Hz, C_{ipso}P), 131.2 (CH_{ar}), 132.1 (pt, J_{CP} = 6 Hz, CH_{ar}P), 133.1 (CH_{ar}), 134.9 (pt, J_{CP} = 6.8 Hz, CH_{ar}P), 135.1 (dd, J_{CP} = 135.1, 93.8 Hz, C_{ipso}P), 136.8 C_{ipso}Bn ³¹P NMR (121.4 MHz, CD₂Cl₂, rt): δ = 121.79; ν_{max} (IR, KBr, pellet)/cm⁻¹ 1047 (P-O-C, st, s), 745 (P-O-C, st, w), 717 (O-C, st, w), HRMS (Cl-CH₄) *m/z*: 702.0712 [M]⁺·Cl. C₃₅H₃₃NO₂P₂ClPd requires 702.0710.

4.4.3. Catalytic experiments

4.4.3.1. General procedure for catalytic Suzuki C-C coupling in ionic liquid

Dichloro(cycloocta-1,5-diene)palladium(II) (2.8 mg, 0.01 mmol) and the corresponding ligand (0.012 or 0.024 mmol) were dissolved in 1 mL of the corresponding ionic liquid, [BMI][PF₆] or [EMI][HPO(O)Me] and stirred for 30 min. under vacuum at room temperature, giving a colorless or yellowish solution. After this time, the substrate (1 mmol), the boronic acid (1.5 mmol) and Na₂CO₃ (265.0 mg, 2.5 mmol) dissolved in 2 mL of deoxygenated water were consecutively added, forming a biphasic system. The mixture was then heated at 60 or 100 °C during 1, 24 or 48 h and then cooled at room temperature. The catalytic mixture was extracted with ethyl ether (5 X 2 mL) then the organic phase washed with 1 mL of NaOH 1M, 1 mL of water and dried with anhydrous Na₂SO₄, filtered and concentrated under reduced pressure, yielding the product either as a solid or as a yellow oil.

4.4.3.2. General procedure for catalytic Suzuki C-C coupling in toluene

Dichloro(cycloocta-1,5-diene)palladium(II) (2.8 mg, 0.01 mmol) and the corresponding ligand (0.012 or 0.024 mmol) were dissolved in 1 mL of freshly distilled toluene and allowed to stir for 30 min, forming a colourless or yellowish solution. After this time, the substrate (1 mmol), the boronic acid (1.5 mmol) and Na₂CO₃ (265.0 mg, 2.5 mmol) dissolved in 2 mL of deoxygenated water were consecutively added, forming a biphasic system. The mixture was then heated at 60 or 100 °C during 1, 24 or 48 h and then cooled at room temperature. The catalytic mixture was extracted with ethyl ether (5 X 2 mL) then the organic phase washed with 1 mL of NaOH 1M, 1 mL of water and dried with anhydrous Na₂SO₄, filtered and concentrated under reduced pressure, yielding the product either as a solid or as a yellow oil.

4.4.3.3. General procedure for catalytic asymmetric allylic alkylation in [BMI][PF₆]

3.7 mg (0.02 mmol) of [Pd(μ -Cl)(η^3 -C₃H₃)]₂ and 0.1 mmol of ligand were dissolved in 1 mL of [BMI][PF₆] and stirred under vacuum for 30 minutes then 252 mg (1 mmol) of substrate (rac-3-acethoxy-1,3-diphenyl-1-propene, 396 mg (1 mmol) of dimethylmalonate, 610 mg and 3 mg of potassium acetate were added. After the reaction, the products were extracted with diethylether then extracted with aqueous NH₄Cl 10% (3 mL X 3) and water (3 mL X 3). The organic phase was dried over MgSO₄, filtered and solvent was removed under vacuum.

4.4.3.4. General procedure for catalytic asymmetric allylic alkylation in dichloromethane

3.7 mg (0.02 mmol) of [Pd(μ -Cl)(η^3 -C₃H₃)]₂ and 0.05 or 0.1 mmol of the corresponding ligand were dissolved in 1 mL of CH₂Cl₂ and stirred for 30 minutes then 252 mg (1 mmol) of substrate (rac-3-acethoxy-1,3-diphenyl-1-propene) dissolved in 1 mL of CH₂Cl₂, 396 mg (1 mmol) of dimethylmalonate in 1 mL of CH₂Cl₂, 610 mg of BSA dissolved in 1 mL of CH₂Cl₂ and 3 mg of potassium acetate were added. After the reaction, 10 mL of diethylether were added and then extracted with aqueous NH₄Cl 10% (3 mL X 3) and water (3 mL X 3). The organic phase was dried over MgSO₄, filtered and solvent was removed under vacuum.

4.5. References

- ¹ W. S. Knowles and M. J. Sabacky. *Chem. Commun.* **1968**, 1445.
- ² L. Horner, H. Siegel and H. Büthe. *Angew. Chem. Int. Ed. Engl.* **1968**, **7**, 941.
- ³ a) H. B. Kagan and T. P. Dang. *Chem. Commun.* 1971, 481; b) H. B. Kagan and T. P. Dang. *J. Am. Chem. Soc.* **1972**, **94**, 64298.
- ⁴ For recent selected reviews, see: a) A. Marinetti and D. Carmichael. *Chem. Rev.* **2002**, **102**, 201. b) W. Thang and X. Zhang. *Chem. Rev.* **2003**, **103**, 3029.
- ⁵ *Phosphorus Ligands in Asymmetric Catalysis*, A. Börner, (Ed). Wiley-VCH, Weinheim, **2008**, chapter 2.
- ⁶ M. J. Burk, J. E. Feaster and R. L. Harlow. *Organometallics*. **1990**, **9**, 2653.
- ⁷ For selected reviews, see: a) C. Lescop and M. Hissler in *Tomorrow's Chemistry Today* B. Pignataro. (Ed.) Wiley-VCH, New York, **2008**, pp 295. b) K. M. Pietrusiewicz, M. Zablocka. *Chem. Rev.* **1994**, **94**, 1375.
- ⁸ a) *Phosphorus-carbon heterocyclic chemistry: The rise of a new domain*, ed.: F. Mathey, Pergamon, Oxford, **2001**; b) F. Leca, M. Sauthier, B. le Guennic, C. Lescop, L. Toupet and J.-F. Halet and R. Réau. *Chem. Commun.* **2003**, 1774. c) F. Leca, C. Lescop, L. Toupet and R. Réau. *Organometallics*. **2004**, **23**, 6191. d) Z. Pakulski, R. Kwiatosz and K. M. Pietrusiewicz. *Tetrahedron*. **2005**, **61**, 1481. e) F. Leca, F. Fernández, G. Muller, C. Lescop, R. Réau and M. Gómez. *Eur. J. Inorg. Chem.* **2009**, 5583.
- ⁹ a) G. C. Fu. *Acc. Chem. Res.* **2006**, **39**, 853. b) C. Ganter in *Phosphorus Ligands in Asymmetric Catalysis*, ed. A. Börner, Wiley-VCH, Weinheim, **2008**, chapter 4.3
- ¹⁰ Selected papers: a) F. Mathey, F. Mercier and C. Charrier. *J. Am. Chem. Soc.* **1981**, **103**, 4595. b) M. Siutkowski, F. Mercier, L. Ricard and F. Mathey. *Organometallics*. **2006**, **25**, 2585. c) M. Clochard, E. Mattmann, F. Mercier, L. Ricard and F. Mathey. *Org. Lett.* **2003**, **5**, 3093.
- ¹¹ E. Vedejs and O. Daugulis. *J. Am. Chem. Soc.* **1999**, **121**, 5813.
- ¹² Z. Pakulski, O. M. Demchuk, J. Frelek, R. Luboradzki and K. M. Pietrusiewicz. *Eur. J. Org. Chem.* **2004**, 3913.
- ¹³ Y-Y. Yan and T. V. RajanBabu. *Org. Lett.* **2000**, **2**, 199.

- ¹⁴ a) J. M. Brunel, T. Constantieux and G. Buono. *J. Org. Chem.* **1999**, 64, 8940. b) G. Delapierre, T. Constantieux, J. M. Brunel and G. Buono. *Eur. J. Org. Chem.* **2000**, 2507. c) G. Delapierre, J. M. Brunel, T. Constantieux and G. Buono. *Tetrahedron: Asymmetry*. **2001**, 12, 1345.
- ¹⁵ a) S. Breedon and M. Wills. *J. Org. Chem.* **1999**, 64, 9735. b) S. E. Lyubimov, V. A. Davankov, P. V. Petrovskii and N. M. Loim. *Rus. Chem. Bull.* **2004**, 56, 2094. c) K. N. Gavrilov, S. E. Lyubimov, O. G. Bondarev, M. G. Maksimova, S. V. Zheglov, P. V. Petrovskii, V. A. Davankov and M. T. Reetz. *Adv. Synth. Catal.* **2007**, 349, 609. d) K. N. Gavrilov, S. E. Lyubimov, S. V. Zheglov, E. B. Benetsky, P. V. Petrovskii, E. A. Rastorguev, T. B. Grishina and V. A. Davankov. *Adv. Synth. Catal.* **2007**, 349, 1085. e) K. N. Gavrilov, E. B. Benetsky, T. B. Grishina, E. A. Rastorguev, M. G. Maksimova, S. V. Zheglov, V. A. Davankov, B. Schäffner, A. Börner, S. Rosset, G. Bailat and A. Alexakis. *Eur. J. Org. Chem.* **2009**, 3923.
- ¹⁶ O. G. Bondarev, R. Goddard. *Tetrahedron Lett.* **2006**, 47, 9013.
- ¹⁷ a) M. Köck, A. Grube, I. B. Seiple and P. S. Baran. *Angew. Chem. Int. Ed.* **2007**, 46, 6586. b) L. A. Paquette and T. M. Morwick. *J. Am. Chem. Soc.* **1997**, 119, 1230. c) L. A. Paquette, A. T. Hamme II, L. H. Kuo, J. Doyon and R. Kreuzholz. *J. Am. Chem. Soc.* **1997**, 119, 1242. d) L. A. Paquette, L. H. Kuo and J. Tae. *J. Org. Chem.* **1998**, 63, 2010.
- ¹⁸ M. Mori, F. Saitoh, N. Uesaka, K. Okamura and T. Date. *J. Org. Chem.* **1994**, 59, 4993.
- ¹⁹ a) N. Miyaura, K. Yamada and A. Suzuki. *Tetrahedron Lett.* **1979**, 36, 3437. b) B. H. Lipshutz, S. Tasler, W. Chrisman, B. Spliethoff and B. Tesche. *J. Org. Chem.* **2003**, 68, 1177.
- ²⁰ a) N. T. S. Pham, M. Van Der Sluys and C. W. Jones. *Adv. Synth. Catal.* **2006**, 348, 609. For recent reviews, see: b) N. Miyaura and A. Suzuki. *Chem. Rev.* **1995**, 95, 2457. c) A. Suzuki. *J. Organomet. Chem.* **1999**, 576, 147. d) N. Miyaura, in: *Topics in Current Chemistry*, (Ed.: N. Miyaura), Springer-Verlag: Berlin, **2002**, Vol. 219, p 11. e) S. Kotha, K. Lahiri and D. Kashinath. *Tetrahedron*. **2002**, 58, 9633. f) F. Bellina, A. Carpita and R. Rossi. *Synthesis*. **2004**, 2419.
- ²¹ W. Stunkel, H. Wang and Z. Ying. WO/2005/040161.

- ²² G. W. Gray, M. Hird, A. D. Ifill, W. E. Smith and K. J. Toyne. *Liquid Crystals.* **1995**, 19, 77.
- ²³ H. Yasuda and V. Orlov. US Patent No. AC07C20900FI.
- ²⁴ A. O. Aliprantis and J. W. Canary. *J. Am. Chem. Soc.* **1994**, 116, 6985.
- ²⁵ a) A. F. Littke, C. Dai and G. C. Fu. *J. Am. Chem. Soc.* **2000**, 122, 4020. b) T. E. Barder, S. D. Walker, J. R. Martinelli and S. L. Buchwald. *J. Am. Chem. Soc.* **2005**, 127, 4685. c) N. Marion, O. Navaroo, J. Mei, E. D. Stevens, N. M. Scott and S. P. Nolan. *J. Am. Chem. Soc.* **2006**, 128, 4101. d) K. W. Anderson and S. L. Buchwald. *Angew. Chem. Int. Ed.* **2005**, 44, 6173.
- ²⁶ A. F. Trindade, P. M. P. Gois and C. A. M. Afonso. *Chem. Rev.* **2009**, 109, 418-514.
- ²⁷ R. Singh, M. Sharma, R. Mamgain and D. S. Rawat. *J. Braz. Chem. Soc.* **2008**, 19, 357. and references included therein.
- ²⁸ B. Zhao, X. Peng, Z. Wang, C. Xia and K. Ding. *Chem. Eur. J.* **2008**, 14, 7847.
- ²⁹ M. T. Reetz and G. Mehler, *Angew. Chem. Int. Ed.* **2000**, 39, 3889.
- ³⁰ L. D. Quin. *A Guide to Organophosphorus Chemistry.* Wiley Interscience, **2000**. New York.
- ³¹ a) D. A. Couch, S. D. Robinson and J. N. Wingfield. *J. Chem. Soc. Dalton Trans.* **1974**, 1309. b) M. Giménez-Pedrós, A. Aghmiz, N. Ruiz and A. M. Masdeu-Bultó. *Eur J. Inorg. Chem.* **2006**, 1067.
- ³² R. K. Sharma, M. Nethaj and A. G. Samuelson. *Tetrahedron: Asymmetry.* **2008**, 19, 655.
- ³³ B. Xin, Y. Zhang, L. Liu and Y. Wang. *Synlett.* **2005**, 20, 3083.
- ³⁴ a) Y. C. Lai, H. Y. Chen, W. C. Hung, C. C. Lin and F. E. Hong. *Tetrahedron.* **2005**, 61, 9484. b) A. Jutand and A. Mosleh. *Organometallics.* **1995**, 14, 1810.
- ³⁵ F. Fernández, B. Cordero, J. Durand, G. Muller, F. Malbosc, Y. Kihn, E. Teuma and M. Gómez. *Dalton Trans.* **2007**, 47, 5572 and references therein.
- ³⁶ S. Jansat, J. Durand, I. Favier, F. Malbosc, C. Pradel, E. Teuma and M. Gómez. *ChemCatChem.* **2009**, 1, 244.
- ³⁷ B. M. Trost and D. J. Murphy. *Organometallics.* **1985**, 4, 1143.
- ³⁸ B. M. Trost and M. L. Crawley, *Chem. Rev.* **2003**, 103, 2921.

- ³⁹P. Goodrich, C. Hardacre, C. Paun, V. I. Pârvulescu and I. Podolean. *Adv. Synth. Catal.* **2008**, *350*, 2473.
- ⁴⁰D. D. Perrin and W. L. F. Armarego. *Purification of Laboratory Chemicals*. 3^a Ed. Pergamon Press, Oxford, **1988**.
- ⁴¹a) M. Genov, A. Almorín and P. Espinet. *Chem. Eur. J.* **2006**, *12*, 9346. b) P. von Matt, G. C. Lloyd Jones, A. B. E. Minidis, A. Pfaltz, L. Macko, M. Neuberger, M. Zehnder, H. Rüegger and P. S. Pregosin. *Helv. Chim. Acta*. **1995**, *78*, 265.
- ⁴²A. Hui, J. Zhang, J and Z. Wang. *Synth. Commun.* **2008**, *38*, 2374.
- ⁴³M. Yatagai, T. Yamagishi and M. Hida. *Bull. Chem. Soc. Jpn.* **1984**, *57*, 823.

Chapter 5

Rh-catalysed
Asymmetric
Hydrogenation in
Non-Conventional
Solvents

UNIVERSITAT ROVIRA I VIRGILI
ORGANOMETALLIC COMPOUNDS AND METAL NANOPARTICLES AS CATALYSTS IN LOW ENVIRONMENTAL IMPACT SOLVENTS
Martha Verónica Escárcega Bobadilla
ISBN:978-84-694-1249-7/DL:T-324-2011

5.1. Introduction

Asymmetric hydrogenation of unsaturated substrates (alkenes, ketones or imines) stands for an economical and environmental friendly strategy to produce biologically active compounds such as drugs, agrochemicals and fragrances without generation of by-products.¹ Prochiral olefins, *e.g.* α -dehydroamino acids and itaconic acid derivatives, enamides and β -aminoacrylates, represent model substrates for the evaluation of chiral ligands in enantioselective hydrogenation processes,² in particular catalysed by rhodium systems containing P-donor ligands (Scheme 5.1). Since the successful results published in the 1970s using Rh complexes containing DIOP,³ CAMP⁴ and DIPAMP⁵ optically pure phosphines (Figure 5.1), a plethora of P-donor ligands has been described, especially C_2 -symmetrical chiral diphosphines.⁶ Later, in the 2000s, monophosphorus donor ligands have also applied inducing high enantioselectivities in the hydrogenation of unsaturated functions, in particular in the reduction of carbon-carbon double bonds.^{2c,7} For the first time, Reetz and co-workers designed a chiral monophosphite ligand containing a BINOL (1,1'-Bi-2-naphthol) backbone, leading to high asymmetric inductions for the asymmetric hydrogenation of dehydroamino-acids and dimethyl itaconate.^{7b} Since that, ligands of type (BINOL)P-OR have been successfully applied in the hydrogenation of model substrates,⁸ also atropoisomeric ligands containing a biphenyl skeleton have been also developed for Rh-catalysed asymmetric hydrogenations.⁹

During the last years, homogeneous enantioselective hydrogenations have been also carried out in reaction medium other than that commonly used organic solvents. The most applied alternative media concern aqueous systems, ionic liquids and supercritical fluids. In water, Sinou *et al.* reported a decrease of enantioselectivity using sulphonated phosphines.¹⁰ Therefore, the best results were observed with sulphonated versions of CHIRAPHOS and PROPHOS ligands (Figure 5.1), but in general the tendency in this reaction medium is an enantioselectivity decrease in comparison with that obtained in organic solvents. However, in some cases, reactions in water gave higher enantiomeric excesses values than in methanol or ethanol, when sulphonated version of BINAP was used (Figure 5.1).¹¹

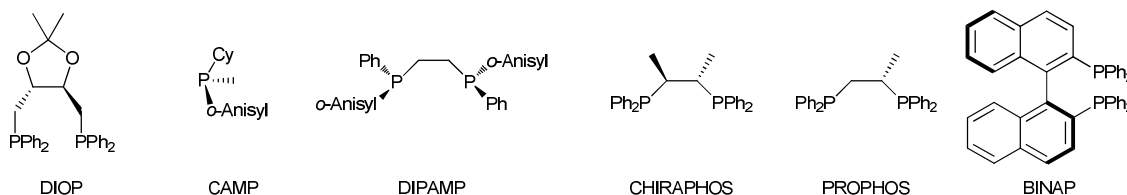


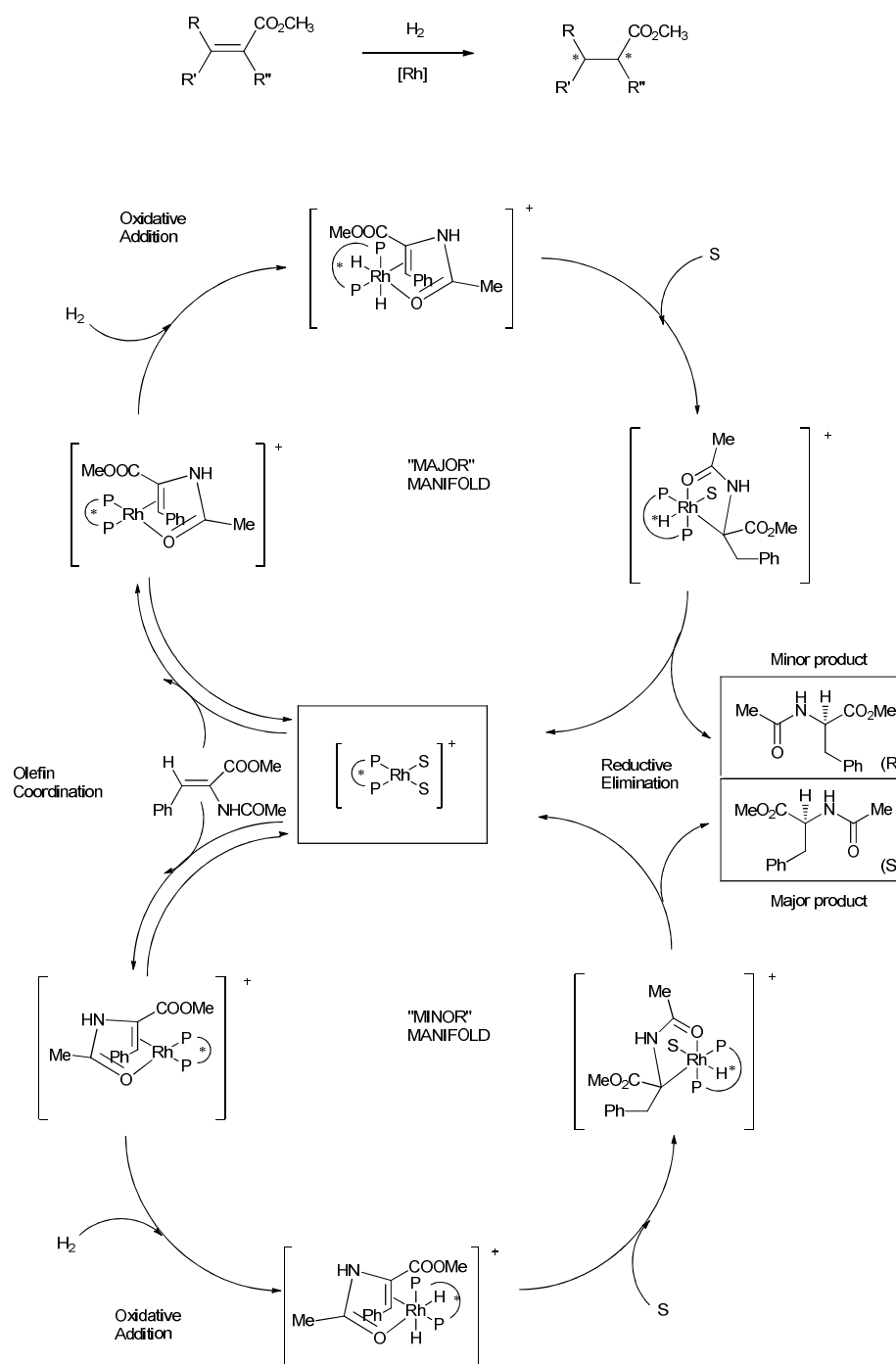
Figure 5.1. Chiral P-donor ligands used in asymmetric hydrogenation of functionalised olefins.

Using scCO₂ as solvent, few works have been reported using monophosphorus ligands in asymmetric hydrogenation, in contrast to those employing bidentate P-donor ones.¹² Recently, Lyubimov and co-workers have applied BINOL derived chiral monodentate phosphites and phosphoramidites in Rh-catalysed asymmetric hydrogenation of dimethyl itaconate obtaining high conversions and enantioselectivities (up to 90%), close to those obtained in dichloromethane but at 100 atm of dihydrogen pressure,¹³ in contrast to previous works where lower selectivities were obtained in scCO₂ in comparison to those in conventional organic solvents by using both, chiral mono and bidentate P-donor ligands.¹⁴

The use of ionic liquids in asymmetric synthesis has been reviewed in the last years.¹⁵ In relation to Rh-catalysed enantioselective hydrogenation containing monodentate ligands, Gavrilov, Reetz and co-workers have recently designed monophosphorus ligands bearing ionic moieties in order to efficiently immobilize the catalytic system in ionic liquid medium.¹⁶ In addition, chiral ionic liquids can enhance the enantioselectivity of the metal-catalysed asymmetric hydrogenations in the presence of racemic ligands and favour the formation of the opposite enantiomer obtained when organic solvents are involved, as demonstrated by Leitner and co-workers.¹⁷

The “classical” catalytic cycle for enantioselective hydrogenation, has been described for the first time by Halpern *et al.*¹⁸ and is described in Scheme 5.1. The first step, which is reversible, is the olefin coordination to the metal centre, forming the diastereoisomeric minor and major species (shown by separate manifolds). The following step is the oxidative addition of dihydrogen, which in fact, determines the enantioselectivity. Studies based on measuring equilibrium constants, have proposed

that the enantioselectivity is given by the higher reactivity with hydrogen of the minor olefinic complex (thermodynamically unfavoured) than their major homologue, which gives the most thermodynamically favoured minor product of the oxidant addition. The next step is the insertion of the olefin in the Rh-H bond to form the corresponding species M-alkyl and finally, by reductive elimination, the formation of the *R* as the minor and *S* as the major organic products.



Scheme 5.1. General reaction and catalytic cycle for the asymmetric hydrogenation reaction of functionalised olefins.

In this chapter, the synthesis of two new fluorinated phosphite ligands, **1** and **2** derived from (*R*)-BINOL as well as phosphonite **3** and phosphite **4** derived from natural tartaric acid (Figure 5.2), previously discussed in Chapter 4, have been applied in Rh-catalysed asymmetric hydrogenation. New cationic Rh(I) complexes, **Rh1** and **Rh3**, as well as supported **Rh1** on functionalised multi-walled carbon nanotubes (MWCNT), **Rh1-IL-MWCNT**, have been used as catalytic precursors in asymmetric hydrogenation reaction in different solvents, such as dichloromethane, scCO₂, [BMI][PF₆] and the mixture [BMI][PF₆]/scCO₂.

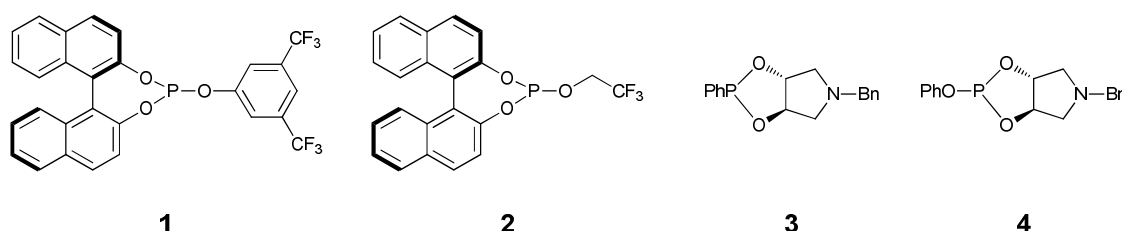
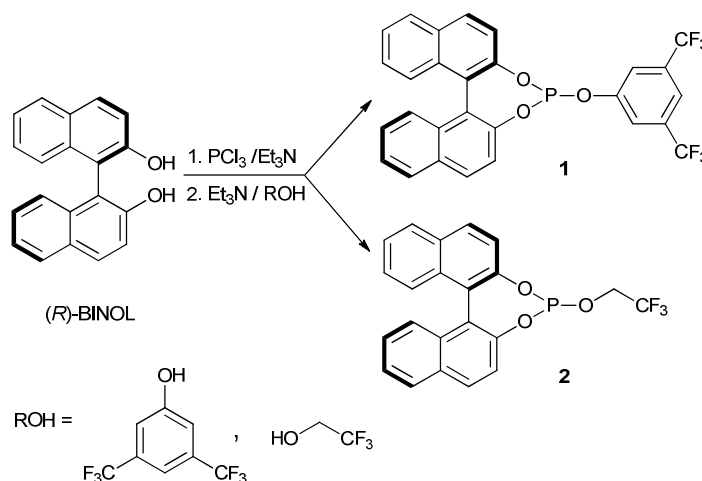


Figure 5.2. Chiral P-donor ligands, **1-4**.

5.2. Results and Discussion

5.2.1. Synthesis of BINOL derived chiral fluorinated ligands **1** and **2**

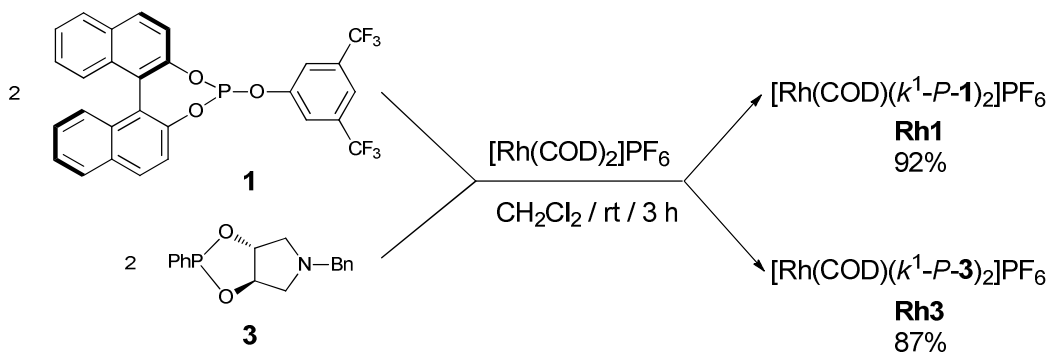
In the course of this study, we have prepared two new binaphthol-derived fluorinated phosphite ligands, **1** and **2**. The synthetic route started from the reaction between (*R*)-BINOL in the presence of triethylamine at 0 °C with phosphorous trichloride and after further slow warming up to room temperature, the corresponding phosphochlorhydrite was obtained. The mixture was then treated with the appropriate fluorinated alcohol in the presence of triethylamine at 0 °C and then slowly warmed up to room temperature overnight, leading to the corresponding ligands **1** and **2** (Scheme 5.2). The reactions were monitored by ³¹P{¹H} NMR.¹⁹ The ligands were obtained in moderate yields (52-60%). Ligands **1** and **2** were fully characterised by ¹H, ¹³C, ³¹P and ¹⁹F NMR, as well as by infrared spectroscopy, elemental analysis and polarimetry. ³¹P{¹H} NMR spectra showed the corresponding singlets in the characteristic region for phosphites.^{7b} Ligand **2** exhibited two multiplets at 3.83 and 4.23 ppm for the methylene diastereotopic protons in the corresponding ¹H NMR spectrum.



Scheme 5.2. Synthesis of chiral ligands **1** and **2**.

5.2.2. Synthesis of Rh(I) complexes, **Rh1** and **Rh3**

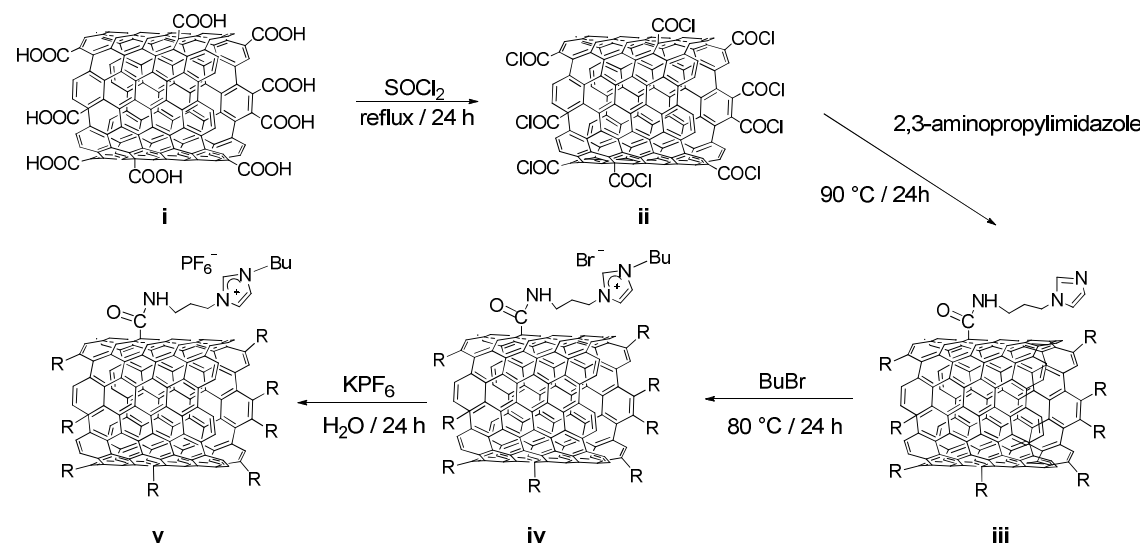
The synthesis of cationic Rh(I) complexes, **Rh1** and **Rh3**, was carried out by reaction of $[\text{Rh}(\text{COD})_2]\text{PF}_6$ with the appropriate ligand, **1** and **3** respectively, in CH_2Cl_2 at room temperature (Scheme 5.3). After solvent evaporation, the corresponding new complexes **Rh1** and **Rh3** were isolated in good yields (87-92%). The coordination of phosphite ligands was monitored by $^{31}\text{P}\{^1\text{H}\}$ NMR, observing a doublet due to the P-Rh coupling ($^1J_{\text{P}-\text{Rh}}$ 321 Hz and 260 Hz, for **Rh1** and **Rh3** respectively). The displacement of one cyclooctadiene ligand by two P-donor ligands was evidenced by the full characterization of these rhodium (I) complexes by multi-nuclear (^1H , ^{13}C , ^{31}P and ^{19}F) NMR, infrared spectroscopy and elemental analysis.



Scheme 5.3. Synthesis of Rh(I) complexes, **Rh1** and **Rh3**.

5.2.3. Supported catalytic ionic liquid phase

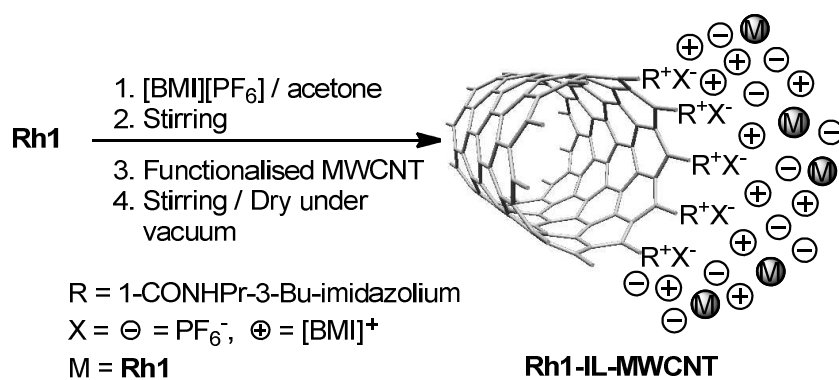
In order to efficiently immobilise and recycle the catalytic ionic liquid phase, a new material was prepared using imidazolium-functionalised MWCNT as support. This support was prepared following the previous reported procedure,²⁰ starting from oxidised MWCNT, **i**, in a four-step sequence (Scheme 5.4).



Scheme 5.4. Synthesis of functionalised MWCNT, **v**.

The first step consisted in the conversion of the carboxylic acid group to acid chloride using an excess of thionyl chloride to obtain **ii**. These carbon nanotubes reacted with an excess of 3-(aminopropyl)imidazole at 120 °C for 24 h under nitrogen atmosphere. The resulting MWCNT, **iii**, were purified by THF washing. Then, the resulting (3-aminopropyl)imidazolium-functionalised MWCNT were treated with an excess of n-butyl bromide, to obtain the N-butylimidazolium bromide-functionalised MWCNT, **iv**. Finally, an exchange reaction with potassium hexafluorophosphate led to the imidazolium-like ionic functionalised MWCNT, **v**.

Imidazolium-functionalised MWCNT (**v** in Scheme 5.4) were added to a solution of **Rh1** in acetone in the presence of $[BMI][PF_6^-]$ (Scheme 5.5). The volatile components were then evaporated under reduced pressure. The resulting material contained an ionic liquid loading of 37 % w/w. **Rh1-IL-MWCNT** was obtained as a black free flowing powder.



Scheme 5.5. Synthesis of **Rh1-IL-MWCNT**.

The high-resolution transmission electron microscopy (HR-TEM) analysis of **Rh1-IL-MWCNT** showed the presence of the ionic liquid phase over the functionalised MWCNT (Figure 5.3). EDX (Energy Dispersive X-ray spectrometry) analysis revealed the presence of Rh on the surface. The presence of both the catalyst and ionic liquid in this material was confirmed by infrared spectroscopy as well as by elemental analysis.

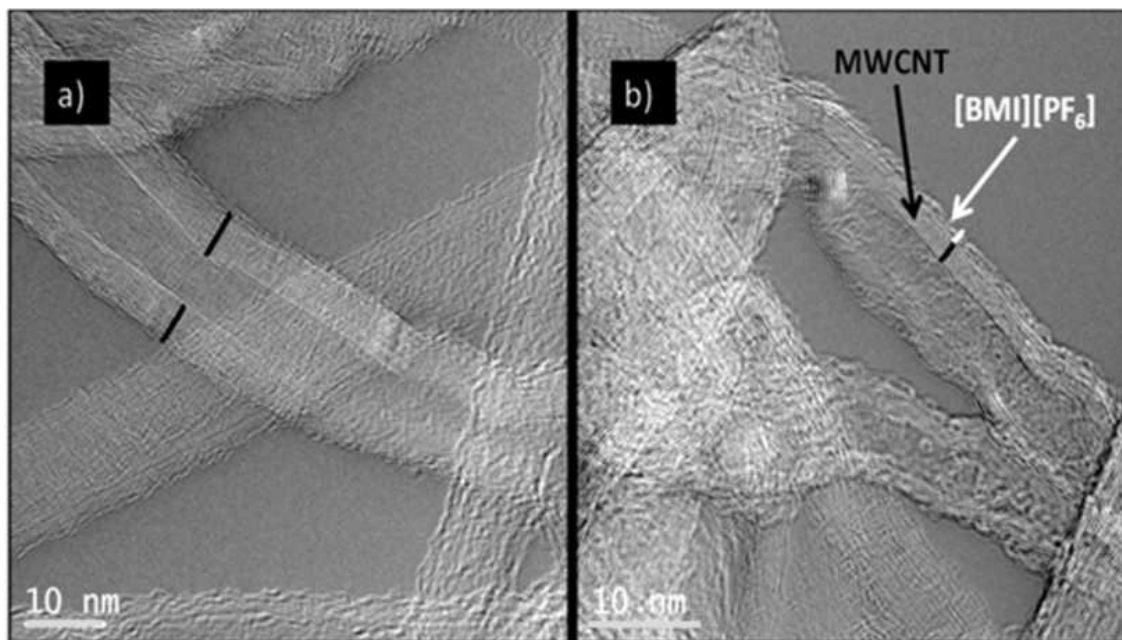


Figure 5.3. HR-TEM micrographs of: a) imidazolium-functionalised MWCNT and b) **Rh1-IL-MWCNT**. Black bar means walls of MWCNT; white bar, **Rh1-IL** film.

In order to assess the effect of the support on the catalytic system, the rhodium catalyst was also supported on SiO_2 instead of functionalised MWCNT by similar method. The composite **Rh1-IL-SiO₂** was analyzed by infrared spectroscopy and

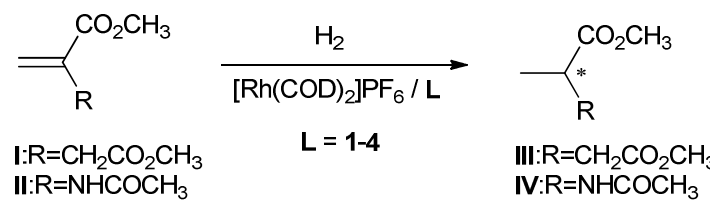
Rh-catalysed asymmetric hydrogenation in non-conventional solvents

elemental analysis. The IR spectrum showed the characteristic bands of [BMI][PF₆] (840 (F-P, st, s), 1575 (C=C, st, w), 2967 (CH, st, w) cm⁻¹), and the elemental analysis evidenced the presence of Rh.

5.2.4. Rh-catalysed asymmetric hydrogenation

5.2.4.1. Rh-catalysed asymmetric hydrogenation in CH₂Cl₂

We have studied the asymmetric hydrogenation of model substrates dimethyl itaconate **I** and methyl-2-acetamidoacrilate **II** catalysed by Rh systems containing ligands **1-4**, under soft conditions (1-3 bar of H₂ pressure; room temperature or 40 °C), in different solvents such as CH₂Cl₂, [BMI][PF₆] (BMI = 1-butyl-3-methyl imidazolium), supercritical carbon dioxide (scCO₂) and mixture of [BMI][PF₆]/scCO₂ (Scheme 5.6). Supported catalysts **Rh1-IL-MWCNT** and **Rh1-IL-SiO₂** were also evaluated.



Scheme 5.6. Rh-catalysed asymmetric hydrogenation.

The reaction of **I** and **II** with hydrogen in the presence of *in situ* formed Rh/L (**L = 1-4**) catalyst in CH₂Cl₂ under 1 bar of hydrogen pressure and at 298 K, afforded the corresponding hydrogenated products in good (entries 1-3, 5 and 6 in Table 5.1) to moderate (entries 4 and 7 in Table 5.1) conversions in one hour. Only the Rh/**4** catalytic system led to low conversions for the hydrogenation of **II** (entry 8 in Table 5.1). In all the cases, low enantioselectivities were achieved (*ee* up to 36% for **III**, entry 4 in Table 5.1).

Table 5.1. Asymmetric hydrogenation of dimethyl itaconate (**I**) and methyl-2-acetamidoacrilate (**II**) catalysed by Rh/**L** systems (**L=1-4**) in CH₂Cl₂.^a

Entry	L	Substrate	%Conversion ^b	%ee ^c
1	1	I	89	27 (<i>R</i>)
2	2	I	100	34 (<i>R</i>)
3	3	I	90	25 (<i>R</i>)
4	4	I	30	36 (<i>S</i>)
5	1	II	100	7 (<i>S</i>)
6	2	II	98	25 (<i>S</i>)
7	3	II	44	32 (<i>R</i>)
8	4	II	13	0

^a) Results from duplicate experiments. Reaction conditions: Rh precursor [Rh(COD)₂]PF₆; Rh:**L** = 1:2.4 (**L** = **1-4** respectively) in 1 mL of CH₂Cl₂; substrate:Rh = 40; t = 1 h; rt; P_{H₂} = 1 bar. ^b) Determined by ¹H NMR.

^c) Determined by chiral GC.

5.2.4.2. Rh-catalysed asymmetric hydrogenation in scCO₂

In scCO₂, only the catalytic systems containing fluorinated ligands **1** and **2** were active (entries 1, 2, 4 and 5 in Table 5.2). This effect can be attributed to the higher solubility of the catalytic systems containing fluorinated substituents in scCO₂ than that exhibited by Rh/**3** system. However, only Rh/**2** was enantioselective under these reaction conditions (entries 2 and 5 in Table 5.2) throwing approximately the same enantioselectivities that those obtained using CH₂Cl₂ as reaction medium.

Rh-catalysed asymmetric hydrogenation in non-conventional solvents

Table 5.2. Asymmetric hydrogenation of dimethyl itaconate (**I**) and methyl-2-acetamidoacrilate (**II**) catalysed by Rh/**L** systems (**L** = **1-3**) in scCO₂.^a

Entry	L	Substrate	%Conversion ^b	%ee ^c
1	1	I	100	0
2	2	I	100	22 (<i>R</i>)
3	3	I	0	-
4	1	II	100	0
5	2	II	100	25 (<i>S</i>)
6	3	II	0	-

^a) Results from duplicate experiments. Reaction conditions: Rh precursor [Rh(COD)₂]PF₆; Rh:L = 1:2.4 (L = **1-3**) 25 mL of scCO₂ at P = 75 bar and T = 35 °C; substrate:Rh = 40; t = 24 h; P_{H2} = 1 bar. ^b) Determined by ¹H NMR. ^c) Determined by chiral GC.

5.2.4.3. Rh-catalysed asymmetric hydrogenation in [BMI][PF₆]

Rh/L (**L** = **1-4**) systems were evaluated in the asymmetric hydrogenation of substrates **I** and **II** in [BMI][PF₆] (Table 5.3) under the same soft conditions used in CH₂Cl₂ (entries 1, 3, 4, 7, 8, 10, 11 and 14 in Table 5.3). Moderate conversions were achieved, presumably due to the poor solubility of H₂ in this reaction medium ([BMI][PF₆] = 0.73 mM in comparision with CH₂Cl₂ = 3.5 mM at T = 298 K; P = 1 atm).²¹ Moderate to good enantioselectivities were obtained, especially for Rh/**2** catalytic system (ee = 62% (*R*) for **III** and 80% (*S*) for **IV**, entries 1 and 8 respectively in Table 5.3). The same reactivity was achieved using the preformed complex [Rh(COD)(κ¹-P-**1**)₂]PF₆ (entries 15 and 16 in Table 5.3). As an attempt to increase the conversion, higher hydrogen pressure (3 bar) was tested, but no significant enhancement was observed (entries 2, 5, 9, 12 in Table 5.3). Unfortunately, the enantioselectivities decreased, in particular for Rh/**1** for which no enantioselectivity was induced (entries 2 and 9 in Table 5.3). This behaviour has been also previously reported by Dupont *et al.* in ionic liquid medium, in which the drop in the enantioselectivities was a function of the increase of hydrogen pressure, at lower pressures the enantioselectivities increased because the enantioface discrimination was most efficient.²² Under both higher dihydrogen pressure (3 bar) and temperature (40 °C), full conversions were attained but without inducing any enantioselectivity (entries 6 and 13 in Table 5.3).

Table 5.3. Asymmetric hydrogenation of dimethyl itaconate and methyl-2-acetamidoacrilate catalyzed by Rh/L systems (**L=1-4**) in [BMI][PF₆].^a

Entry	L	Substrate	P _{H₂} (bar)	%Conversion ^b	%ee ^c
1	1	I	1	70	62 (R)
2	1	I	3	73	0
3	2	I	1	37	36 (R)
4	3	I	1	39	42 (R)
5	3	I	3	43	29 (R)
6	3	I	3	100 ^d	0
7	4	I	1	15	27 (S)
8	1	II	1	35	80 (S)
9	1	II	3	44	0
10	2	II	1	14	0
11	3	II	1	39	26 (R)
12	3	II	3	42	21 (R)
13	3	II	3	100 ^d	0
14	4	II	1	25	0
15	1^e	I	1	68	62 (R)
16	1^e	II	1	36	80 (S)

^a) Results from duplicate experiments. Reaction conditions: Rh precursor [Rh(COD)₂]PF₆; Rh:L = 1:2.4 (L = **1-4**) in 1 mL of [BMI][PF₆]; substrate:Rh = 40; t = 24; rt. ^b) Determined by ¹H NMR. ^c) Determined by chiral GC. ^d) T = 40 °C. ^e) Preformed catalyst **Rh1**.

5.2.4.4. Rh-catalysed asymmetric hydrogenation in [BMI][PF₆]/scCO₂

The increase of dihydrogen solubility in [BMI][PF₆] by using scCO₂ is well known.²³ With the aim to improve the activities of the catalytic systems in [BMI][PF₆], tests in the mixture of [BMI][PF₆]/scCO₂ were evaluated (Table 5.4).

Rh-catalysed asymmetric hydrogenation in non-conventional solvents

Table 5.4. Asymmetric hydrogenation of dimethyl itaconate (**I**) and methyl-2-acetamidoacrilate catalysed (**II**) by Rh/L systems (**L** = **1-3**) in the mixture [BMI][PF₆]/scCO₂.^a

Entry	L	Substrate	%Conversion ^b
1	1	I	100
2	2	I	93
3	3	I	100
4	1	II	100
5	2	II	100 (12(S)) ^c
6	3	II	100

^a) Results from duplicate experiments. Reaction conditions: Rh precursor [Rh(COD)₂]PF₆; Rh:L = 1:2.4 (L = **1-3**) in 1 mL of [BMI][PF₆] and 25 mL of scCO₂ at P = 75 bar and T = 35 °C; substrate:Rh = 40; t = 24; P_{H2} = 1bar. ^b) Determined by ¹H NMR. ^c) Determined by chiral GC.

In this solvent mixture, the catalytic systems were more active than those in neat [BMI][PF₆] (Table 5.3), probably due to the higher dihydrogen solubility in the mixture [BMI][PF₆]/scCO₂ mixture. Unfortunately, the enantioselectivity decreased and only for Rh/**2** catalytic system, some asymmetric induction was observed for substrate **II** (entry 5 in Table 5.4).

5.2.4.5. Recycling experiments

Recycling tests were carried out using the catalytic system Rh/**1** in [BMI][PF₆]. For the hydrogenation of substrates **I** and **II** under 1 bar of dihydrogen pressure at room temperature, the catalytic phase containing Rh/**1** was recycled up to ten times preserving the conversion, but the enantioselectivity was lost after the first run (Figure 5.4).

Inductively coupled plasma mass spectrometry (ICP-MS) post-catalysis analysis of the hydrogenated product indicated that no metal leaching was produced during the recycling (rhodium content for the organic product was found in the range of 0.01-0.03 ppm). But ³¹P{¹H} NMR analysis of the ethyl ether extraction phase proved the presence of free ligand. When the catalytic phase was reused without extraction of the

organic product, the conversion remained unchangeable without enantioselectivity loss.

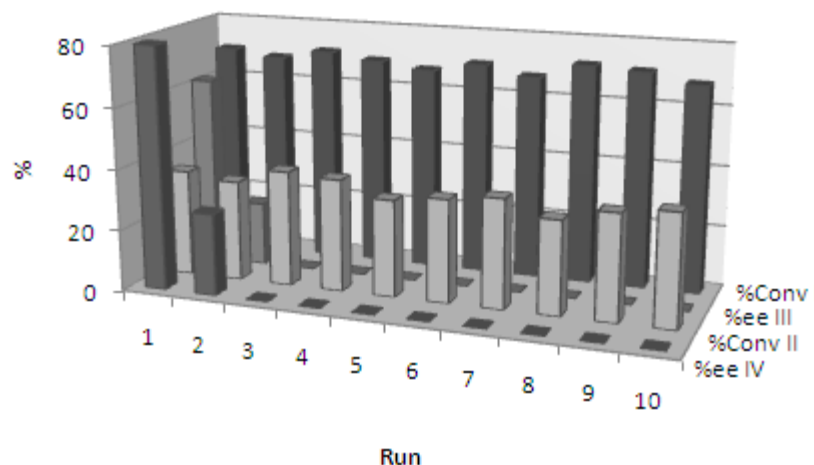


Figure 5.4. Recycling experiments of substrates **I** (in black) and **II** (in gray) using Rh/**1** as catalyst in [BMI][PF₆].

5.2.4.6. Rh-catalysed asymmetric hydrogenation in supported ionic liquid phase

With the aim to improve the catalyst immobilisation, the catalytic precursor **Rh1** dissolved in [BMI][PF₆] was supported on both functionalised MWCNT and silica to form **Rh1-IL-MWCNT** and **Rh1-IL-SiO₂** materials respectively (see above), in order to be tested in the asymmetric hydrogenation of **I** and **II** (Table 5.5).

The catalytic behaviour of **Rh1-IL-MWCNT** system was compared with that observed using **Rh-IL-SiO₂** in order to assess both the feasibility and the performance of the MWCNT-supported system. Both MWCNT- and SiO₂-supported catalytic systems were moderately active (entries 1, 2, 7 and 8 in Table 5.5) under the softest conditions studied (1 bar H₂ at 298 K), showing similar conversions without inducing asymmetry. When dihydrogen pressure was increased (3 bar), the conversion for **Rh1-IL-MWCNT** increased (entries 3 and 9 in Table 5.5) and on the contrary, for **Rh1-IL-SiO₂** decreased (entries 4 and 10 in Table 5.5), without improving the enantioselectivity in any case. The conversion for substrate **I** was increased working under harsher conditions (3 bar H₂ at 40 °C) using both supported catalytic systems (entries 5 and 6 in Table 5.5), giving total conversion for MWCNT-supported system. Under the same conditions,

Rh-catalysed asymmetric hydrogenation in non-conventional solvents

conversion considerably increased for substrate **II** using **Rh1-IL-MWCNT**, in contrast to the inactivity observed using **Rh1-IL-SiO₂** (entries 11 and 12 in Table 5.5).

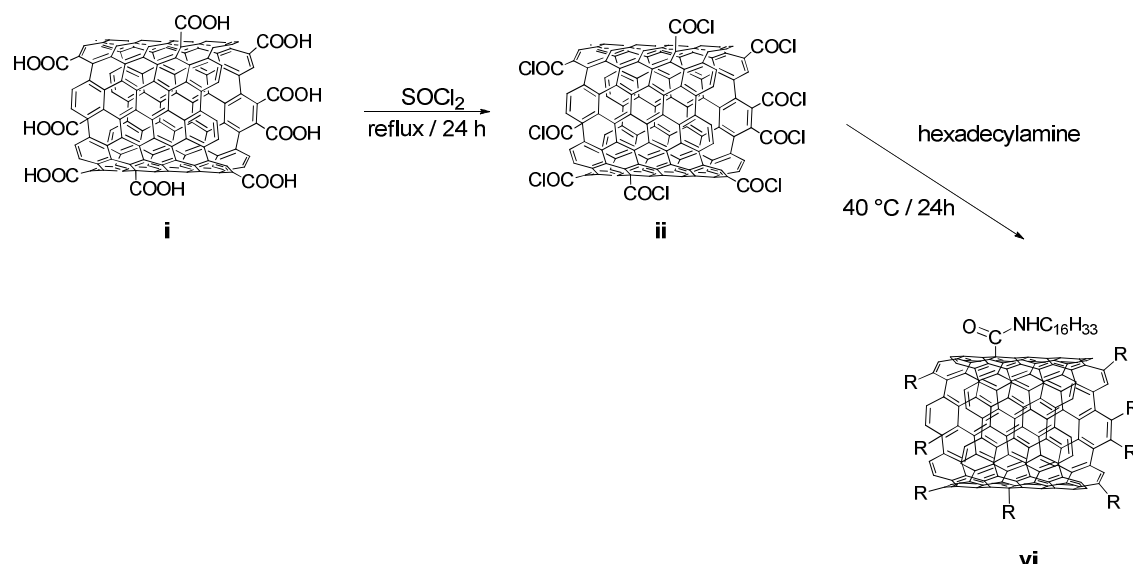
Table 5.5. Asymmetric hydrogenation of dimethyl itaconate (**I**) and methyl-2-acetamidoacrilate (**II**) catalysed by **Rh1-IL-MWCNT** and **Rh1-IL-SiO₂**.^a

Entry	Substrate	Catalyst	P _{H₂} (bar)	%Conversion ^b
1	I	Rh1-IL-MWCNT	1	17
2	I	Rh1-IL-SiO₂	1	14
3	I	Rh1-IL-MWCNT	3	27
4	I	Rh1-IL-SiO₂	3	0
5	I	Rh1-IL-MWCNT	3	100 ^c
6	I	Rh1-IL-SiO₂	3	91 ^c
7	II	Rh1-IL-MWCNT	1	17
8	II	Rh1-IL-SiO₂	1	20
9	II	Rh1-IL-MWCNT	3	44
10	II	Rh1-IL-SiO₂	3	1
11	II	Rh1-IL-MWCNT	3	60 ^c
12	II	Rh1-IL-SiO₂	3	1 ^c

^a) Results from duplicate experiments. Reaction conditions: 1 mL of ethyl ether; substrate:Rh = 40; t = 24h; rt. ^b) Determined by ¹H NMR. ^c) T = 40 °C

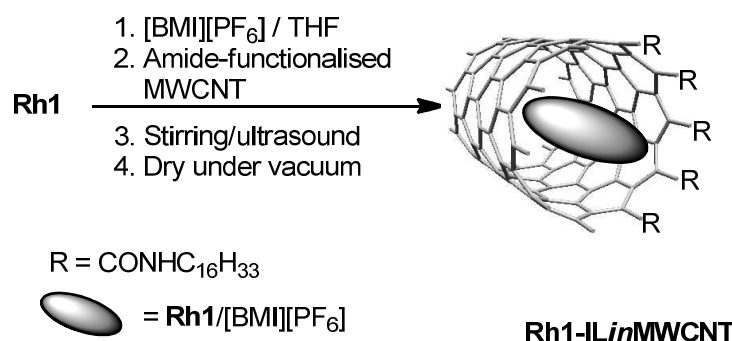
5.2.5. Confined catalytic ionic liquid phase

With the aim to explore the effect of the confinement of the catalytic ionic liquid phase in order to get asymmetric induction, amide-functionalised MWCNT, **vi**, were used as support (Scheme 5.7). The hydrophobic –C₁₆H₃₃ group was introduced to force the IL-**Rh1** mixture to be confined in the MWCNT. This support was prepared following the previously described methodology,²⁴ starting from oxidised MWCNT in a two-step sequence (Scheme 5.7).



Scheme 5.7. Synthesis of amide-functionalised MWCNT, **vi**.

Amide-functionalised MWCNT (**vi** in Scheme 5.7) were added to a solution of **Rh1** in THF in the presence of $[\text{BMI}][\text{PF}_6]$ and this catalytic phase confined by alternative stirring/ultrasonic cycles (Scheme 5.8). The volatile components were evaporated under reduced pressure and the resulting material containing the ionic liquids loading of 37% w/w, **Rh1-ILinMWCNT**, was obtained as a black free flowing powder.



Scheme 5.8. Synthesis of **Rh1-ILinMWCNT**.

The HR-TEM analysis of this new material, showed the presence of the ionic liquid phase confined in the MWCNT (Figure 5.5). The presence of both the catalyst and the ionic liquid in this material was confirmed by infrared spectroscopy as well as by elemental analysis.

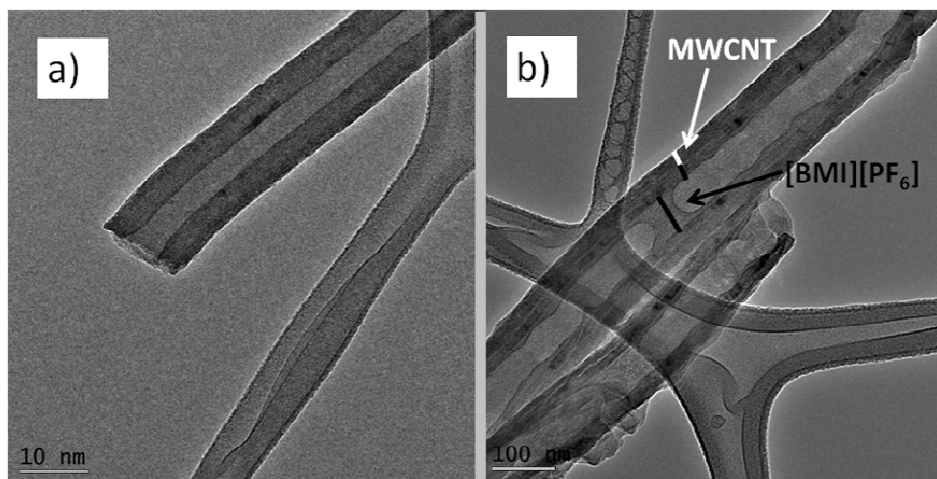


Figure 5.5. HR-TEM micrographs of: a) Amide-functionalised MWCNT and b) **Rh1-ILinMWCNT**. White bar means walls of MWCNT; black bar, **Rh1-IL** film.

This new material was preliminary tested in the asymmetric hydrogenation reaction of functionalised olefins in diethyl ether as solvent. Unfortunately, no conversion was observed under the same reaction conditions used for **Rh1-IL-MWCNT** system (see above). Post-catalysis HR-TEM micrographs showed that the ionic liquid phase was dispersed inside and also outside the MWCNT support (Figure 5.6).

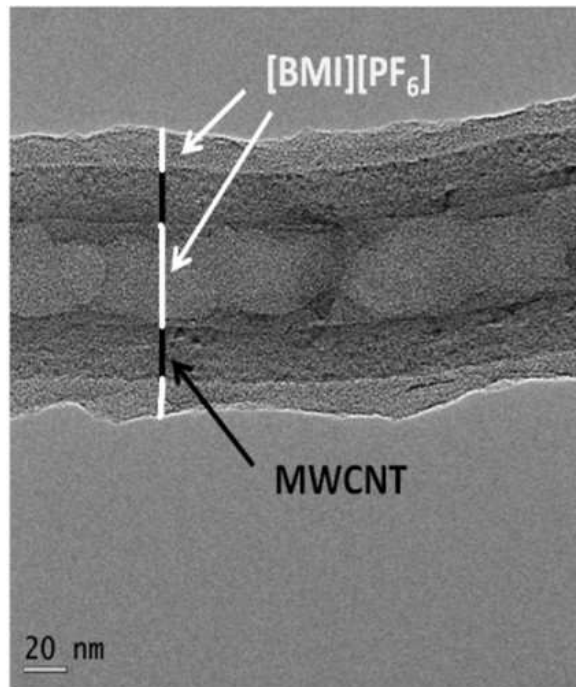


Figure 5.6. Post-catalysis HR-TEM micrograph of **Rh1-ILinMWCNT**. Black bar means walls of amide-functionalised MWCNT; white bar, ionic liquid film.

5.3. Conclusions

The catalytic systems evaluated were active in CH_2Cl_2 , but showing low enantioselectivities. In scCO_2 , only the systems containing fluorinated groups were active, probably due to their solubility in this solvent, achieving slightly asymmetric induction in the case of Rh/**2** catalyst (*ee* = 25% for **IV**). In [BMI][PF₆], good enantioselectivities were afforded in the case of Rh/**1** (*ee* = 80% for **IV**), under mild reaction conditions (1 bar of H₂ pressure at 298 K). However, the enantioselectivity was lost when hydrogen pressure and/or temperature increased. This effect is due to the ligand leaching as evidenced by NMR and ICP-MS analysis of organic phases. In relation to catalyst recycling, the best catalytic system, Rh/**1** in [BMI][PF₆], was reused up to 10 times preserving the activity, but loosing the enantioselectivity due to the ligand leaching.

In order to better immobilize the catalyst, **Rh1** complex dissolved in ionic liquid was supported on functionalised multi-walled carbon nanotubes. This system exhibited moderate conversion, being more active than the analogous catalytic material supported on silica, probably due to the carbon nanotubes open structure in relation to silica, which avoided mass transfer limitations.

5.4. Experimental

All syntheses were performed using standard Schlenk techniques under nitrogen or argon atmosphere. Organic solvents were dried following the procedures described in literature.²⁵ [Rh(COD)₂]PF₆²⁶ and compound (3*S*,4*S*)-1-benzylpyrrolidine-3,4-diol²⁷ were synthesized following the methodology described in the literature. PhPCl₂, PCl₃, 2,2,2-trifluoroethanol, 3,5-bis(trifluoromethyl)phenol, (*R*)-(+)1,1'-binaphthol ((*R*)-BINOL), phenol, dimethyl itaconate and methyl 2-acetamidoacrylate were purchased from Sigma-Aldrich and Acros chemicals and used without further purification. [BMI][PF₆] (99.5%) was purchased from Solvionic and treated under reduced pressure at 60 °C for 48 h prior to use. Multi-walled carbon nanotubes were prepared by C-CVD²⁸ (catalytic chemical vapour deposition) in the “Laboratoire de Genie Chimique” of the Université de Toulouse (purity >95 %, <5 % remainig iron particles; active surface =

227 cm²/g; pore volume = 0.66 cm³/g; average pore diameter = 6-20 nm; external diameter = 21-8 nm; internal diameter = 12-4 nm). Ionic functionalization of the MWCNT surface was carried out following the procedure described in literature,^[20] and Pyrograph III MWCNT, Applied Science, 98% purity and hexadecylamine functionalisation was carried out as described in the literature.²⁴ Mesoporous silica (EP10X amorphous silica, Crosfield Ltd., pore volume = 1.81 cm³ g⁻¹, particle size ≈ 100 µm) was purchase from INEOS Silicas. ¹H, ¹³C and ³¹P NMR spectra were recorded on a Bruker AV-300 spectrometer (300.13 MHz). ¹H and ¹³C correlation spectra were obtained using standard procedures. The MWCNT samples were dispersed in ethanol, sonicated for 5 minutes and the resulting suspension was dropped onto a holey carbon copper grid and the solvent was allowed to evaporate. The images were obtained in a JEOL JEM 1011 running at 100kV for routine images (resolution 4, 5 Å), acquisition by camera slow scans SIS (Megaview III) and a JEOL JEM 2100F running at 100kV with high resolution images (resolution 2,3 Å), X-ray analysis PGT (light elements detection, resolution 135 eV), images acquisition by camera slow scan Gatan 1K x 1K. IR spectra were recorded on a FTIR Nicolet Impact 400 spectrometer. Optical rotations were measured in a Perkin Elmer 241MC polarimeter. Gas chromatography analyses were performed with a Hewlett-Packard 5890A instrument in a CHIRALDEX G-TA (30 m x 025mm) or Permabond L-Chirasil-Val column (25 m x 0.25 mm), equipped with a Hewlett-Packard HP3396 series II integrator. Catalytic experiments in scCO₂ were performed in a Parr autoclave (25 mL) with magnetic stirring. The autoclave was equipped with a liquid inlet, a gas inlet, a CO₂ inlet and a thermocouple. An electric heating mantle kept the temperature constant. Catalytic experiments with CH₂Cl₂, [BMI][PF₆] and SILPs were performed in a Fisher Porter bottle with magnetic stirring.

5.4.1. Synthesis of P-donor ligands

5.4.1.1. (11b*R*)-4-(3,5-bis(trifluoromethyl)phenoxy)dinaphtho[2,1-d:1',2'f][1,3,2]dioxaphosphepine 1

(*R*)-BINOL (1 g, 3.5 mmol) was azeotropically dried with toluene and dissolved in THF (20 mL) and triethylamine (1 mL). The reaction mixture was cooled at 0 °C and then PCl₃ (0.4 mL, 4.6 mmol) were drop wise added and stirred for 6 hours at room

temperature. Then 3,5-tris(trifluoromethyl)phenol (0.5 mL, 3.5 mmol) in THF (10 mL) and triethylamine (1 mL) were drop wise added at 0 °C over a period of time of 15 minutes and then, the reaction mixture was stirred at room temperature overnight. The resulting mixture was filtered through a basic alumina under nitrogen atmosphere and the solvent was evaporated. The final product was obtained as white powder (0.750 g, 52%). $[\alpha]_D^{25}=+37.13$ ($c=1.02$, CH_2Cl_2). ^1H NMR (400 MHz, CDCl_3 , rt) $\delta=$ 6.54-8.05 (15H, ar); ^{13}C NMR (75 MHz, CDCl_3 , 298 K) $\delta=$ 111.9 (C_{ipsoar}), 114.4 (CH_{ar}), 115.8 (CH_{ar}), 117.5 (CH_{ar}), 121.3 (C_{ipsoar}), 123.1 (q, $^1\text{J}_{\text{C}-\text{F}}=271$ Hz, CF_3), 124.3 (CH_{ar}), 124.4 (CH_{ar}), 127.7 (CH_{ar}), 128.5 (CH_{ar}), 129.7 (C_{ipsoar}), 131.5 (CH_{ar}), 133 (q, $\text{C}_{ipso}\text{CF}_3$, $^1\text{J}_{\text{C}-\text{F}}=33$ Hz), 133.6 (C_{ipsoar}), 152 (C_{ipsoar}), 156.3 (C_{ipsoar}) ^{19}F NMR (376.5 MHz, CDCl_3 , 298 K) $\delta=$ -63.64; ^{31}P NMR (162 MHz, CDCl_3 , 298 K) $\delta=$ 145.18. ν_{max} (KBr, pellet)/ cm^{-1} 1215 (C-F, st, w), 1151 (P-O-Car, st,w), 948 (P-O, st, w), 786 (P-C, st, w), 746 (C-F, st, w) Elemental analysis. Found C 61.90, H 2.83 %. $\text{C}_{28}\text{H}_{15}\text{F}_6\text{O}_3\text{P}$ requires C 61.78, H 2.78 %.

5.4.1.2. Synthesis of (11bR)-4-(2,2,2-trifluoroethoxy)dinaphtho[2,1-d:1',2'-f][1,3,2]dioxaphosphepine, 2

(*R*)-BINOL (1 g, 3.5 mmol) was azeotropically dried with toluene and dissolved in THF (20 mL) and triethylamine (1 mL). The reaction mixture was cooled at 0 °C and then PCl_3 (0.4 mL, 4.6 mmol) were drop wise added and stirred for 6 hours at room temperature. Then 2,2,2-trifluoroethanol (0.6 mL, 3.5 mmol) in THF (10 mL) and triethylamine (1 mL) were drop wise added at 0 °C over a period of time of 15 minutes and then, the reaction mixture was stirred at room temperature overnight. The resulting mixture was filtered through a basic alumina under nitrogen atmosphere and the solvent was evaporated. The final product was obtained as white powder (0.864 g, 60%). $[\alpha]_D^{25}=+22.92$ ($c=1.06$, CH_2Cl_2). ^1H NMR (400 MHz, CDCl_3 , 298 K) $\delta=$ 3.83 (m, 1H, CHH), 4.23 (m, 1H, CHH), 7.2-8 (m, 12H, ar); ^{13}C NMR (100 MHz, CDCl_3 , 298 K) $\delta=$ 60.7 (q, $^1\text{J}_{\text{C}-\text{F}}=35$ Hz, CH_2CF_3), 111.6 (C_{ipsoar}), 117.6 (CH_{ar}), 124.1 (CH_{ar}), 124.2 (q, $^1\text{J}_{\text{C}-\text{F}}=277$ Hz, CF_3), 124.3 (CH_{ar}), 127.5 (CH_{ar}), 128.4 (CH_{ar}), 129.5 (C_{ipsoar}), 131.3 (CH_{ar}), 133.6 (C_{ipsoar}), 152.3 (C_{ipsoar}); ^{19}F NMR (376.5 MHz, CDCl_3 , 298 K) $\delta=$ -75.59; ^{31}P NMR (162 MHz, CDCl_3 , 298 K) $\delta=$ 136.30. ν_{max} (KBr, pellet)/ cm^{-1} 1215 (C-F, st, w), 977 (P-O-Cal, st,

w), 823 (P-C, st, w), 743 (CF₃, st, w). Elemental analysis Found C 63.81, H 3.44 %. C₂₂H₁₄F₃O₃P requires C 63.78, H 3.41 %.

5.4.1.3. (3a*S*,6a*S*)-5-benzyl-2-phenyltetrahydro-3a*H*-[1,3,2]dioxaphospholo[4,5-*c*]pyrrole, 3

This ligand was synthesized following the procedure described in Chapter 4.

5.4.1.4. (3a*R*,6a*R*)-5-benzyloxytetrahydro-3a*H*-[1,3,2]dioxaphospholo[4,5-*c*]pyrrole, 4

This ligand was synthesized following the procedure described in Chapter 4.¹⁸

5.4.2. Synthesis of Rh complexes

5.4.2.1. Cyclooctadiene-bis-(11b*R*)-4-(2,2,2-trifluoroethoxy)dinaphtho[2,1-d:1',2'-f]-[1,3,2]dioxaphosphepine)rhodium(I)hexafluorophosphate, Rh1

[Rh(COD)₂]PF₆ (30 mg, 0.065 mmol) and **1** (74 mg, 0.14 mmol) were dissolved in CH₂Cl₂ (5 mL) and stirred for 3 h. Then the solvent was evaporated and the orange solid washed with pentane (97 mg 92%). ¹H NMR (300 MHz, CDCl₃, 298 K) δ = 1.33 (bs, 1H, CH₂COD), 1.75 (bs, 1H, CH₂COD), 2.05 (bs, 1H, CH₂COD), 2.23 (bs, 2H, CH₂COD), 2.45 (bs, 1H, CH₂COD), 2.56 (bs, 2H, CH₂COD), 4.48 (bs, 2H, CH_{COD}), 5.88 (bs, 2H, CH_{COD}), 6.75-8.24 (30H, CH_{ar}); ¹³C NMR (75.47 MHz, CDCl₃, 298 K) δ = 28.6 (CH₂COD), 29.7 (CH₂COD), 29.9 (CH₂COD), 105.5 (CH_{COD}), 107.4 (CH_{COD}), 107.5 (CH_{COD}), 111.4 (CH_{COD}), 117.8 (CH_{ar}), 120.2 (CH_{ar}), 120.6 (CH_{ar}), 121.5 (CF₃), 122 (CF₃), 122.7 (C_{ipsoar}), 124 (CH_{ar}), 124.3 (CH_{ar}), 125.9 (CH_{ar}), 126.4 (CH_{ar}), 126.7 (CH_{ar}), 127 (CH_{ar}), 127.5 (CH_{ar}), 128.3 (CH_{ar}), 128.4 (CH_{ar}), 128.7 (CH_{ar}), 129.5 (C_{ipsoar}), 131.2 (CH_{ar}), 131.4 (CH_{ar}), 131.8 (C_{ipsoar}), 132.2 (C_{ipsoar}), 133.4 (C_{ipsoar}), 134 (C_{ipsoar}), 152.8 (C_{ipsoar}); ¹⁹F NMR (282.4 MHz, CDCl₃, 298 K) δ = -62.92 CF₃, ³¹P NMR (121.5 MHz, CDCl₃, 298 K) δ = 134.8 (d, ¹J_{P-Rh} 321 Hz). ν_{max} (KBr, pellet)/cm⁻¹ 1213 (C-F, st, w), 816 (P-C, st, w), 748 (P-O-Car, st, w), 726 (CF₃, st, w). Elemental analysis Found C 57.54, H 3.13 %. C₆₄H₄₂F₁₈O₆P₃ requires C 57.28, H 3.15 %.

5.4.2.2. Cyclooctadiene-bis-((3aS,6aS)-5-benzyl-2-phenyltetrahydro-3aH-[1,3,2]dioxaphospholo[4,5-c]pyrrole)rhodium(I)hexafluorophosphate, Rh3

[Rh(COD)₂]PF₆ (15 mg, 0.033 mmol) and **3** (41 mg, 0.14 mmol) were dissolved in CH₂Cl₂ (5 mL) and stirred for 3 h. Then the solvent was evaporated and the yellow solid washed with pentane (31 mg 87%). ¹H NMR (500 MHz, CD₂Cl₂, 298 K) δ = 2.22 (bs, 4H, CH₂COD), 2.39 (bs, 4H, CH₂CH), 2.49 (bs, 4H, CH₂CH) 3.08 (bs, 4H, CH₂N), 3.81 (bs, 4H, CH₂COD), 4.72 (bs, 2H, OCH), 4.81 (bs, 1H, CH_{COD}), 4.98 (bs, 2H, OCH), 4.99 (bs, 1H, CH_{COD}), 5.90 (bs, 1H, CH_{COD}), 6.24 (bs, 1H, CH_{COD}), 7.09-765 (20H, CH_{ar}); ¹³C NMR (125.77 MHz, CH₂Cl₂, 298 K) δ = 28 (CH₂CH), 29.7 (CH₂CH), 30.7 (NCH₂), 57.8 (CH₂COD), 58.5 (CH₂COD), 82.7 (CH_{COD}), 82.9 (CH_{COD}), 83 (CH_{COD}), 83 (CH_{COD}), 107.2 (OCH), 107.3 (OCH), 127.9 (CH_{ar}), 128.7 (CH_{ar}), 128.8 (CH_{ar}), 128.9 (CH_{ar}), 128.9 (CH_{ar}), 129 (CH_{ar}), 129.3 (CH_{ar}), 129.4 (CH_{ar}), 130.5 (CH_{ar}), 132 (CH_{ar}), 132.8 (CH_{ar}), 133.6 (CH_{ar}), 134.2 (CH_{ar}); ³¹P NMR (121.5 MHz, CDCl₃, 298 K) δ = 128 (d, ¹J_{P-Rh} 260 Hz). ν_{max} (KBr, pellet)/cm⁻¹ 1259 (C-N, st, w), 1061 (P-O-Car, st, w), 751 (P-C, st, w). Elemental analysis. Found C 53.23, H 3.81, N 2.92 %. C₄₂H₃₆F₆N₂O₄P₃Rh requires C 53.52, H 3.85, N 2.97 %

5.4.3. Immobilization of [Rh(COD)(1)₂]PF₆ over a supported ionic liquid phase (SILP), Rh1-IL-MWCNT, Rh1-IL-SiO₂

Supports MWCNT ionic functionalized or SiO₂ (200 mg), were immersed for 15 min at room temperature with a solution of [Rh(COD)(1)₂][PF₆] (20 mg, 1.39·10⁻² mmol) in [BMI][PF₆] (74 mg, corresponding to 37% w/w) in acetone (15 mL); acetone was then removed under vaccum.

Rh1-IL-MWCNT: ν_{max} (KBr, pellet)/cm⁻¹ 836 (F-P, st), 1573 (C=C, st, w), 2964 (CH, st, w). Elemental analysis: Found C 59.66, H 2.78, N 5.68, Rh 0.18 %.

Rh1-IL-SiO₂: ν_{max} (KBr, pellet)/cm⁻¹ 840 (F-P, st), 1575 (C=C, st, w), 2967 (CH, st, w). Elemental analysis: Found C 20.77, H 2.73, N 5.03, Rh 0.38 %.

5.4.4. Immobilization of [Rh(COD)(1)₂]PF₆ over a supported ionic liquid phase (SILP) inside of CNTs, Rh1-ILinMWCNT

200 mg of hexadecylamine functionalised MWCNTs were immersed into a solution of [Rh(COD)(2)₂][PF₆] (20 mg, 1.39·10⁻² mmol) in [BMI][PF₆] (74 mg, corresponding to 37% w/w) in 2 ml of THF, under alternative stirring and ultrasonic treatment. After 2 h, the THF was removed under vacuum.

Rh1-ILinMWCNT: ν_{max} (KBr, pellet)/cm⁻¹ 837 (FP, st), 1576 (C=C, st, w), 2966 (CH, st, w). Elemental analysis: Found C 48.49, H 4.67, N 7.09, Rh 0.18 %.

5.4.5. Catalytic experiments

5.4.5.1. General procedure for catalytic asymmetric hydrogenation in organic solvent

[Rh(COD)₂][PF₆] (2 mg, 0.0043 mmol) and the corresponding ligand (0.0051 or 0.01 mmol) were dissolved in dichloromethane (1 mL) and stirred for 30 min under argon atmosphere. After this time, the substrate (0.175, 0.86 or 2.15 mmol) was added and then the system was pressurized at P_{H₂} = 1 or 3 bar and stirred at room temperature or at 40 °C for 1 h. The catalytic mixture was filtered through a celite column and solvent evaporated, yielding the product as a colourless oil.

5.4.5.2. General procedure for catalytic asymmetric hydrogenation in [BMI][PF₆]

[Rh(COD)₂][PF₆] (2 mg, 0.0043 mmol) and the corresponding ligand (0.0051 or 0.01 mmol) were introduced in a Fisher-Porter bottle and dissolved in [BMI][PF₆] (1 mL) and stirred for 30 min under vacuum at room temperature, giving a yellowish solution. After this time, the substrate (0.175, 0.86 or 2.15 mmol) was added and then the system was pressurized at P_{H₂} = 1 or 3 bar and stirred at room temperature or at 40 °C for 24 h. The catalytic mixture was extracted with ethyl ether (3 x 2mL) and solvent evaporated yielding the product as a colourless oil.

5.4.5.3. General procedure for catalytic asymmetric hydrogenation in supercritical carbon dioxide ($scCO_2$)

[Rh(COD)₂][PF₆] (2 mg, 0.0043 mmol) and the corresponding ligand (0.0051 or 0.01 mmol) were dissolved in dichloromethane (1 mL) and stirred for 30 min under argon atmosphere. Then the solution was introduced in a Parr autoclave and solvent evaporated under vacuum. Substrates were then added and the reactor presurized with 1 atm of dihydrogen and pressurized with CO₂ at 75 atm of total pressure. The autoclave was stirred and heated at 35 °C for 24 h. The autoclave was then cooled at 0 °C and slowly depressurized through a cold trap. The reaction mixture was extracted with diethylether and filtered through a celite column.

5.4.5.4. General procedure for catalytic asymmetric hydrogenation in $scCO_2/[BMI][PF_6]$

[Rh(COD)₂][PF₆] (2 mg, 0.0043 mmol) and the corresponding ligand (0.0051 or 0.01 mmol) were introduced in a Parr autoclave and dissolved in [BMI][PF₆] (1 mL) and stirred for 30 min under vacuum at room temperature. After this time, the substrate (0.175 mmol) was added and the reactor presurized with 1 atm of dihydrogen and pressurized with CO₂ at 75 atm of total pressure. The autoclave was stirred and heated at 35 °C for 24 h. The autoclave was then cooled at 0 °C and slowly depressurized through a cold trap. The reaction mixture was extracted with diethylether and filtered through a celite column.

5.4.5.5. General procedure for catalytic asymmetric hydrogenation in supported ionic liquid phase (SILP)

Rh1-IL-SiO₂ or Rh1-IL-MWCNT (55.5 mg) were introduced in a Fisher-Porter bottle and diethylether (1 mL) and the corresponding substrate (0.175 mmol) was added and the system was pressurized at 1 or 3 bar and stirred at room temperature or 40 °C for 24 h. The catalytic mixture was extracted with ethyl ether (3 x 1 mL) and then the solution was filtered through celite column.

5.5. References

- ¹ *Catalytic Asymmetric Synthesis*, I. Ojima, (Ed.). 2nd edition, Wiley-VCH, **2000**.
- ² For selected reviews, see: a) F. Lagasse and H. B. Kagan. *Chem. Pharm. Bull.* **2000**, 48, 315. b) T. P. Clark and C. R. Landis. *Tetrahedron: Asymmetry*. **2004**, 15, 2123. c) T. Jerphagnon, J.-L. Renaud and C. Bruneau. *Tetrahedron: Asymmetry*. **2004**, 15, 2101.
- ³ T. P. Dang and H. B. Kagan, *J. Chem. Soc., Chem. Commun.*, **1971**, 481.
- ⁴ W. S. Knowles, M. J. Sabacky and B. D. Vineyard. *J. Chem. Soc., Chem. Commun.* **1972**, 10.
- ⁵ B. D. Vineyard, W. S. Knowles, M. J. Sabacky, G. L. Bachman and D. J. Weinkauff. *J. Am. Chem. Soc.* **1977**, 99, 5946.
- ⁶ S. Gladiali and E. Alberico, *Chiral Chelating Diphosphines with Stereogenic C-centers in the Interconnecting Spacer in Phosphorus Ligands in Asymmetric Catalysis*, Edited by A. Börner, Wiley-VCH, Weinheim, **2008**.
- ⁷ a) D. J. Ager, A. H. M. de Vries and J. G. de Vries. *Platinum Metals Rev.* **2006**, 50, 54. b) M. T. Reetz and G. Mehler. *Angew. Chem. Int. Ed.* **2000**, 39, 3889. c) C. Claver, E. Fernandez, A. Gillon, K. Heslop, D. J. Hyett, A. Martorell, A. Guy Orpen, P. and G. Pringle. *Chem. Commun.* **2000**, 961.
- ⁸ For selected papers, see: a) M. Ostermeier, B. Brunneer, C. Korff and G. Helmchen. *Eur. J. Org. Chem.* **2003**, 3453. b) W. Chen and J. Xiao. *Tetrahedron Lett.* **2001**, 42, 2897. c) T. Jerphagnon, J.-L. Renaud, P. Demonchaux, A. Ferreira and C. Bruneau. *Adv. Synth. Catal.* **2004**, 346, 33.
- ⁹ For selected papers, see: a) Z. Hua, V. C. Vassar and I. Ojima. *Org. Lett.* **2003**, 5, 3831. b) P. Hannen, H. -C. Militzer, E. M. Vogl and F. A. Rampf. *Chem. Commun.* **2003**, 2210. c) M. van den Berg, A. J. Minnaard, E. P. Schudde, J. van Esch, A. H. M. de Vries, J. H. de Vries and B. L. Feringa. *J. Am. Chem. Soc.* **2000**, 122, 11539.
- ¹⁰ a) F. Alario, Y. Amrani, Y. Colleuille, T. P. Dang, J. Jenck, D. Morel and D. Sinou. *J. Chem. Soc. Chem. Commun.* **1986**, 202. b) Y. Amrani, L. Lecomte, D. Sinou, J. Bakos, I. Tóth and B. Heil. *Organometallics*. **1989**, 8, 542.
- ¹¹ a) Kam-to Wan and M. E. Davis. *J. Chem. Soc. Chem. Commun.* **1993**, 1262. b) Kam-to Wan and M. E. Davis. *Tetrahedron: Asymmetry*. **1993**, 4, 2461.

- ¹² D. J. Cole-Hamilton. *Adv. Synth. Catal.* **2006**, 348, 1341.
- ¹³ S. E. Lyubimov, E. E. Said-Galiev, A. R. Khokhlov, N. M. Loim, L. N. Popova, P. V. Petrovskii and V. A. Davankov. *J. Supercritical Fluids.* **2008**, 45, 70.
- ¹⁴ a) D. J. Adams, W. Chen, E. G. Hope, S. Lange, A. M. Stuart, A. West and J. Xiao. *Green Chem.* **2003**, 5, 118. b) S. Lange, A. Brinkmann, P. Trautner, K. Woelk, J. J. Bargon and W. Leitner. *Chirality.* **2000**, 12, 450.
- ¹⁵ For selected reviews, see: a) J. Durand, E. Teuma and M. Gómez. *C. R. Chimie.* **2007**, 10, 152. b) C. Baudequin, J. Baudoux, J. Levillain, D. Cahard, A-C. Gaumont and J-C. Plaquevent. *Tetrahedron: Asymmetry.* **2003**, 14, 3081. c) H. Olivier-Bourbigou, L. Magna and D. Morvan. *Applied Catalysis A: General.* **2010**, 373, 1. For applications in asymmetric hydrogenation, see: d) P. S. Schulz, *Ligands for catalytic reactions in ionic liquids in Phosphorus Ligands in Asymmetric Catalysis*, Edited by A. Börner, Wiley-VCH, Weinheim, **2008**.
- ¹⁶ K. N. Gavrilov, S. E. Lyubimov, O. G. Bondarev, M. G. Maksimova, S. V. Zheglov, P. V. Petrovskii, V. A. Davankov and M. T. Reetz. *Adv. Synth. Catal.* **2007**, 349, 609.
- ¹⁷ D. Chen, M. Schmitkamp, G. Franciò, J. Klankermayer and W. Leitner. *Angew. Chem. Int. Ed.* **2008**, 47, 7339.
- ¹⁸ a) J. Halpern, *Science.* **1982**, 217, 401. b) C. R. Landis and J. P. Halpern. *J. Am. Chem. Soc.* **1987**, 109, 1746.
- ¹⁹ M. T. Reetz, A. Meiswinkel, G. Mehler, K. Angermund, M. Graf, W. Thiel, R. Mynott and D. G. Blackmond. *J. Am. Chem. Soc.* **2005**, 127, 10305.
- ²⁰ L. Rodríguez-Pérez, E. Teuma, A. Falqui, M. Gómez and P. Serp. *Chem Commun.* **2008**, 4201.
- ²¹ P. J. Dyson and T. J. Geldbach. *Metal Catalysed Reactions in Ionic Liquids*, Springer, Dordrecht, **2005**.
- ²² A. Berger, R. F. de Souza, M. R. Delgado and J. Dupont. *Tetrahedron: Asymmetry.* **2001**, 12, 1825.
- ²³ P. G. Jessop, R. R. Stanley, R. A. Brown, C. A. Eckert, C. L. Liotta, T. T. Ngo and P. Pollet. *Green Chem.* **2003**, 5, 123.

- ²⁴ E. Castillejos, P.-J. Debouttère, L. Roiban, A. Solhy, V. Martinez, Y. Kihn, O. Ersen, K. Philippot, B. Chaudret and P. Serp, *Angew. Chem. Int. Ed.* **2009**, 48, 2529.
- ²⁵ D. D. Perrin and W. L. F. Armarego. *Purification of Laboratory Chemicals. 3^a Ed.* Pergamon Press, Oxford, **1988**.
- ²⁶ R. Usón, L. A. Oro and J. Cabeza. *Inorg. Synth.* **1985**, 23, 126.
- ²⁷ A. Hui, J. Zhang, Z. Wang. *Synthetic Communications.* **2008**, 38, 2374.
- ²⁸ M. Corrias, B. Caussat, A. Ayral, J. Durand, Y. Kihn, P. Kalck and P. Serp. *Chem. Eng. Sci.* **2003**, 58, 4475.

Chapter 6

Conclusions
Conclusions
Conclusiones
Conclusions

UNIVERSITAT ROVIRA I VIRGILI
ORGANOMETALLIC COMPOUNDS AND METAL NANOPARTICLES AS CATALYSTS IN LOW ENVIRONMENTAL IMPACT SOLVENTS
Martha Verónica Escárcega Bobadilla
ISBN:978-84-694-1249-7/DL:T-324-2011

6.1. Concluding remarks

The aim of this Thesis was to study the catalytic behaviour of different molecular and nano-catalytic metallic systems in low environmental impact solvents, such as scCO₂ and ILs.

- New Rh and Ru nanoparticles stabilised by mono-arylphosphines (Figure 6.1) were used as catalysts in arene hydrogenation reactions in organic solvent as well as in scCO₂.

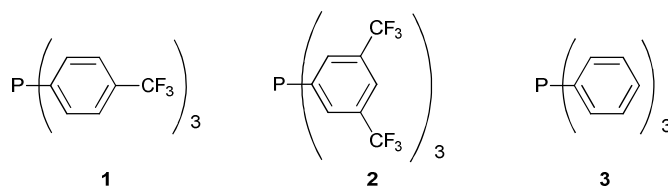


Figure 6.1. Mono-arylphosphines used as stabilisers of ruthenium and rhodium nanoparticles (Chapter 3).

The results obtained permitted to conclude the following features:

- ⇒ The synthesis of small MNP (ca. 1.50 nm) was highly dependent on the metal and the ligand nature. Therefore, PPh₃ stabilised both, RuNP and RhNP, but when trifluoromethyl groups are present on the ligands structure, the less-fluorine containing ligand, **1**, only stabilised Rh nanoparticles, and the more-fluorine containing ligand, **2**, only stabilised the Ru ones. **Ru2** and **Ru3** nanoparticles exhibited smaller size (1.30-1.40 nm) than **Rh1** and **Rh3** (1.70-2.50 nm); for both metals, good dispersions could be observed.
- ⇒ The presence of phosphine ligands at the metallic surface was evidenced by vibrational spectroscopies (IR and Raman) and elemental analysis. In addition, ligand exchange reaction between **Ru2** and dodecanethiol in THF showed a slow displacement of **2** by the thiol derivative (monitored by NMR), pointing to a strong interaction of the ligand with the metallic surface.

Conclusions

- ⇒ The relative higher metallic surface observed for RuNP, in comparison with that for RhNP, agrees with the higher activity observed for Ru systems than that given for Rh ones. In addition, the selectivity observed points to a strong interaction between the aryl groups of the substrates with the surface, mainly in the presence of oxygenated groups.
- ⇒ Concerning the catalytic behaviour, substrate conversions obtained revealed that the catalytic systems are in general slower in scCO₂ than in THF, probably due to the different solubility of the MNP in these solvents, even for materials stabilized by the more-fluorinated ligand **2**. RuNP remain dispersed after hydrogenation under scCO₂, in contrast to the agglomerates observed for RhNP. After catalysis, only agglomerates were observed when the catalytic reactions were carried out in THF.
- Novel azaphosphabicyclo[3,3,0]octane ligands **1** and **2** and the diphosphinite ligand **3** (Figure 6.2), derived from natural tartaric acid, were used in Pd-catalysed C-C bond formation reactions: Suzuki C-C cross-coupling and asymmetric allylic alkylation reactions in organic solvent as well as in ILs.

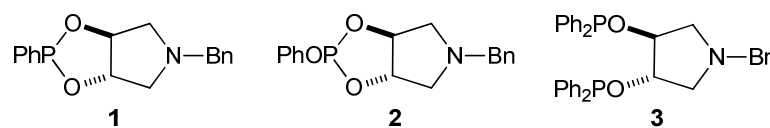


Figure 6.2. Chiral P-donor ligands derived from natural tartaric acid used in Pd-catalysed C-C bond formation processes (Chapter 4).

This study leads to the following conclusions:

- ⇒ NMR studies of ligands **1** and **2** revealed that at least three conformers are present in solution due to the relative spatial disposition of benzyl on nitrogen atom and phosphorus substituent, giving both *syn* and *anti* arrangements. Modelling studies (DFT level) are in good agreement with the isomeric ratios observed by NMR spectroscopy. Nevertheless upon Pd coordination to give [PdCl₂(κ^1 -P-**1**)₂], the conformers are not thus far distinguished.

- ⇒ The catalytic systems Pd/**1-3** were highly active and chemoselective in Suzuki C-C cross-couplings with substrates bearing both electron-donor and electron-withdrawing groups for 4-R-bromobenzene and 4-R-chlorobenzene derivatives. Using [BMI][PF₆] as solvent, the systems worked without formation of by-products allowing the activation of C-Cl bonds even for substrates containing electron-donor substituents. However, the activities were lower in most of the cases when the reactions were performed in toluene.
- ⇒ It is noteworthy that ligands **1-3** showed higher stability under catalytic basic biphasic conditions in [BMI][PF₆] than that observed in toluene and [EMI][PH(O)OMe]. This behaviour allowed the recycling of the catalytic phase in [BMI][PF₆] up to ten cycles without loss of activity.
- ⇒ Unfortunately, asymmetric Suzuki reactions were not selective towards the desired cross-coupling product, only giving the expected product in very low conversion and low chemoselectivity (substrate conversion less than 30% using Pd/**1** catalytic system in toluene).
- ⇒ The catalytic evaluation for the formation of new stereogenic centre in the Pd-catalysed asymmetric allylic alkylation model reaction gave low enantioselectivities (*ee* up to 26% (*S*) in CH₂Cl₂). Surprisingly, even if the enantiomeric excess was also low, the opposite enantiomer was obtained in [BMI][PF₆] (*ee* = 11% (*R*)).
- Chiral P-donor ligands derived from BINOL (**1** and **2**) and azadioxaphosphabicyclo[3.3.0]octane (**3** and **4**) (Figure 6.3) were tested in Rh-catalysed asymmetric hydrogenation in different solvents, such as CH₂Cl₂, scCO₂, IL and by supporting the catalytic-IL phase over/inside functionalised MWCNT.

Conclusions

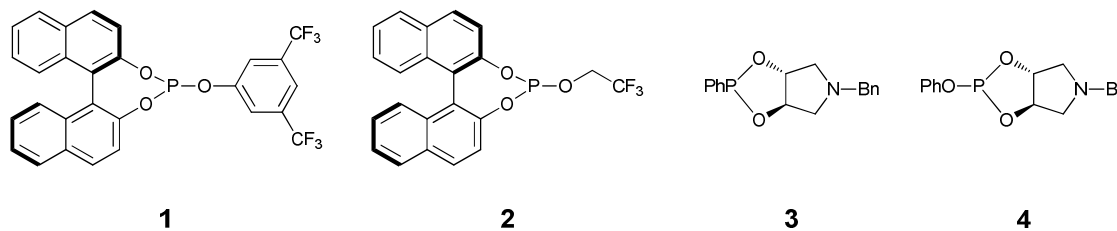


Figure 6.3 Chiral P-donor ligands used in Rh-catalysed asymmetric hydrogenation reactions (Chapter 5).

The conclusions of this study are following summarised:

- ⇒ The catalytic systems evaluated were active in CH_2Cl_2 , but showed low enantioselectivities (ee up to 36% (*S*)).
- ⇒ In scCO_2 , only the systems containing fluorinated groups were active, probably due to their solubility under these conditions, achieving slightly asymmetric induction in the case of Rh/**2** catalyst ($ee = 25\% (S)$ for **IV**).
- ⇒ In $[\text{BMI}][\text{PF}_6]$, good enantioselectivities were afforded (Rh/**1** system led to an $ee = 80\% (S)$ for **IV**), under soft reaction conditions (1 bar of H_2 pressure, room temperature). However, the enantioselectivity was lost when hydrogen pressure and temperature increased.
- ⇒ The best catalytic system found in this work, Rh/**1** in $[\text{BMI}][\text{PF}_6]$, was reused up to 10 times without activity lost, but loosing the enantioselectivity due to the ligand leaching, as evidenced by NMR analysis of organic phases.
- ⇒ In order to better immobilize the catalytic phase, **Rh1** complex dissolved in ionic liquid was supported on ionic-functionalised multi-walled carbon nanotubes. This system exhibited moderate conversion in comparison with the corresponding non-supported system, but it was more active than the analogous catalytic material supported on silica, probably due to the carbon nanotubes opened structure in relation to silica, which avoids mass transfer limitations.

6.2. Conclusions

L'objectif de cette Thèse a été d'étudier le comportement catalytique des différents systèmes métalliques moléculaires et nano-catalytiques dans des solvants à faible impact sur l'environnement, tels que le CO₂ supercritique et les liquides ioniques.

- Nouvelles nanoparticules de Rh et Ru stabilisées par de mono-phosphines aromatiques (voir Figure 6.1) ont été utilisées comme catalyseurs dans les réactions d'hydrogénéation des arènes dans solvant organique, ainsi que dans le scCO₂. Les résultats obtenus nous permettent de proposer les conclusions suivantes:
 - ⇒ La synthèse de MNP de petite taille (ca. 1.50 nm) a été fortement dépendante de la nature du métal et du ligand. Par conséquent, la PPh₃ a stabilisé RuNP et RhNP, mais lorsque des groupes trifluorométhyle sont présents sur la structure des ligands, le ligand moins riche en fluor, **1**, ne stabilise que des nanoparticules de Rh, et le ligand le plus riche en fluor, **2**, stabilise seulement les nanoparticules de Ru. Les nanoparticules **Ru2** et **Ru3** montrent la plus petite taille (1,30 à 1,40 nm) en comparaison avec celles de **Rh1** et **Rh3** (1,70 à 2,50 nm); pour ces deux métaux, des bonnes dispersions ont été observées.
 - ⇒ La présence des ligands sur la surface métallique a été mise en évidence par des spectroscopies vibrationnelles (IR et Raman) et analyse élémentaire. En particulier, la réaction entre **Ru2** et le dodécanethiol dans le THF a montré le déplacement lent du ligand **2** par le thiol (suivi par RMN), démontrant une forte interaction du ligand avec la surface métallique.
 - ⇒ La surface métallique relativement plus grande pour les RuNP, en comparaison avec celle des RhNP, est en concordance avec la plus haute activité observée pour les systèmes de Ru que pour ceux de Rh. En plus, la sélectivité observée démontre une forte interaction entre les groupes aryle

Conclusions

des substrats avec la surface métallique, principalement ceux comportant des groupes oxygénés.

- ⇒ Les conversions obtenues ont montré que les systèmes catalytiques sont en général plus faibles dans le scCO₂ que dans le THF, probablement dû des différentes solubilités des MNP dans le scCO₂ que dans le THF, même pour le ligand le plus fluoré, **2**. RuNP ont resté bien dispersées après hydrogénéation dans le scCO₂; au contraire, les RhNP ont donné lieu à des agglomérats. Après catalyse dans le THF, des agglomérats ont été uniquement observés.
- Des nouveaux ligands azaphosphabicyclo[3,3,0]octane, **1** et **2** aussi que le ligand diphosphinite **3** (voir Figure 6.2), dérivés de l'acide tartrique naturel, ont été utilisés pour la réaction de couplage croisé de Suzuki et la réaction d'alkylation allylique asymétrique catalysées par du palladium dans solvant organique et ILs. Les conclusions de cette étude sont les suivantes :
 - ⇒ Les études de RMN des ligands **1** et **2** ont montré qu'au moins trois conformères sont présents en dissolution dû à la disposition spatiale relative des substituents des groupes benzyle et phosphorés donnant lieu à deux arrangements, *syn* et *anti*. Les études de modélisation moléculaire (au niveau DFT) sont en bonne concordance avec les proportions isomériques observées par RMN. Néanmoins après coordination pour former le complexe [PdCl₂(κ^1 -*P*-**1**)₂], les conformères ne sont plus distingués.
 - ⇒ Les systèmes catalytiques Pd/**1-3** ont été très actifs et sélectifs pour la réaction de couplage croisé de Suzuki avec des substrats comportant des groupes électro-attracteurs et aussi électro-donneurs dérivés de 4-R-bromobenzène et 4-R-chlorobenzène. En utilisant [BMI][PF₆] comme solvant, les systèmes catalytiques ont fonctionné sans formation des sous-produits, permettant l'activation de la liaison C-Cl pour des substrats contenant substituents électro-donneurs. Au contraire, dans le toluène, les activités sont en général plus basses.

- ⇒ Les ligands **1-3** présentent une plus grande stabilité sous des conditions catalytiques basiques dans le [BMI][PF₆] que dans le toluène et le [EMI][PH(O)OMe]. Ce comportement permet le recyclage de la phase catalytique dans le [BMI][PF₆] au moins dix fois sans perdre l'activité.
- ⇒ Malheureusement, les réactions asymétriques de Suzuki n'ont pas été sélectifs vers le produit de couplage croisé désiré ; le produit espéré a été uniquement obtenu avec une conversion et chimiosélectivité très faibles (conversion de substrat inférieur à 30% avec le système Pd/**1** dans le toluène).
- ⇒ L'évaluation catalytique de ces ligands pour la formation d'un nouveau centre stéréogénique par voie de la réaction d'alkylation allylique asymétrique catalysée par du palladium, a conduit à des énantiosélectivités faibles (ee jusqu'à 26% (*S*) dans le CH₂Cl₂. Surprenant, dans le dichlorométhane la réaction a conduit à son énantiomère (ee = 11% (*R*)).
- Les ligands P-donneurs dérivés du BINOL (**1** et **2**) et azadioxaphosphabicyclo[3.3.0]octane (**3** et **4**) (voir Figure 6.3) ont été appliqués pour la réaction d'hydrogénéation asymétrique catalysée par du rhodium dans différents solvants comme le CH₂Cl₂, ILs et également en supportant la phase catalytique dans le IL sur/dedans MWCNT fonctionnalisés par des fonctions ioniques. Les conclusions de cette étude sont les suivantes :
- ⇒ Tous les systèmes catalytiques testés ont été actifs dans le CH₂Cl₂, mais pas très énantiosélectifs (ee jusqu'au 36% (*S*))).
- ⇒ Dans le scCO₂, seulement les systèmes comportant des groupes fluorés ont été actifs, probablement grâce à la solubilité dans ce solvant, donnant une faible énantiosélectivité avec le catalyseur Rh/**2** (ee = 25% (*S*) pour **IV**).
- ⇒ Dans le [BMI][PF₆], des bonnes énantiosélectivités ont été obtenues (pour Rh/**1**: ee = 80% (*S*) pour **IV**), sous des conditions douces de réaction (P_{H2} = 1 bar, température ambiante). Toutefois l'énantiosélectivité chute quand la pression d'hydrogène et la température montent.

Conclusions

- ⇒ Le meilleur système catalytique, Rh/**1** dans le [BMI][PF₆], a été réutilisé plus de dix fois sans perte d'activité mais l'énaniosélectivité est rapidement perdue à cause du « leaching » du ligand comme a été mise en évidence par RMN des phases organiques.
- ⇒ Avec la finalité de mieux immobiliser le catalyseur, le complexe **Rh1** a été solubilisé dans le IL et supporté sur des MWCNT fonctionnalisés par des groupes imidazolium. Ce système a montré des conversions modérées et a été plus actif que le matériel catalytique analogue supporté sur silice, probablement grâce a la structure ouverte des MWCNT qu'évite les limitations de transfert de masse.

6.3. Conclusiones

El objetivo de esta Tesis ha sido el estudio del comportamiento catalítico de diferentes sistemas metálicos tanto moleculares como nanopartículas en disolventes de bajo impacto ambiental como CO₂ supercrítico y líquidos iónicos.

- Se han utilizado nuevas nanopartículas (MNP) de Rh y Ru estabilizadas por monoarilfosfinas (ver Figura 6.1) como catalizadores en la reacción de hidrogenación de arenos tanto en disolvente orgánico como en scCO₂, obteniendo las siguientes conclusiones:
 - ⇒ La síntesis de MNP pequeñas (ca. 1.50 nm) dependió del metal y de la naturaleza del ligando. El ligando PPh₃ estabilizó ambas nanopartículas, tanto RuNP como RhNP. Sin embargo, al utilizar ligandos fluorados, el ligando que contiene menos grupos fluorados, **1**, estabilizó RhNP, mientras que el ligando que contiene más grupos fluorados, **2**, estabilizó RuNP. Las nanopartículas **Ru2** y **Ru3** mostraron tener un tamaño más pequeño (1.30-1.40 nm) que las nanopartículas de rodio **Rh1** y **Rh3** (1.70-2.50 nm); para ambos metales, se observaron buenas dispersiones.
 - ⇒ La presencia de los ligandos fosfina en la superficie metálica se confirmó por espectroscopias vibracionales (IR y Raman) y análisis elemental. En particular, la reacción entre **Ru2** y dodeciltiol en THF mostró un desplazamiento lento de **3** por el derivado tiolado (seguido por RMN), apuntando a una interacción fuerte del ligando con la superficie metálica.
 - ⇒ Las nanopartículas de rutenio tienen una superficie metálica relativamente más grande que las de rodio lo cual está en concordancia con la mayor actividad observada para los sistemas de rutenio. Además, la selectividad observada apunta a una fuerte interacción entre los grupos arilo de los sustratos con la superficie metálica, principalmente en presencia de grupos oxigenados.

Conclusions

- ⇒ Las conversiones obtenidas pusieron de manifiesto que los sistemas catalíticos son en general más lentos en scCO₂ que en THF, probablemente debido a las diferentes solubilidades de las MNP en scCO₂ en comparación con THF, incluso para el ligando con más contenido de flúor, **2**. Las RuNP permanecieron dispersas después de la hidrogenación en scCO₂, contrariamente a lo observado para las nanopartículas de rodio en las que se observaron aglomerados. En THF, se observaron en todos los casos aglomerados después de las reacciones catalíticas.
- Los nuevos ligandos de tipo octan[3,3,0]azafosfaciclo **1** y **2** y el ligando difosfinito **3** (ver Figura 6.2), derivados del ácido tartárico natural, han sido utilizados en la reacción de acoplamiento C-C cruzado de Suzuki así como en la reacción de alquilación alílica asimétrica catalizadas por paladio, tanto en disolvente orgánico como en ILs. Las conclusiones de esta parte de la Tesis son:
 - ⇒ Los estudios por RMN de los ligandos **1** y **2**, mostraron la presencia de al menos tres confórmeros en disolución debido a la disposición espacial relativa de los sustituyentes bencilo del nitrógeno y del substituyente del fósforo, dando lugar a los isómeros *syn* y *anti*. Los estudios de modelización molecular (a nivel DFT) están en buena concordancia con las relaciones isoméricas observadas por espectroscopia de RMN.
 - ⇒ Los sistemas catalíticos Pd/**1-3** han sido altamente activos y selectivos en los acoplamientos cruzados C-C de Suzuki tanto con sustratos de tipo 4-R-bromobenceno y 4-R-clorobenceno con grupos electro-attractores así como con grupos electro-dadores. Utilizando [BMI][PF₆] como disolvente, los sistemas fueron activos sin la formación de subproductos de reacción, permitiendo la activación del enlace C-Cl incluso para sustratos que contenían sustituyentes electro-dadores. En cambio, los sistemas catalíticos muestran actividades generalmente menores en tolueno.
 - ⇒ Cabe destacar que los ligandos **1-3** han mostrado una alta estabilidad bajo las condiciones catalíticas básicas utilizadas en [BMI][PF₆] en comparación con las

observadas en tolueno y en [EMI][PH(O)OMe]. Este comportamiento ha permitido el reciclaje de la fase catalítica en [BMI][PF₆] hasta diez veces sin pérdida de actividad.

- ⇒ Desafortunadamente, las reacciones de Suzuki en versión asimétrica, no han sido selectivas hacia el producto deseado de acoplamiento cruzado, dando solamente el producto esperado con conversiones y quimioselectividades muy bajas (menos de 30% utilizando el sistema Pd/**1** en tolueno).
- ⇒ La evaluación catalítica de los sistemas de paladio con estos ligandos quirales en la reacción de alquilación alílica asimétrica modelo, catalizada por paladio, ha dado lugar a bajas enantioselectividades (*ee* hasta 26% (*S*) en CH₂Cl₂). Sorprendentemente, a pesar de que el exceso enantiomérico también fue bajo, en [BMI][PF₆] se ha obtenido el enantiómero opuesto (*ee* = 11% (*R*)).
- Los sistemas catalíticos de rodio con ligandos quirales P-dadores derivados del BINOL (**1** y **2**) y de tipo octan[3,3,0]azafosfaciclo (**3** y **4**) (ver Figura 6.3) se han probado en la reacción de hidrogenación asimétrica en diferentes disolventes como son CH₂Cl₂, scCO₂ y ILs. También se ha soportado la fase con el catalizador en el IL sobre/dentro de MWCNT funcionalizados con grupos imidazolio. Las conclusiones de este trabajo son las siguientes:
 - ⇒ Los sistemas catalíticos evaluados han sido activos en CH₂Cl₂ pero han mostrado bajas enantioselectividades (*ee* hasta 36% (*S*)).
 - ⇒ En scCO₂, sólo los sistemas que contenían grupos fluorados fueron activos, probablemente debido a su solubilidad en este disolvente, pero mostraron una baja inducción asimétrica, sólo significativa en el caso del sistema Rh/**2** (*ee* = 25% (*S*) para **IV**).
 - ⇒ En [BMI][PF₆] se obtuvieron buenas enantioselectividades (Rh/**1**: *ee* = 80% (*S*) para **IV**) bajo condiciones de reacción suaves (1 bar de presión de hidrógeno, temperatura ambiente). De cualquier manera, la enantioselectividad se perdió al incrementar la presión de hidrógeno y la temperatura.

Conclusions

- ⇒ El mejor sistema catalítico, Rh/**1** en [BMI][PF₆], fue reutilizado diez veces manteniendo la actividad, pero perdiendo la enantioselectividad debido al “leaching” de ligando.
- ⇒ Con la finalidad de inmovilizar el catalizador, el complejo **Rh1** se disolvió en el IL y se soportó sobre MWCNT funcionalizados. Este sistema presentó conversiones moderadas, siendo más activo que el material catalítico homólogo soportado en sílice, probablemente debido a la estructura abierta de los nanotubos de carbono con respecto a la sílice, lo cual evita las limitaciones debidas a la transferencia de masa.

6.4. Conclusions

L'objectiu d'aquesta tesi ha estat l'estudi del comportament catalític de diferents sistemes metà·lics tant moleculars com nanopartícules en dissolvents de baix impacte ambiental com són el CO₂ supercrític i els líquids iònics.

- S'han utilitzat noves nanopartícules de Rh i Ru estabilitzades per monoarilfosfines (vegeu Figura 6.1) com catalitzadors en la reacció d'hidrogenació d'arens tant en dissolvent orgànic com en scCO₂, establint-se les següents conclusions:
 - ⇒ La síntesi de MNP de grandària petita (ca. 1.50 nm) va dependre altament del precursor organometà·lic i de la naturalesa del lligand. El lligand PPh₃ ha estabilitzat ambdós tipus de MNP, tant de Ru com de Rh. Però, en utilitzar lligands fluorats, aquell amb menys contingut de fluor, **1**, va estabilitzar únicament les RhNP, mentre que el lligand amb més contingut de fluor, **2**, va estabilitzar únicament les RuNP. Les nanopartícules **Ru2** i **Ru3** han mostrat una grandària més petita (1.30-1.40 nm) que les nanopartícules de rodi **Rh1** i **Rh3** (1.70-2.50 nm); per a ambdós metalls, s'han observat bones dispersions.
 - ⇒ La presència dels lligands en la superfície metà·lica es va posar de manifest per les espectroscòpies vibracionals IR i Raman, i anàlisi elemental. En particular, la reacció entre **Ru2** i dodeciltiol en THF va mostrar un desplaçament lent de **3** pel derivat tiolat (seguit per RMN), apuntant a una interacció forta del lligand amb la superfície metà·lica.
 - ⇒ Les nanopartícules de ruteni tenen una superfície metà·lica relativament més gran que les de rodi, el que està d'acord amb l'activitat més elevada observada per als sistemes de ruteni. A més, la selectivitat observada apunta a una forta interacció entre els grups aril dels substrats amb la superfície metà·lica, principalment en presència de grups oxigenats.
 - ⇒ Les conversions obtingudes han posat de manifest que els sistemes catalítics són en general més lents en scCO₂ que en THF, probablement degut a les

Conclusions

diferents solubilitats de les MNP en scCO₂ en comparació amb aquella obtinguda en THF, fins i tot pel lligand amb més contingut de fluor, **2**. Les RuNP van romandre disperses després de la hidrogenació en scCO₂, a diferència del que es va observar amb les de Rh en el que es van obtenir aglomerats. En THF, s'han observat en tots els casos aglomerats després de les reaccions catalítiques.

- Els nous lligands de tipus octà[3,3,0] azafosfacicicle **1** i **2** i el lligand difosfonit **3** (vegeu Figura 6.2), derivats de l'àcid tartàric natural, han estat utilitzats en la reacció d'acoblament C-C creuat de Suzuki així com en la reacció d'alquilació al·lílica asimètrica catalitzades per palladi, tant en dissolvent orgànic com en ILs. Les conclusions d'aquesta part de la Tesi són:
 - ⇒ Els estudis per RMN dels lligands **1** i **2** van mostrar la presència d'almenys tres confòrmers en dissolució a causa de la disposició espacial relativa dels substituents del benzil del nitrogen i del substituent del fòsfor, donant lloc als isòmers *syn* i *anti*. Els estudis de modelatge molecular (a nivell DFT) es troben en bona concordança amb les relacions isomèriques observades per espectroscòpia de RMN.
 - ⇒ Els sistemes catalítics Pd/**1-3** han estat altament actius i selectius en els acoblaments C-C creuats de Suzuki, tant amb substrats del tipus 4-R-bromobencè com 4-R-clorobencè, amb grups electro-attractors així com electro-dadors. Utilitzant [BMI][PF₆] com a dissolvent, els sistemes catalítics van funcionar sense formació de subproductes de reacció, permetent l'activació de l'enllaç C-Cl inclús per a substrats amb substituents electro-donadors. En canvi, els sistemes mostren activitats generalment menors en toluè.
 - ⇒ Cal destacar que els lligands **1-3** han mostrat una alta estabilitat sota les condicions catalítiques bàsiques utilitzades en [BMI][PF₆] en comparació de l'observada en toluè i en [EMI][PH(O)OMe]. Aquest comportament ha permès

el reciclatge de la fase catalítica en [BMI][PF₆] fins a deu vegades sense pèrdua d'activitat.

- ⇒ Malauradament, les reaccions de Suzuki en versió asimètrica, no han estat selectives cap al producte desitjat d'acoblament creuat, donant solament el producte esperat amb rendiments i químioselectivitats molt baixos (menys de 30% utilitzant el sistema Pd/**1** en toluè).
- ⇒ L'avaluació catalítica de sistemes de pal·ladi amb aquests lligands quirals en la reacció d'alquilació al·lílica asimètrica model ha donat baixes enantioselectivitats (*ee* fins a 26% (*S*) en CH₂Cl₂). Sorprendentment, a pesar que l'excés enantiòmeric obtingut en [BMI][PF₆] ha estat baix, l'enantiomer obtingut presenta la configuració absoluta oposada (*ee* = 11% (*R*)).
- Els sistemes catalítics de rodí amb lligands quirals P-donadors derivats del BINOL (**1** i **2**) i de tipus octà[3,3,0]azafosfacicicle (**3** i **4**) (vegeu Figura 6.3) s'han provat en la reacció d'hidrogenació asimètrica en diferents dissolvents com són CH₂Cl₂, scCO₂ i ILs. També s'ha suportat la fase del catalitzador en IL sobre/dins de MWCNT funcionalitzats amb grups imidazoli. Les conclusions d'aquest treball són les següents:
 - ⇒ Els sistemes catalítics evaluats han estat actius en CH₂Cl₂ però han mostrat baixes enantioselectivitats (*ee* fins a 36% (*S*)).
 - ⇒ En scCO₂, solament els sistemes amb grups fluorats han estat actius, probablement a causa de la seva solubilitat en aquest dissolvent però han mostrat baixa inducció asimètrica només significativa en el cas del sistema més selectiu Rh/**2** (*ee* = 25% (*S*) per a **IV**).
 - ⇒ En [BMI][PF₆] s'han obtingut bones enantioselectivitats (Rh/**1**: *ee* = 80% (*S*) per a **IV**) sota condicions de reacció suaus (1 bar de pressió d'hidrogen, temperatura ambient). De qualsevol manera l'enantioselectivitat s'ha perdut en incrementar la pressió d'hidrogen i la temperatura.

Conclusions

- ⇒ El millor sistema catalític, Rh/**1** en [BMI][PF₆], ha estat reutilitzat deu vegades sense pèrdua d'activitat però perdent l'enantioselectivitat a causa del "leaching" del lligand.
- ⇒ Amb la finalitat d'immobilitzar el catalitzador, el complex **Rh1** es va dissoldre en el IL i es va suportar sobre MWCNT funcionalitzats. Aquest sistema va presentar conversions moderades, essent més actiu que el material catalític homòleg suportat en sílice, probablement a causa de l'estructura oberta dels nanotubs de carboni pel que fa a la sílice, la qual cosa evita les limitacions de transferència de massa.

Summary

Résumé
Resumen
Resum

UNIVERSITAT ROVIRA I VIRGILI
ORGANOMETALLIC COMPOUNDS AND METAL NANOPARTICLES AS CATALYSTS IN LOW ENVIRONMENTAL IMPACT SOLVENTS
Martha Verónica Escárcega Bobadilla
ISBN:978-84-694-1249-7/DL:T-324-2011

Summary

In the last decades, the design of processes in the framework of the sustainable chemistry has been exponentially growing. The constant searching of cleaner processes has led to a lot of effort to obtain higher yields by activation of specific sites, and improving chemo-, regio- and enantioselectivities, which are crucial from a point of view of an atom economy strategy. In this sense, solvents play a critical role, particularly in catalytic organic synthesis as could be seen through this work.

This PhD thesis focuses on the use of alternative sustainable reaction media such as ionic liquids (ILs), supercritical carbon dioxide (scCO_2) and mixtures of both solvents in different catalytic processes, with the aim of decreasing the use of conventional organic solvents.

Several catalytic reactions like homogeneous and supported rhodium catalysed asymmetric hydrogenation of functionalised olefins, biphasic palladium catalysed Suzuki C-C cross-coupling between aryl halides and aryl boronic acids, homogeneous palladium catalysed asymmetric allylic alkylation, and ruthenium and rhodium nanoparticles catalysed arene hydrogenation were tested.

This PhD Thesis is divided in the following Chapters:

In **Chapter 1**, a general Introduction and historical background is given about Sustainable Chemistry and Catalysis.

The general and also specific Objectives of this work are given in **Chapter 2**.

Chapter 3 describes the synthesis and characterisation of ruthenium and rhodium nanoparticles (MNP), which were prepared in the presence of phosphine ligands containing fluorinated groups. The syntheses of these new materials evidenced the crucial tuning between metal precursor and ligand. These nanocatalysts were used in hydrogenation reactions of arene derivatives in both THF and supercritical carbon dioxide medium. The catalytic behavior observed (activity and selectivity) showed that both Ru and Rh systems are active in scCO_2 although the conversions are lower respect

Summary

to THF, preventing the hydrogenation of the aromatic group when electron-donor groups are present on the substrate.

Chapter 4 deals with the synthesis and characterisation of new chiral azadioxaphosphabicyclo[3.3.0]octane ligands. An accurate structural analysis showed that they were obtained as a mixture of three conformers, in agreement with molecular modelling studies showing a *trans* arrangement with regard to the two condensed five-membered heterocycles. The stability of oxaphosphane ligands in [BMI][PF₆] (1-butyl-3-methyl-imidazolium hexafluorophosphate) under basic catalytic conditions was remarkable (monitored by NMR spectroscopy). Palladium catalytic systems containing these ligands were active in Suzuki C-C cross-coupling reactions between phenyl boronic acid and aryl halides (bromide and chloride derivatives) bearing electron-donor or electron-withdrawing substituents, in both organic and ionic liquid solvents. The catalytic systems showed a high stability even under the most severe reaction conditions used in this work. The ionic liquid catalytic phase could be recycled up to ten times without significant activity loss.

Chapter 5 focuses on Rh catalytic systems containing chiral P-donor ligands, such as new fluorinated (*R*)-BINOL and azadioxaphosphabicyclo[3.3.0]octane derivatives. They were tested in benchmark enantioselective hydrogenation reactions in different solvents (dichloromethane, [BMI][PF₆], scCO₂ and [BMI][PF₆]/scCO₂ mixture). The most efficient medium was the ionic liquid, which provided the best asymmetric induction achieved (up to 80% ee). The IL catalytic phase could be recycled without loss of activity, but with loss of asymmetric induction due to the ligand leaching. The IL catalytic phase was then supported on ionic functionalized multi-walled carbon nanotubes in order to improve the catalyst immobilization. However, no enantioselectivity was observed although good catalytic activity was achieved. This work represents an original comparative study of Rh catalysts containing new monodentate chiral phosphorous ligands in different reaction media, revealing that (*R*)-BINOL derivative ligands containing fluorinated groups lead to efficient catalysts for asymmetric hydrogenation reactions using [BMI][PF₆] as solvent.

Finally, the Conclusions of this work are given in **Chapter 6**.

Résumé

Au cours des dernières décennies, la conception des processus dans le cadre de la chimie durable n'a cessé de croître. La constante recherche de nouvelles cibles moléculaires a conduit beaucoup d'efforts pour obtenir des rendements plus élevés par l'activation des sites spécifiques, en ce qui concerne la chimio-, régio- et énantioselectivités, qui sont cruciales du point de vue d'une stratégie d'économie atomique. En ce sens, les solvants jouent un rôle crucial, en particulier dans la synthèse organique catalytique comme on le voit à travers ce travail.

Cette Thèse se focalise sur l'utilisation des milieux alternatifs de réaction, comme les liquides ioniques (LI), le dioxyde de carbone supercritique (scCO_2) et des mélanges des deux solvants dans les différents processus catalytiques, en comparant avec des solvants organiques classiques.

Plusieurs réactions catalytiques comme l'hydrogénéation asymétrique des oléfines fonctionnalisées catalysée par rhodium en phase homogène et supportée, le couplage C-C croisé de Suzuki biphasique catalysée par palladium, entre des halogénures d'aryle et des acides aryleboroniques, l'alkylation allylique asymétrique homogène catalysée par palladium et l'hydrogénéation des arènes nanoatalysée par le ruthénium et le rhodium ont été testés.

Cette Thèse a été divisée dans les Chapitres suivants:

Dans le **Chapitre 1** une introduction générale aussi que le contexte historique est donné sur la chimie durable et la catalyse.

Les objectifs généraux et spécifiques de ce travail sont donnés dans le **Chapitre 2**.

Le **Chapitre 3** décrit la synthèse et la caractérisation des nanoparticules de ruthénium et de rhodium (MNP) qui ont été préparés en présence de ligands phosphine contenant des groupes fluorés, à partir de composés organométalliques bien définis. Les synthèses de ces nouveaux matériaux ont montré que le « tuning » entre précurseur métallique et le ligand est crucial. Ces nanocatalyseurs ont été utilisés dans des réactions d'hydrogénéation de dérivés arènes dans les deux THF et le dioxyde

Summary

de carbone supercritique. Le comportement catalytique observé (activité et sélectivité) a montré que les deux systèmes de Ru et Rh sont moins actifs dans le scCO₂ que dans le THF, l'hydrogénéation du groupe aromatique a été prévenu lorsque des groupes donneurs d'électrons sont présents sur le substrat.

Le **Chapitre 4** traite de la synthèse et la caractérisation de nouveaux ligands chiraux azadioxaphosphabicycle [3.3.0] octane montrant une disposition *trans* en ce qui concerne les deux hétérocycles condensés à cinq chaînons. Ils ont été obtenus comme un mélange de trois conformères, en accord avec les études de modélisation moléculaire. La stabilité des ligands oxaphosphane dans [BMI][PF₆] dans les conditions catalytiques basiques a été étudiée (suivie par spectroscopie RMN). Les systèmes catalytiques de palladium contenant ces ligands ont été actifs dans les réactions de couplage croisé de Suzuki C-C entre l'acide phényle boronique et d'halogénures d'aryle (dérivés chlorure et bromure) portant substituants électro-donneurs ou électro-attracteurs, dans les deux solvants organiques et liquide ionique. Les systèmes catalytiques ont montré une grande stabilité, même dans les conditions de la réaction la plus forte utilisée dans ce travail. La phase liquide ionique catalytique peut être réutilisée jusqu'à dix fois sans perte importante d'activité.

Le **Chapitre 5** traite sur des systèmes catalytiques homogènes de Rh contenant des ligands chiraux P-donneurs, tels que les nouveaux dérivés fluorés du (*R*)-BINOL et azadioxaphosphabicyclo [3.3.0] octane. Ils ont été testés dans des réactions d'hydrogénéation énantiomérisante de référence dans différents solvants (dichlorométhane, le 1-butyl-3-méthyl-imidazolium hexafluorophosphate ([BMI][PF₆]), le scCO₂ et le mélange [BMI][PF₆] / scCO₂). Le moyen le plus efficace a été le liquide ionique, induisant la meilleure énantiomérisation (jusqu'à 80% ee). La phase IL catalytique peut être recyclé sans perte d'activité, mais avec une perte d'induction asymétrique due à la lixiviation du ligand. La phase catalytique IL a été prise en charge sur nanotubes de carbones multi-parois fonctionnalisées ioniquement afin d'améliorer l'immobilisation du catalyseur. Toutefois, aucune énantiomérisation n'a malheureusement été observée, malgré une haute activité catalytique a été atteinte. Ce travail représente une étude originale comparative des catalyseurs Rh contenant de nouvelles ligands phosphorés chiraux monodentés dans les milieux réactionnels

différentes, révélant que les ligands dérivés du (*R*)-BINOL contenant des groupes fluorés conduisent à des catalyseurs efficaces pour les réactions d'hydrogénéation asymétrique en utilisant [BMI][PF₆] en tant que solvant.

Finalement, les conclusions de ce travail sont donnés dans le **Chapitre 6**.

Resumen

Durante las últimas décadas, el diseño de procesos en el marco de la química sostenible ha ido creciendo de manera exponencial. La constante búsqueda de procesos más benignos con el medio ambiente ha implicado grandes esfuerzos en la obtención de altos rendimientos por activación de sitios específicos y poniendo especial atención en mejorar la quimio-, la regio- y la enantioselectividad, las cuales son cruciales desde el punto de vista estratégico de la economía atómica. En este sentido, los disolventes juegan un papel crítico, particularmente en la síntesis orgánica catalítica como se ha demostrado a lo largo de este trabajo.

Esta Tesis se enfoca en el uso de medios de reacción alternativos y sostenibles, como son los líquidos iónicos (ILs), el dióxido de carbono supercrítico (scCO₂) y mezclas de ambos disolventes en diferentes procesos catalíticos, con el objetivo de disminuir el uso de disolventes orgánicos.

Se ha estudiado un amplio panel de reacciones catalíticas, como son la hidrogenación asimétrica de olefinas catalizada por rodio tanto en fase homogénea como soportada, la reacción de acoplamiento cruzado C-C de Suzuki bifásica entre halogenuros de arilo y ácidos fenilborónicos catalizada por paladio, la reacción de alquilación alílica asimétrica catalizada por paladio y la hidrogenación de arenos nanocatalizada por sistemas de rodio y rutenio.

Esta Tesis Doctoral está dividida en los siguientes Capítulos:

En el **Capítulo 1**, se presenta una Introducción general así como los antecedentes acerca de la química sostenible y la catálisis.

Los Objetivos, tanto generales como específicos, de este trabajo están descritos en el **Capítulo 2**.

El **Capítulo 3** describe la síntesis y caracterización de nanopartículas (MNP) de rodio y rutenio con ligandos fosfina que contienen grupos fluorados. La síntesis de estos nuevos materiales ha evidenciado la importancia crucial de una buena modulación entre el precursor metálico y el ligando. Estos nanocatalizadores se han

utilizado en reacciones de hidrogenación de derivados de arenó tanto en THF como medio dióxido de carbono supercrítico. El comportamiento catalítico observado (actividad y selectividad) ha mostrado que ambos sistemas (de Rh y de Ru) son activos en scCO₂ aunque las conversiones son menores que en THF, previniendo la hidrogenación del grupo aromático cuando en el sustrato están presentes grupos electrodadores.

En el **Capítulo 4** se presenta la síntesis y caracterización de nuevos ligandos octil[3.3.0]azadioxafosfaciclo. Un estudio estructural detallado ha permitido concluir que estos ligandos se han obtenido como una mezcla de tres confórmeros, en concordancia con estudios de modelado molecular mostrando una disposición *trans* con respecto a los dos heterociclos de cinco miembros. Es destacable la elevada estabilidad de los ligandos oxafosfano en [BMI][PF₆] (hexafluorofosfato de 1-butil-3-metilimidazolio) bajo las condiciones catalíticas básicas de reacción (seguimiento por espectroscopía de RMN). Los sistemas de paladio que contienen estos ligandos han sido activos en reacciones de acoplamiento cruzado C-C de tipo Suzuki entre ácidos fenilborónicos y halogenuros de arilo (derivados bromuro y cloruro) con sustituyentes tanto electrodadores como electroattractores en ambos medios, orgánico y líquidos iónicos. Los sistemas catalíticos han mostrado una gran estabilidad incluso bajo las condiciones de reacción más severas utilizadas en este trabajo. Prueba de ello es que la fase catalítica en líquido iónico ha podido ser reciclada hasta diez veces sin pérdida significativa de la actividad.

El **Capítulo 5** trata sobre la reacción de hidrogenación asimétrica catalizada por rodio con ligandos P-dadores, como son los nuevos derivados fluorados del (*R*)-BINOL y derivados de tipo octil [3.3.0]azadioxafosfaciclo. Estos sistemas catalíticos han sido probados en la reacción modelo de hidrogenación asimétrica en diferentes medios de reacción (dclorometano, [BMI][PF₆], scCO₂ y la mezcla [BMI][PF₆] / scCO₂). El medio de reacción más eficiente ha sido el líquido iónico, en el cual se han obtenido las mejores enantioselectividades (hasta 80% ee). La fase catalítica de IL ha podido ser reciclada sin pérdida de actividad, pero la inducción asimétrica se ha perdido debido al “leaching” del ligando. La fase catalítica en IL se ha soportado sobre nanotubos de carbono multipared funcionalizados iónicamente, con la finalidad de mejorar la inmovilización

Summary

del catalizador. Desafortunadamente no se ha observado inducción asimétrica. Este trabajo presenta un estudio comparativo original de catalizadores de Rh con nuevos ligandos fosforados quirales monodentados en medios de reacción diferentes, y ha revelado que los ligandos con grupos fluorados derivados del (*R*)-BINOL pueden ser catalizadores eficientes para reacciones de hidrogenación asimétrica utilizando [BMI][PF₆] como medio de reacción.

Finalmente, las Conclusiones de este trabajo están dadas en el **Capítulo 6**.

Resum

Durant les darreres dècades, el disseny de processos en el marc de la química sostenible ha anat creixent de forma exponencial. La recerca constant de processos més beniges amb el medi ambient ha implicat un gran esforç per obtenir millors rendiments mitjançant l'activació de llocs específics, i possant especial èmfasi amb el control de la quimio-, la regio- i la enantioselectivitat, punts crucials per a l'economia atòmica. En aquest sentit, els dissolvents juguen un paper crític, i com s'ha mostrat al llarg d'aquesta memòria, particularment en la síntesi orgànica catalitzada per metalls.

Aquesta Tesi s'enfoca en l'ús de mitjans de reacció alternatius i sostenibles, com són els líquids iònics (ILs), el diòxid de carboni supercrític (scCO_2) i la barreja de ambdós dissolvents, amb l'objectiu de disminuir l'ús de dissolvents orgànics convencionals.

S'ha estudiat un variat ventall de processos catalítics, com són la reacció d'hidrogenació asimètrica d'olefines funcionalitzades catalitzada per rodi tant en fase homogènia com suportada, la reacció de Suzuki d'acoblament creuat C-C entre halogenurs d'aril i àcids aril borònics catalitzada per pal·ladi en condicions bifàsiques de reacció, la reacció en fase homogènia d'alquilació al·lílica asimètrica catalitzada per pal·ladi i la hidrogenació nanocatalitzada per nanopartícules de rodi i ruteni de arens.

Aquesta Tesi Doctoral es divideix en les següents Capítols:

En el **Capítol 1**, es presenta una Introducció general així com els antecedents sobre la química sostenible i la catàlisis.

Els Objectius, tant generals com específics, són descrits en el **Capítol 2**.

En el **Capítol 3**, es descriu la síntesi i caracterització de nanopartícules (MNP) de rodi i ruteni les quals han estat preparades en presència de lligands fosfina amb grups fluorats. La síntesi d'aquests nous materials ha evidenciat la importància crucial d'una bona modulació entre el precursor metàl·lic i el lligand. Aquests nanocatalitzadors han estat emprats en reaccions d'hidrogenació de derivats d'arè tant en THF com en diòxid de carboni supercrític. El comportament catalític observat (activitat i selectivitat) ha

Summary

mostrat que tots dos sistemes, Rh i Ru, són actius en scCO₂, malgrat que les conversions són inferiors que en THF, evitant la hidrogenació del grup aromàtic quan grups electrodonadors (com funcions èter) estan presents en el substrat.

En el **Capítol 4** es presenta la síntesi i caracterització de nous lligands octil[3.3.0] azadioxafosfacicicle. Un acurat estudi estructural mostra que aquests lligands s'han obtingut com una barreja de tres confòrmers, en concordança amb estudis de modelatge molecular, mostrant una disposició *trans* pel que fa als dos heterocicles de cinc membres. És destacable l'estabilitat dels lligands oxafosfà en [BMI][PF₆] (hexafluorofosfat d'1-butil-3-metilimidazoli) sota les condicions catalítiques bàsiques de reacció (seguida per espectroscòpia de RMN). Els sistemes de pal·ladi amb aquests lligands han estat actius en reaccions d'acoblament creuat C-C de tipus Suzuki entre àcids fenil borònics i halogenurs d'aril (bromur i clorur) amb substituents tant electrodonadors com electroatractors en tots dos medis, orgànic i líquid iònic. Els sistemes catalítics han mostrat una gran estabilitat fins i tot sota les condicions de reacció més severes utilitzades en aquest treball. Prova d'això és que la fase catalítica líquid iònic ha pogut ser reciclada fins a deu vegades sense pèrdua significativa de l'activitat.

El **Capítol 5** versa sobre la reacció d'hidrogenació asimètrica catalitzada per rodí amb lligands P-donadors fluorats derivats del (*R*)-BINOL i octil [3.3.0] azadioxafosfacicicle. Aquests sistemes han estat provats en la reacció model d'hidrogenació asimètrica en diferents mitjans de reacció (diclorometà, [BMI][PF₆], scCO₂ i la barreja [BMI][PF₆] / scCO₂). El mitjà de reacció més eficient ha estat el líquid iònic, en el qual s'han obtingut les millors enantioselectivitats (fins a 80% *ee*). La fase catalítica del líquid iònic s'ha reciclat sense pèrdua d'activitat, però perdent la inducció asimètrica a causa del “leaching” del lligand. La fase catalítica en IL s'ha suportat amb la finalitat de millorar la immobilització del catalitzador. Malauradament, no s'ha obtingut enantioselectivitat. Aquest treball presenta un estudi comparatiu original de catalitzadors de Rh amb nous lligands fosforats quirals monodentats en medis de reacció diferents, i ha revelat que els lligands amb grups fluorats derivats del (*R*)-BINOL poden ser catalitzadors eficients per a reaccions d'hidrogenació asimètrica utilitzant [BMI][PF₆] com a medi de reacció.

Finalment, les Conclusions de aquest treball es presenten en el **Capítol 6**.

UNIVERSITAT ROVIRA I VIRGILI
ORGANOMETALLIC COMPOUNDS AND METAL NANOPARTICLES AS CATALYSTS IN LOW ENVIRONMENTAL IMPACT SOLVENTS
Martha Verónica Escárcega Bobadilla
ISBN:978-84-694-1249-7/DL:T-324-2011

Publications

- M. V. Escárcega-Bobadilla, C. Tortosa, E. Teuma, C. Pradel, A. Orejón, M. Gómez and A. M. Masdeu-Bultó. "Ruthenium and rhodium nanoparticles as catalytic precursors in supercritical carbón dioxide". *Catalysis Today*. **2009**, 148, 398-404.
- M. V. Escárcega-Bobadilla, E. Teuma, A. M. Masdeu-Bultó and M. Gómez. "New bicyclic phosphorous ligands: synthesis, structure and catalytic applications in ionic liquids". *Submitted*.
- M. V. Escárcega-Bobadilla, L. Rodríguez-Pérez, E. Teuma, P. Serp, A. M. Masdeu-Bultó and M. Gómez. "Rhodium complexes containing chiral P-donor ligands as catalysts for asymmetric hydrogenation in non conventional media". *Submitted*.

Conferences and scientific meetings

- "*Organometallic complexes and metal nanoparticles as catalysts in different reaction media*". **Oral presentation**. Démi-journée 'Mi-Thèse', Université Paul Sabatier. Toulouse, France. March, 2010.
- "*Recoverable Palladium Catalytic Systems Containing P-donor Chiral Ligands in Ionic Liquids. Applications in Suzuki C-C Coupling*". **Oral presentation**. '10th FIGIPAS International Meeting in Inorganic Chemistry'. Palermo, Italy. July, 2009.
- "*Metal Nanoparticles in Catalysis in Supercritical Carbon Dioxide*" **Poster**. '10th International Conference on CO₂ utilization (ICCDU-X)'. Tianjin, China. May, 2009.
- "*Metallic Nanoparticles in Catalysis: Application in Sustainable Chemistry*". **Oral presentation**. 'Journée Chimie Grand Sud-Ouest', French Chemical Society. Pau, France. November, 2008.
- "*Metal Nanoparticles in Catalysis using Supercritical Carbon Dioxide*". **Oral presentation**. 'IV Trobada de Joves Investigadors', Universitat Rovira I Virgili. Tarragona, Spain. July, 2008.

Scientific contributions

- “*Ru and Rh Nanoparticles Stabilized by Fluorinated Ligands: Application in Sustainable Chemistry*”. **Poster.** ‘Summer School on Catalysis’, University of Liverpool. Liverpool, England. September, 2007.

UNIVERSITAT ROVIRA I VIRGILI
ORGANOMETALLIC COMPOUNDS AND METAL NANOPARTICLES AS CATALYSTS IN LOW ENVIRONMENTAL IMPACT SOLVENTS
Martha Verónica Escárcega Bobadilla
ISBN:978-84-694-1249-7/DL:T-324-2011

UNIVERSITAT ROVIRA I VIRGILI
ORGANOMETALLIC COMPOUNDS AND METAL NANOPARTICLES AS CATALYSTS IN LOW ENVIRONMENTAL IMPACT SOLVENTS
Martha Verónica Escárcega Bobadilla
ISBN:978-84-694-1249-7/DL:T-324-2011